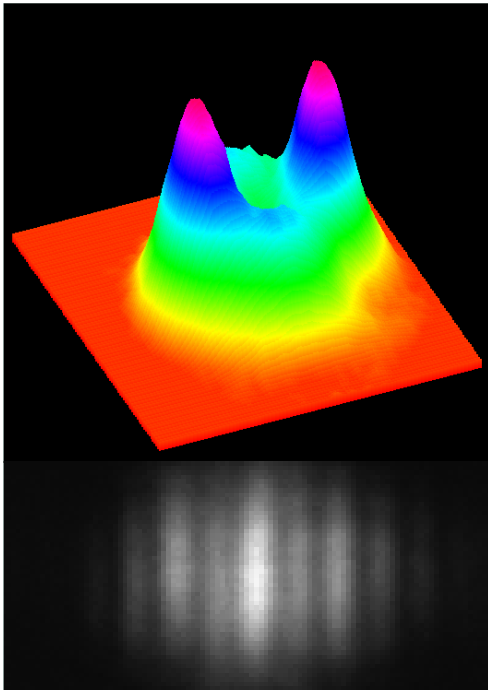


Международная конференция, посвященная юбилею
И.М.ХАЛАТНИКОВА, 22-23 октября 2009 г., Черноголовка



Bose-Einstein Condensation of Dipolar Excitons in Quantum Wells



- BEC in diluted Bose gases ($N a^D \ll 1$, N – density, a – linear size of Bose-particle, D – system dimensionality) occurs when thermal de Broglie wavelength $\lambda_{dB} = (h^2 / 2\pi m k_B T)^{1/2}$ exceeds the interparticles separation
A.EINSTEIN (1924-25)

- BEC is accompanied by
 - a. macroscopic occupation of the ground state with momentum $p=0$
 - b. appearance of the order parameter (coherence, ξ) destroyed by fluctuations

- In 3D Bose-system BEC takes place when $N\lambda_{dB}^3 = 2.612$

- The λ -Phenomenon of Liquid Helium and the Bose-Einstein Degeneracy

F.London *Nature* N3571, 643 (1938)

$$T_\lambda \cong 2.17K \quad T_L \cong 3.09K$$

* Burton, E. F., *NATURE*, 135, 265 (1935); Kapitza, P., *NATURE*, 141, 74 (1938); Allen, J. F. and Misener, A. D., *NATURE*, 141, 75 (1938).

- In atomic Bose-gases BEC occurs at $T \leq 1\mu K$ (1995)
E.Cornell, W.Ketterle and C.E.Wieman, Nobel Prize (2001)

Excitonic scales in semiconductors

$$\underline{R}_{ex} = 1/\epsilon_0^2 (\mu_{ex} / m_0) \underline{R}_H$$

(Ge, GaAs: $R_{ex} \approx 4 \text{ meV}$)

$$\underline{a}_{ex} = \epsilon_0 (m_0/\mu_0) \underline{a}_H$$

(Ge, GaAs : $a_{ex}^B \approx 10^{-6} \text{ cm}$)

$$\underline{\mu}_{ex} \approx 0.1 m_e; M_{ex} = m_e + m_h$$
$$\chi_{ex}^{dia} \approx 10^5 - 10^6 \chi_H^{dia}$$

*BEC (Bose-gases Rb, Na, H...)
in magnetic traps, $T_C \leq 10^{-6} \text{ K}$*

*In the case of GaAs/AlGaAs QWs 2D-
excitons reaches a value $T_C \approx 3\text{K}$
for exciton density per spin
 $N/g = 10^{10} \text{ cm}^{-2}$
($a_B \approx 20 \text{ nm}$, $m_{ex} \approx 0.25m_0$, spin
degeneracy $g = 4$)*

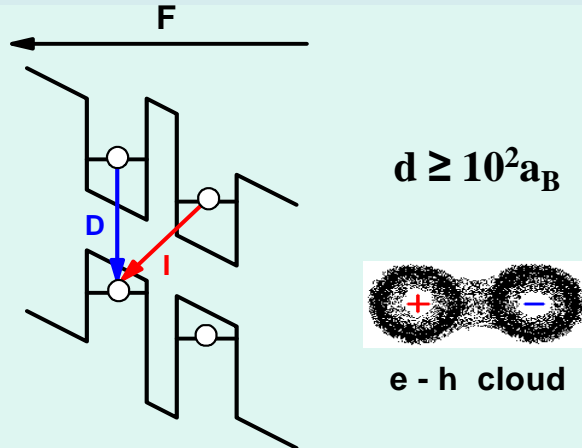
Exciton condensation in semiconductors

- $Na_{ex}^d \ll 1$
**Moskalenko
Blatt
Casella (1962)**
- $Na_{ex}^d \gg 1$
**Keldysh
Kopaev
Kozlov (1964-65)**
- **Kohn
Sherrington (1970)**
- **Electron-hole droplets**
**Keldysh (1968)
Pokrovsky
Rogachev (1969)**
- **Orto- and paraexcitons in C₂O ($\mu \leq 0$)**
**B.a la Guillaume
Mysirovicz
Wolfe (1980-93)**
- **Spin-aligned excitons in Ge ($[\mu]/kT=0.3$)**
**Kulakovskii
Kukushkin
Timofeev (1981)**

Outline

- **Introduction**
- **Schottky-diodes heterostructures with double and single QWs**
- **Electrostatic lateral traps for dipolar excitons and compensation of extra charges**
- **Bose-Einstein condensation of dipolar excitons in a lateral trap exhibited in bimodal luminescence spectra (observation in a far zone)**
- **Patterned photoluminescence structure in real space above condensation threshold**
- **Linear polarization of Bose-condensate photoluminescence and spontaneous symmetry breaking**
- **Long-range coherence of dipolar exciton Bose-condensate: correlator $g^{(1)}(\mathbf{r})$ and two-photon correlator $g^{(2)}(\tau)$**
- **Conclusions**

Double Quantum Well

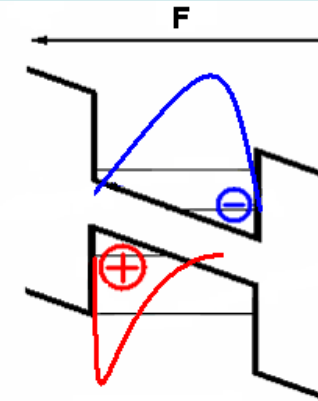


Lozovik and Yudson (1976),
 Shevchenko (1976)
 Fukuzawa et al. (1990),
 Kash et al. (1992)
 Butov et al. (1994-2008),
 Snoke et al. (2002-2008))
 Rapaport et al. (2003-2008)

Spatial separation of electrons and holes

- spatially indirect **dipolar excitons** with large dipole momentum in the ground state
 - dipole-dipole repulsion
 - **no multiexciton complexes.**
- Reduced electron-hole overlap
 - increased radiative decay time
- opportunity **to accumulate** such excitons **and to cool** them.

Wide Single Quantum Well



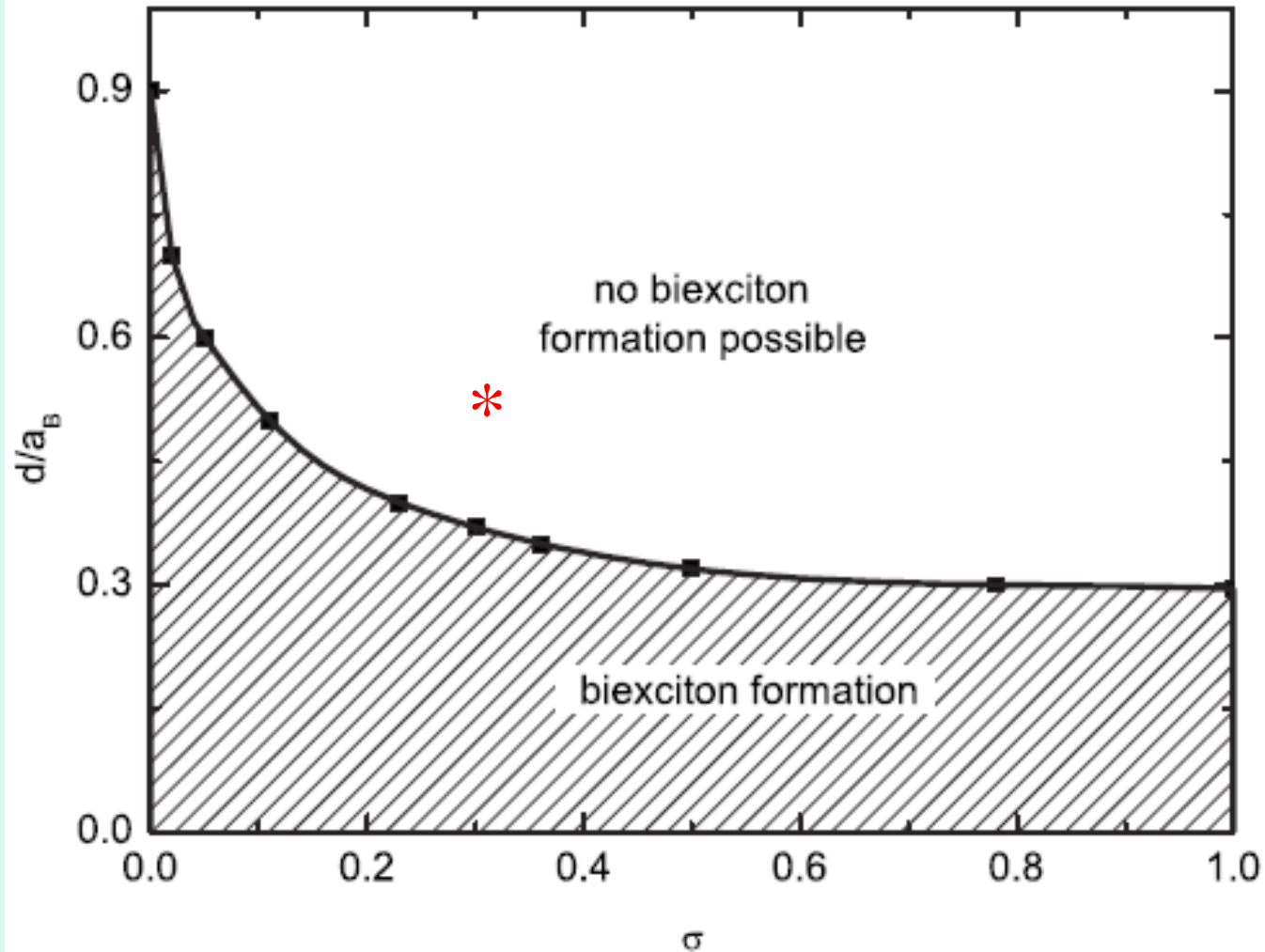
Solov'ev, Kukushkin et al (2006)
 Gorbunov, Timofeev (2006)

SQW GaAs/AlGaAs 250Å: no thin interwell barrier layer

- **structural perfection** is much higher
- the charge of the system under study can be controlled and the condition of **neutrality** can be fulfilled

BEC of 2D excitons can occur only under spatial restriction !

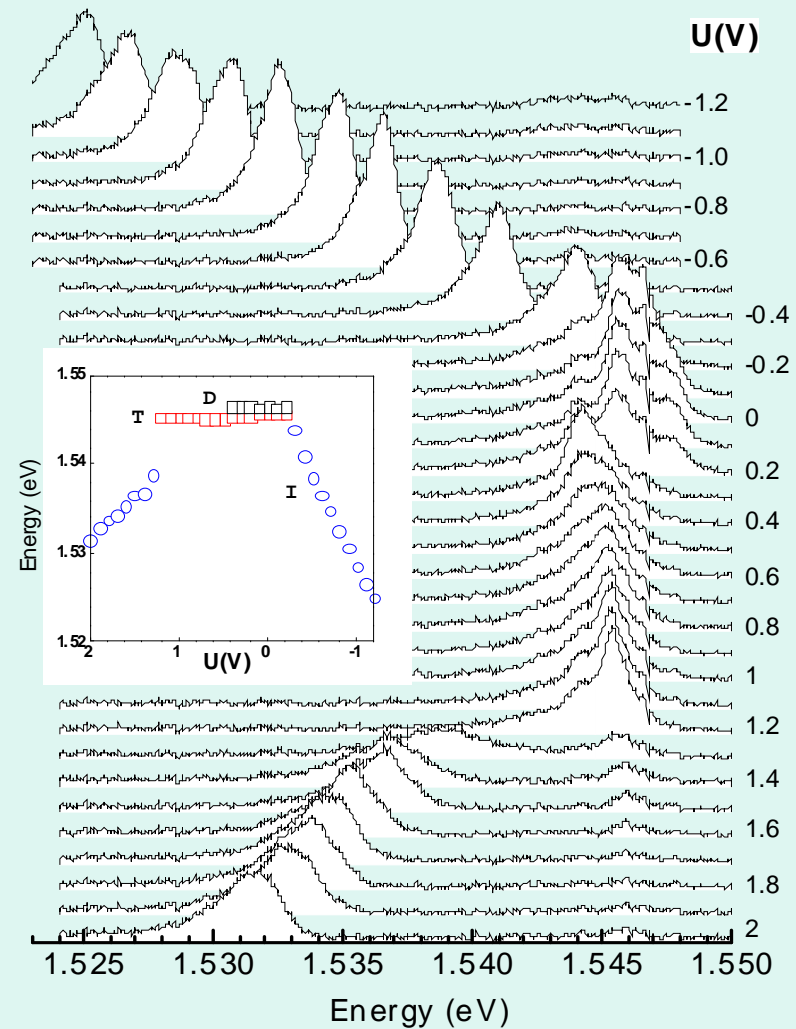
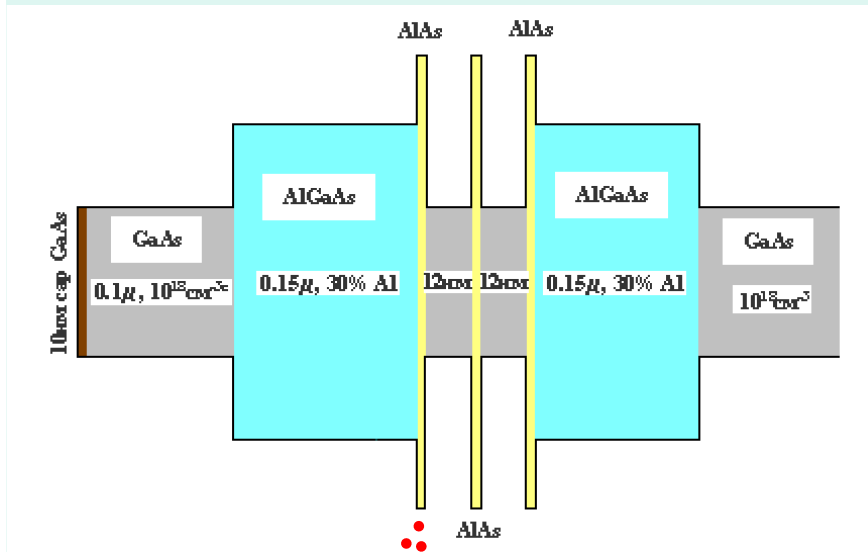
- a lateral potential trap is needed.



Critical charge separation in units of the bulk exciton Bohr radius \mathbf{a}_B plotted vs mass ratio $\sigma = m_e/m_h$ *Schindler and Zimmermann (PR B, 2008)*

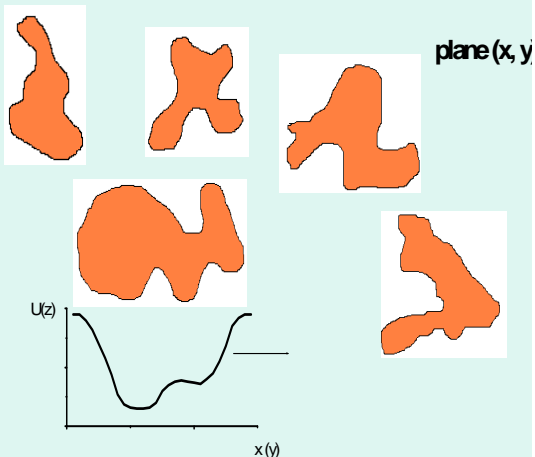
We investigate dipolar exciton systems where biexciton formation is impossible
($\sigma \equiv m_e/m_h = 0.32$ $d/a_B = 0.53$)

(n-i-n) - diod heterostructure with DQW



Ловушки, связанные с крупномасштабными флуктуациями случайного потенциала

The lateral random potential fluctuations



$$\mu(n(r)) + U(r) = \mu$$

$$|\mu(r)| < |\mu|$$

$$\mu(n) = -|E_{ex}| + |\delta U|$$

$$T_C = \frac{2\pi\hbar^2 N_{ex} / g}{m_{ex} k_B \ln(SN_{ex} / g)}$$

Непрозрачная маска с отверстиями микронных размеров на поверхности образца для отбора одиночных доменов в случайном распределении потенциала

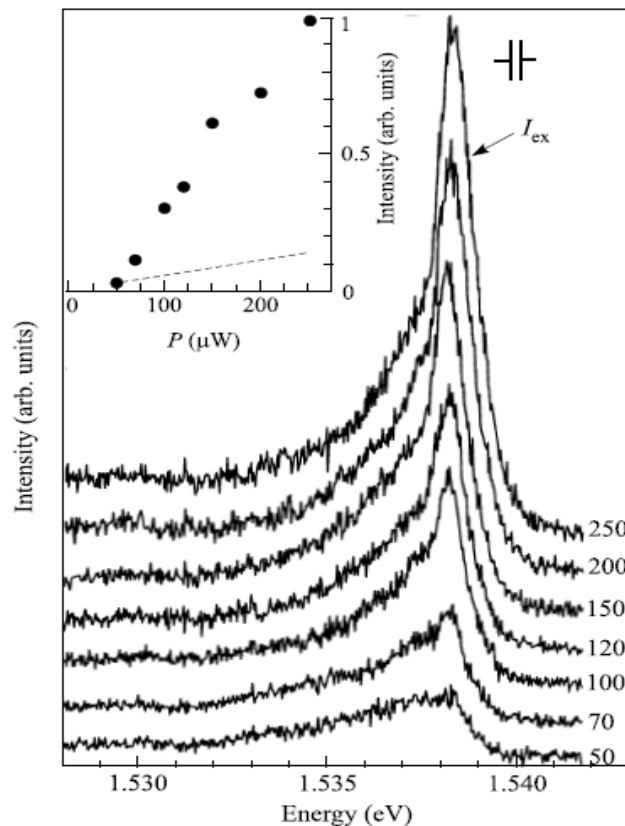


Рис.2. Спектры ФЛ межъямного экситона (линия I_{ex}) при различных мощностях резонансного возбуждения прямого 1sHH экситона, приложенном смещении $U = 0.3$ В и $T = 1.51$ К. Цифры справа от спектров соответствуют мощности возбуждения в мкВт. Вверху справа указано спектральное разрешение прибора. На вставке представлена зависимость интенсивности линии МЭ (точки) в функции мощности оптического возбуждения. Штриховая линия – экстраполяция линейной зависимости интенсивности фона под линией

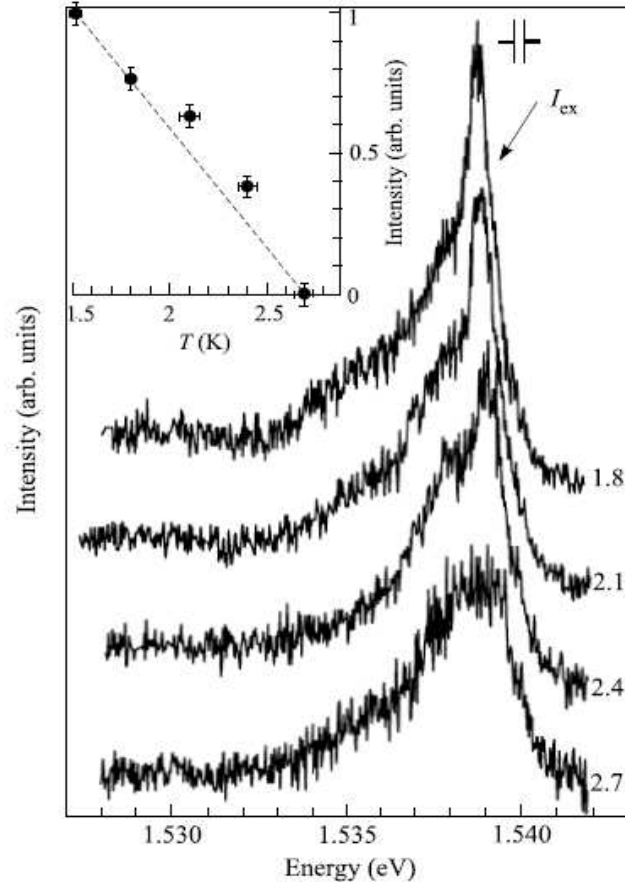
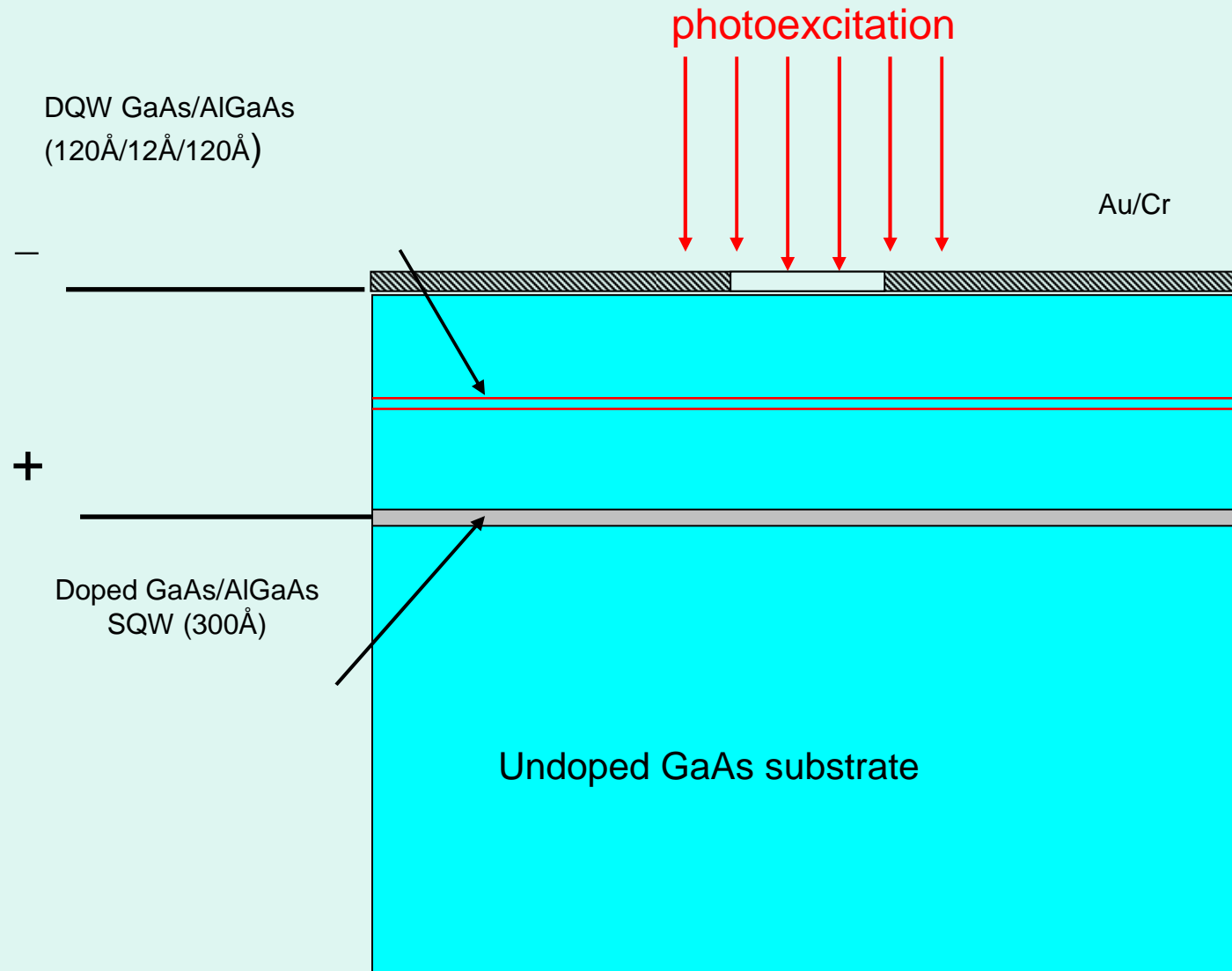
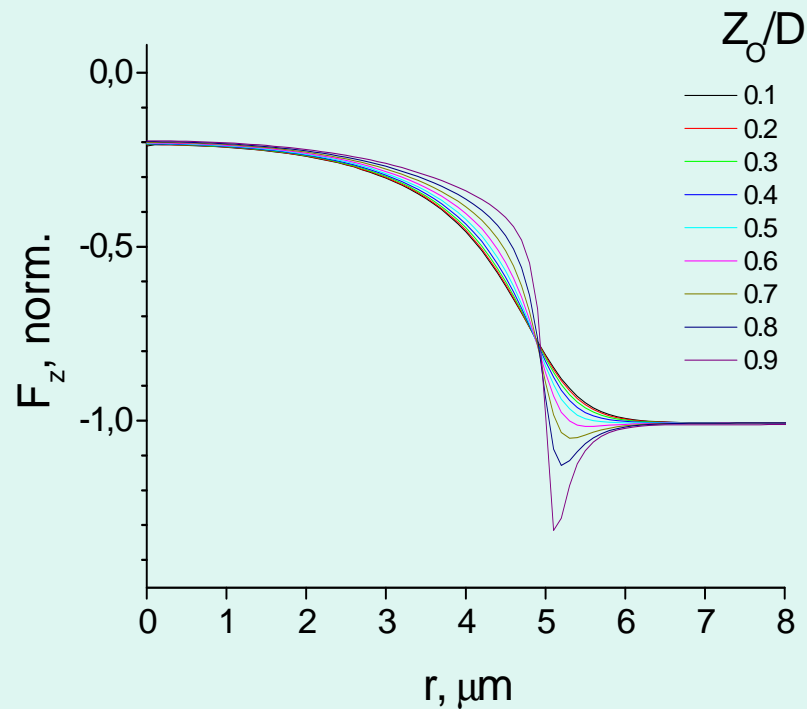


Рис.3. Температурная зависимость интенсивности линии фотолуминесценции МЭ при возбуждении $P = 150$ мкВт и приложенном электрическом смещении $U = 0.3$ В. Цифры справа соответствуют температуре в кельвинах. Точки на вставке показывают поведение интенсивности линии МЭ от температуры, штриховая кривая – экстраполяция зависимости $I_T \propto (1 - T/T_c)$

Circular lateral trap for dipolar excitons appears within perimeter of the circle window in Schottky gate (heterostructures with DQW or SQW).



Calculated radial profiles of the potential circular trap for dipolar excitons (potential trap along perimeter of a circle window in Schottky gate)



N.A.Gippius (2006)

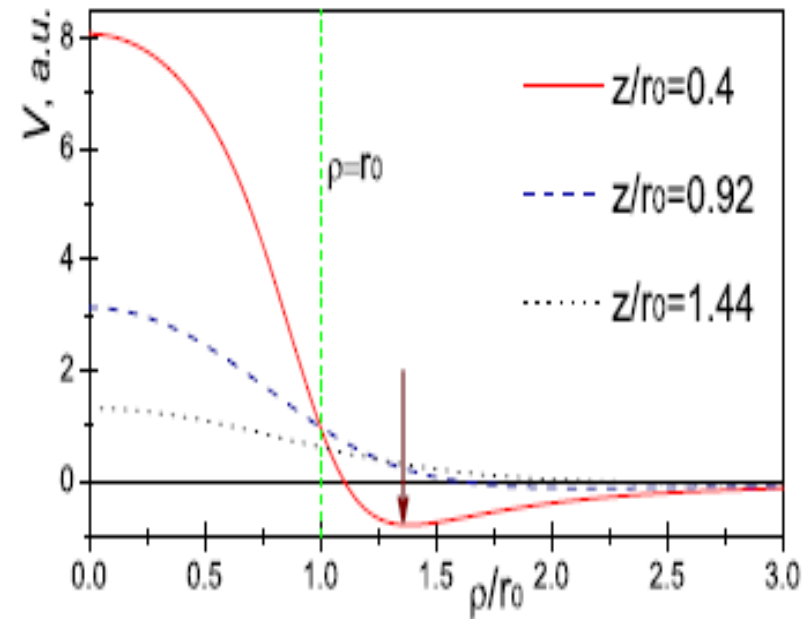
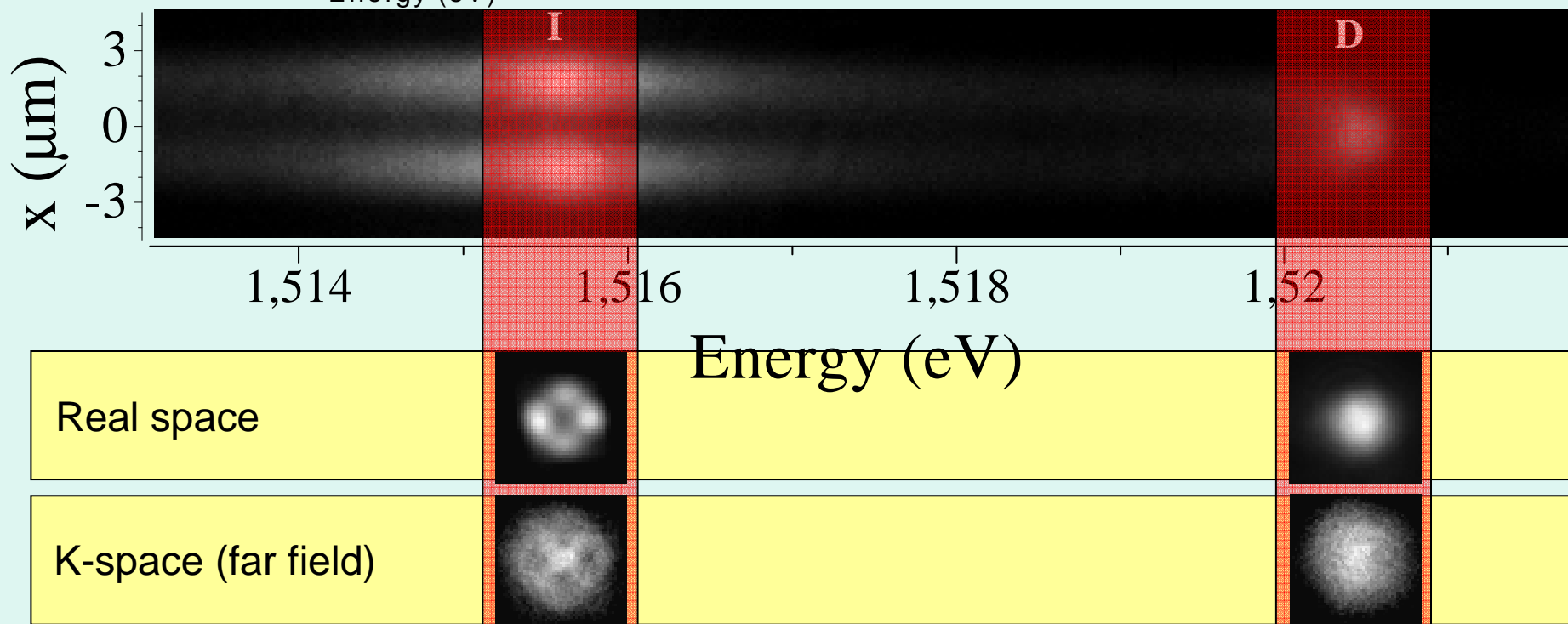
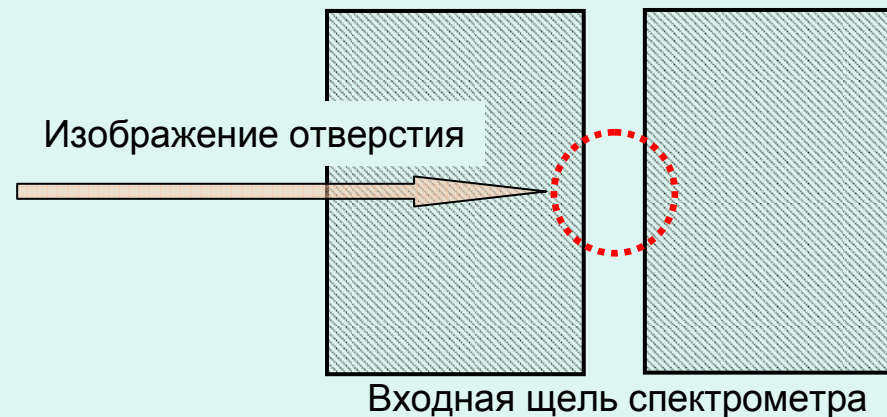
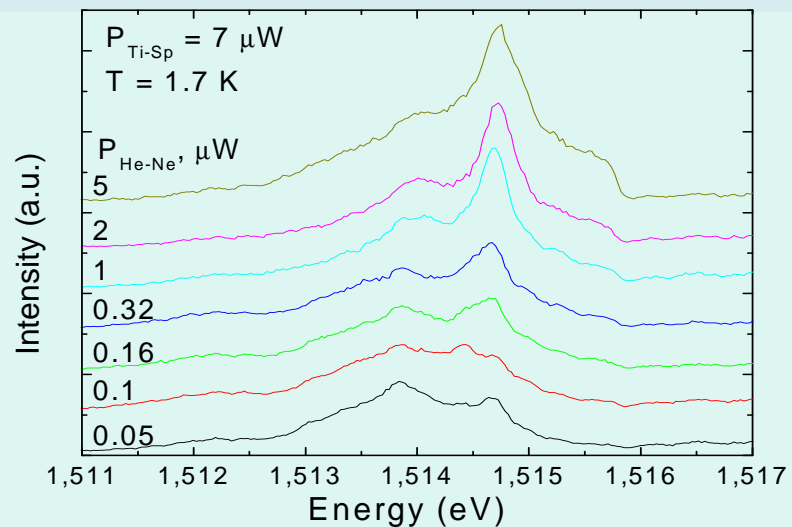


Fig. 2. A radial profile of the exciton potential energy V in nonuniform electric field as a function of the ratio ρ/r_0 at different values of the parameter z/r_0 . The pulling force $\lambda = 90$ is for all curves

V.I.Sugakov, A.A.Chernyuk JETP Lett. (2007)

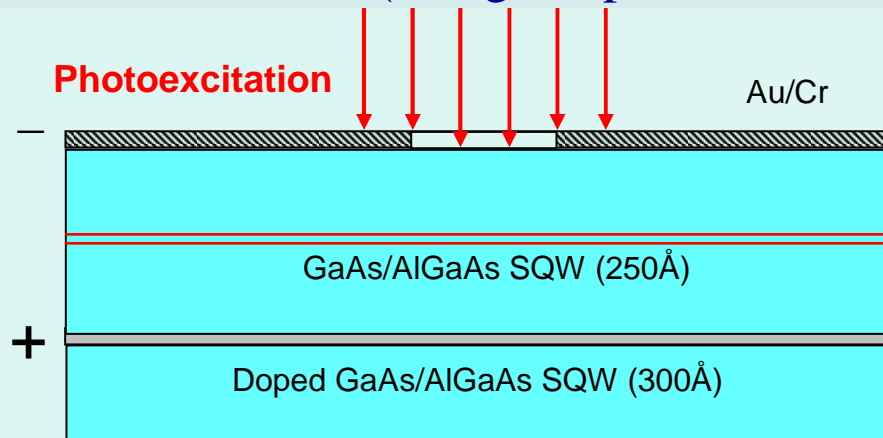
L.A.Maksimov (2006)

Спектр люминесценции внутри отверстия $\varnothing 5 \mu\text{m}$ с пространственным разрешением вдоль щели: одиночная GaAs/AlGaAs квантовая яма 250\AA



Ring-shaped lateral trap for indirect excitons in Schottky-diod

(along the perimeter of a window in top Schottky gate)

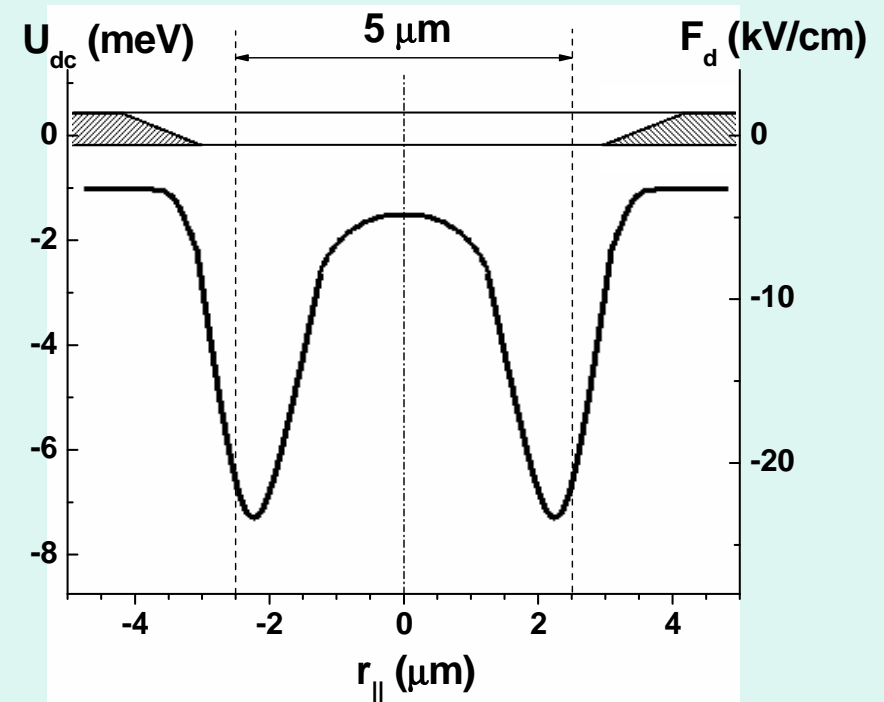
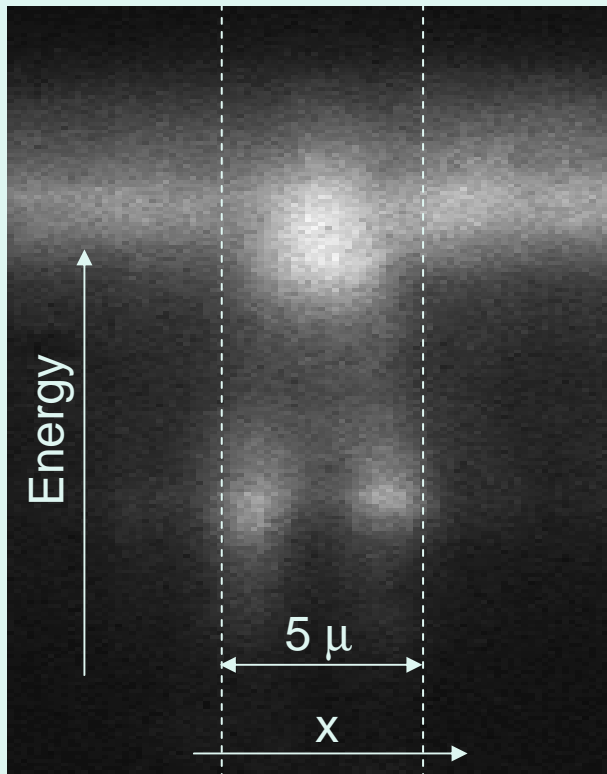


The potential profile of the trap can be described near bottom as:

$$V(r) = \alpha r_{\parallel}^2,$$

with force constant $\alpha \approx 2.2 \text{ meV}/\mu\text{m}^2$.

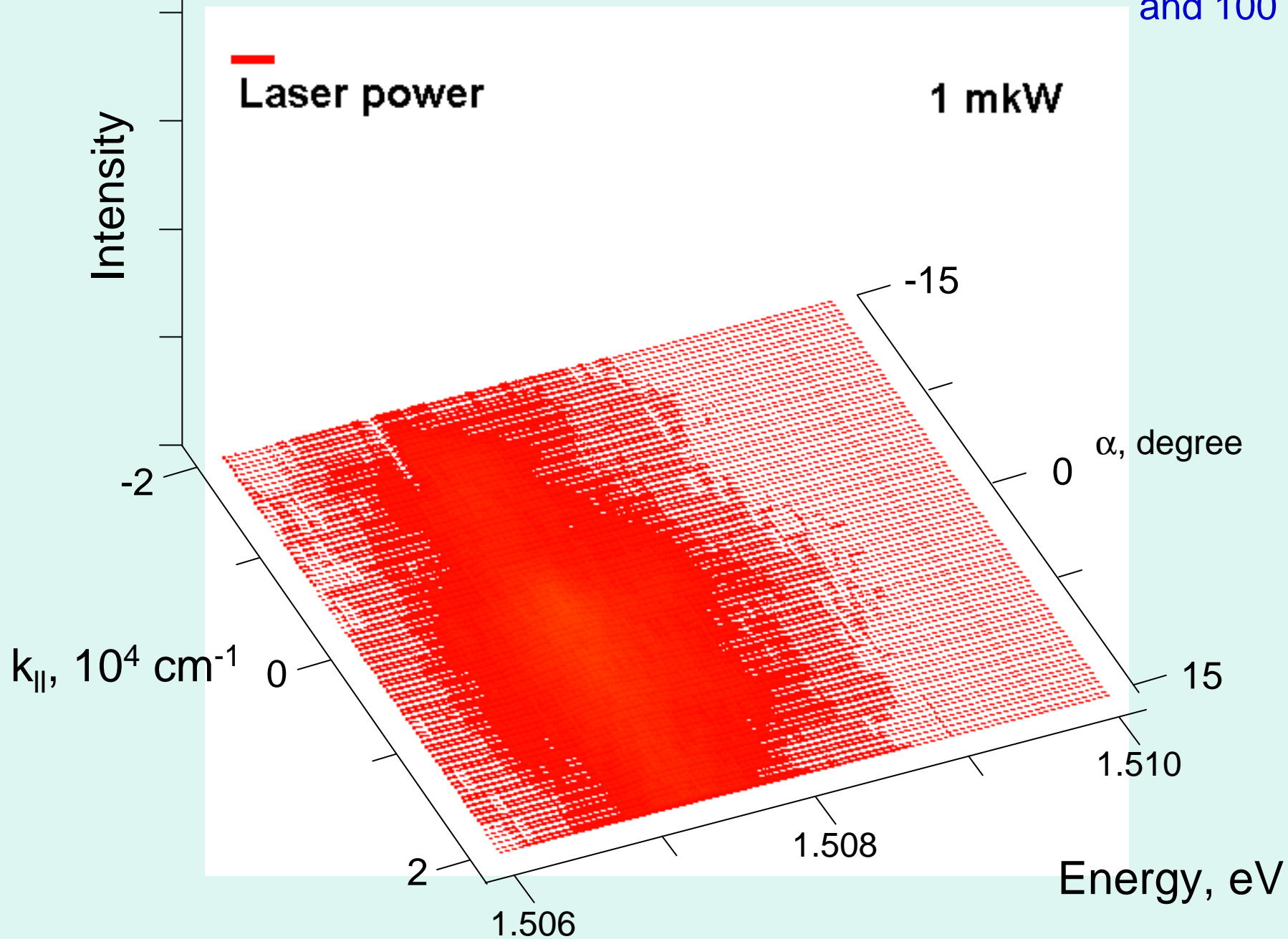
Barrier height $\Delta V \approx 5 \text{ meV} \gg kT$.



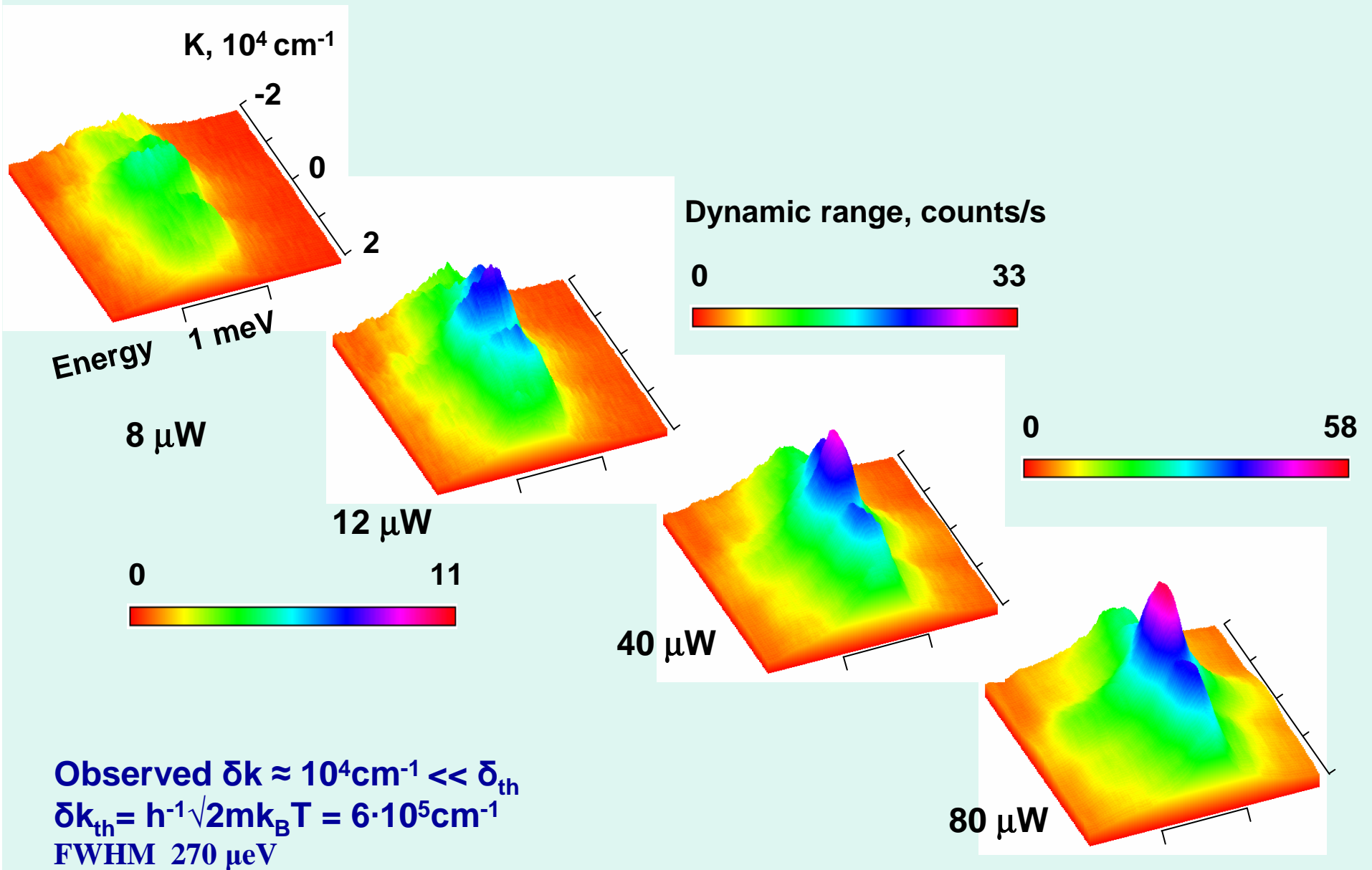
$\langle d_{\text{ex}} \rangle = 115 \text{ \AA}$ (F=20 kV/cm)

Far field bimodal evolution of PL spectra

1 – 20 μW
and 100 μW

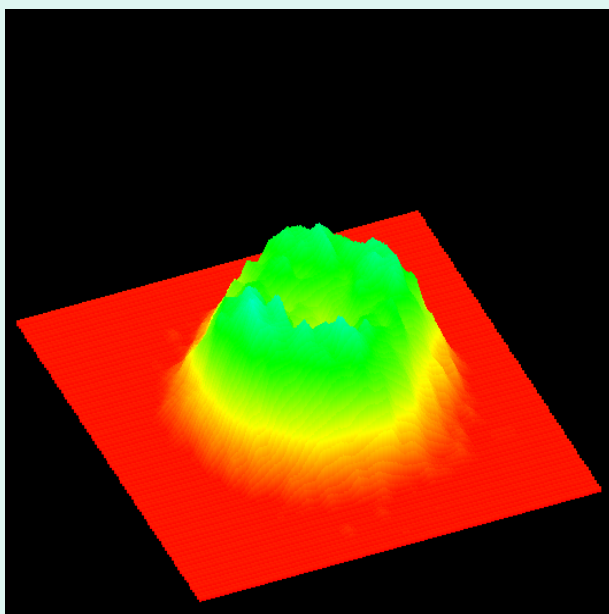


Far field bimodal evolution of PL spectra

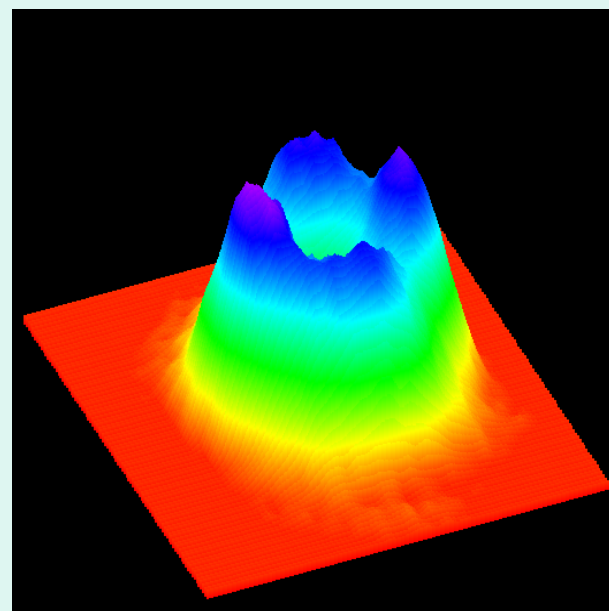


PL 3D pseudo images of BEC luminescence from 5 μm circular trap

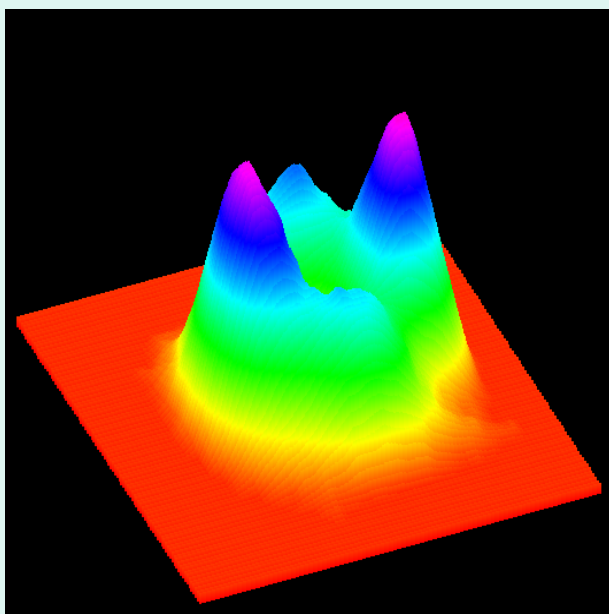
0.1 μWt



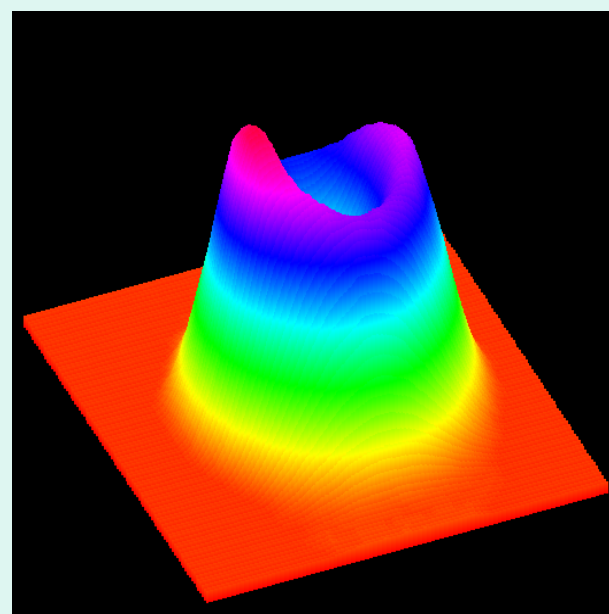
2.5 μWt



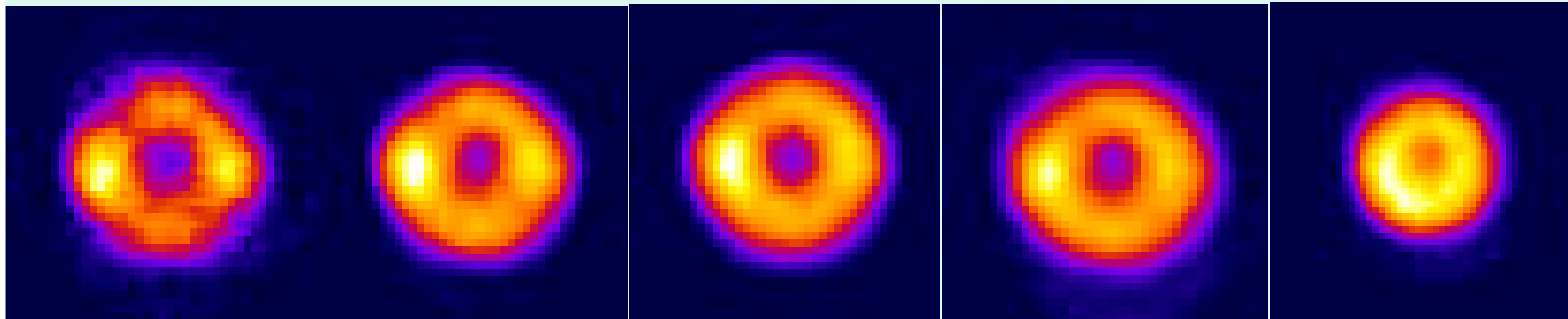
5 μWt



250 μWt



Temperature behavior of the luminescence
spatial structure from $5\ \mu\text{m}$ window $P = 20\ \mu\text{Wt}$
(in plane pseudo images)



4.6K

5.15K

6.0K

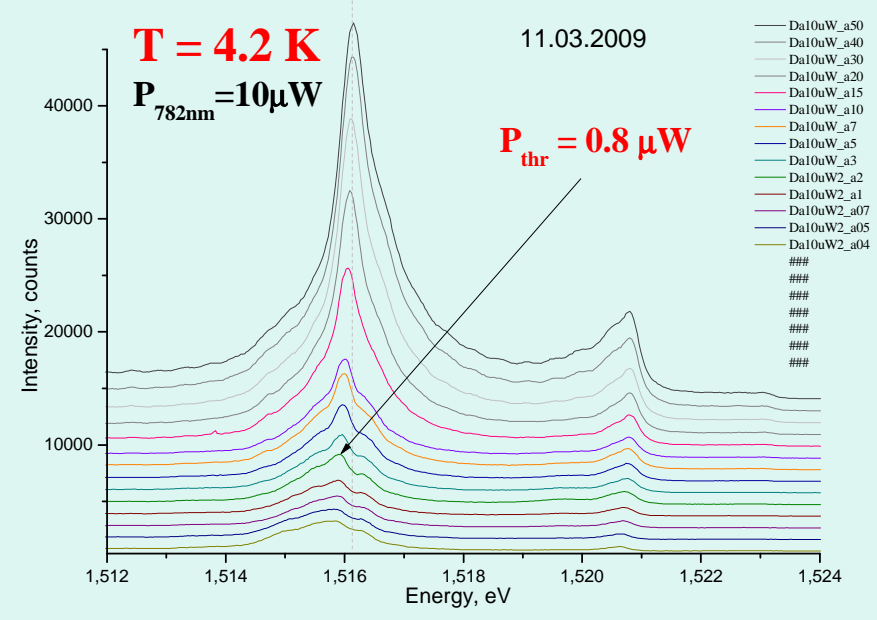
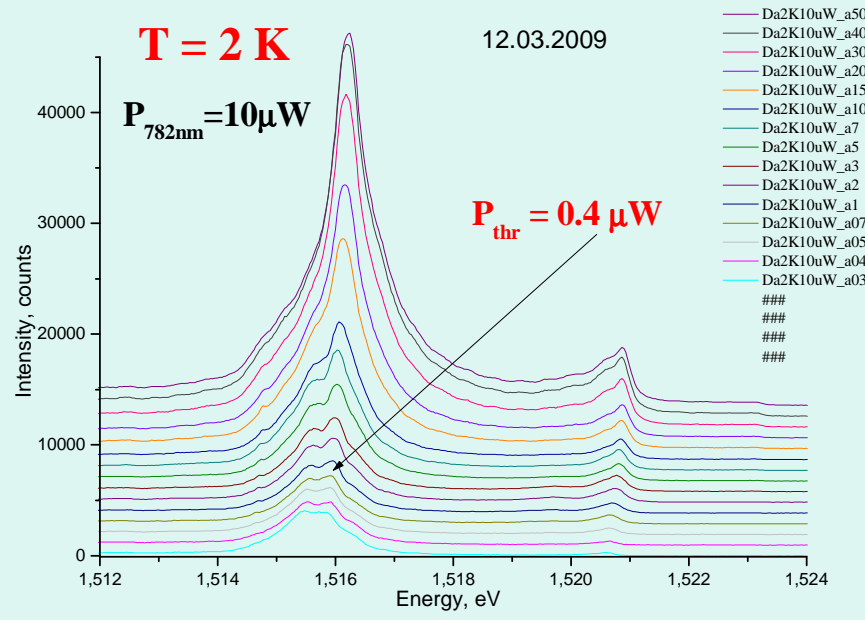
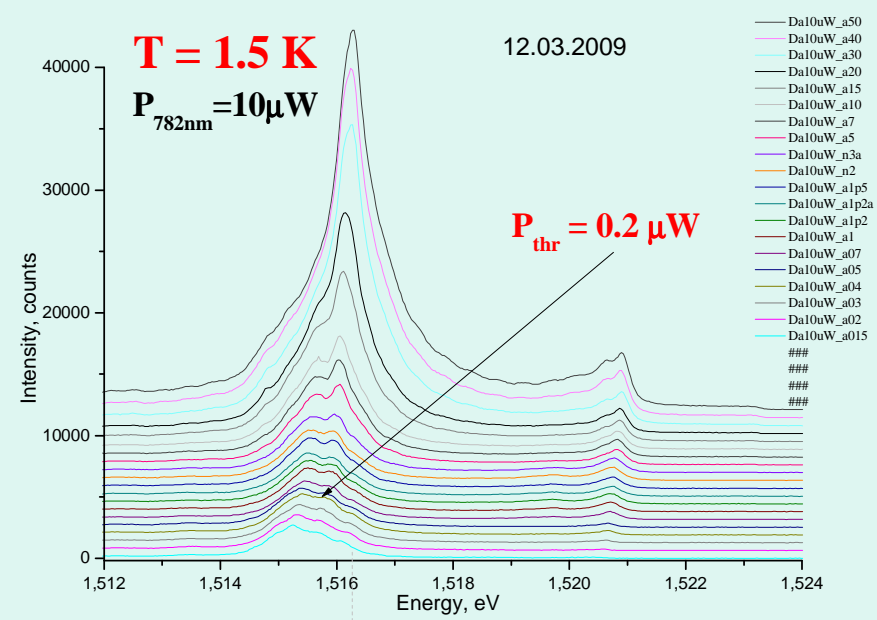
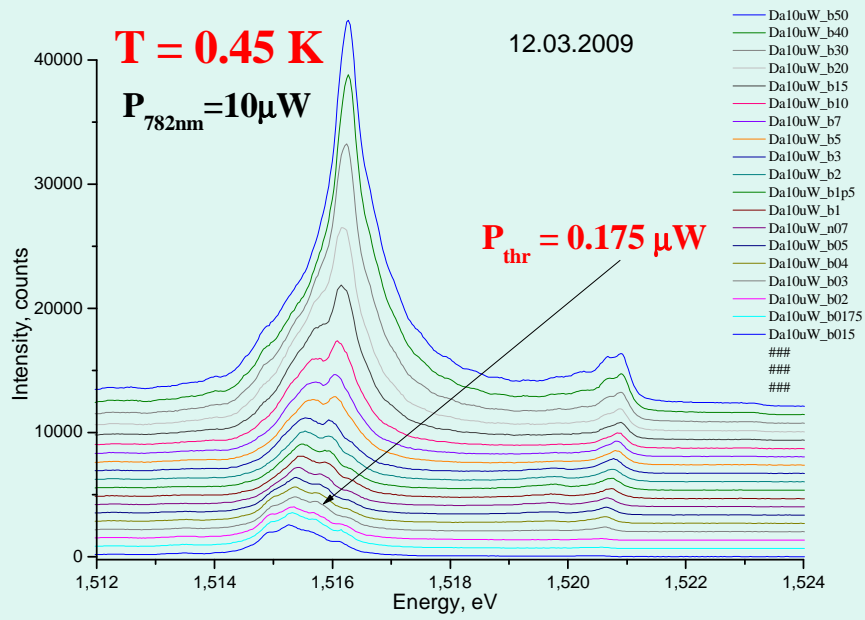
7.2K

10K

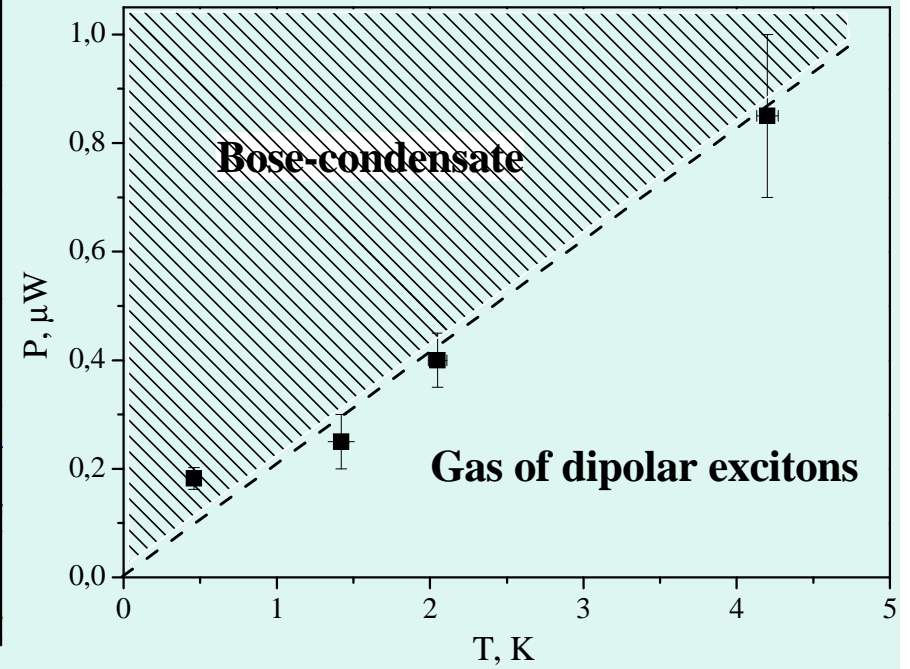
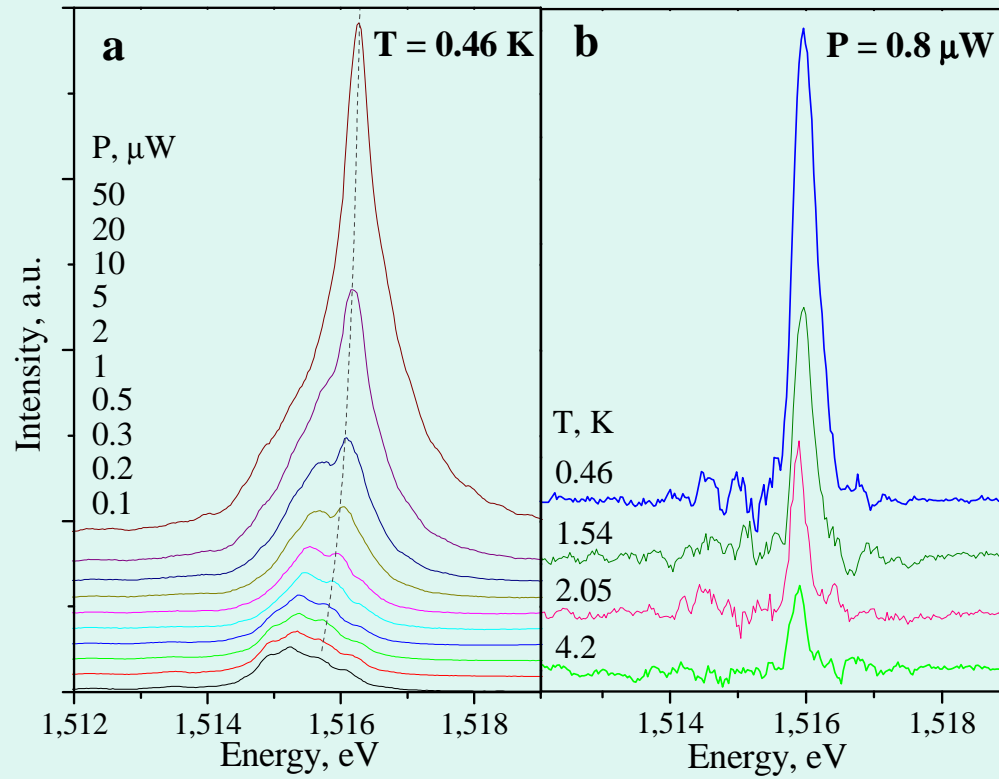


Институт Физики Твёрдого Тела РАН
Institute of Solid State Physics RAS

Threshold of BEC of Dipolar Excitons at Different Temperature

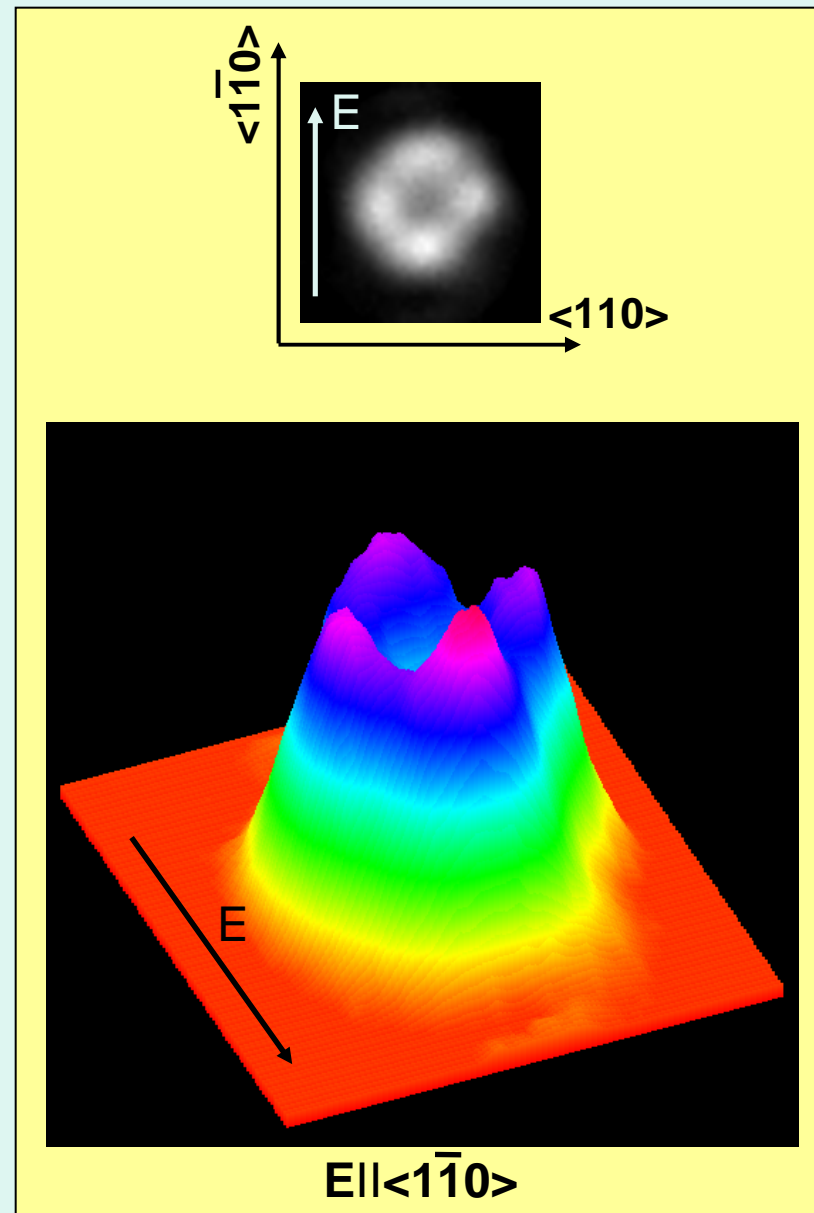
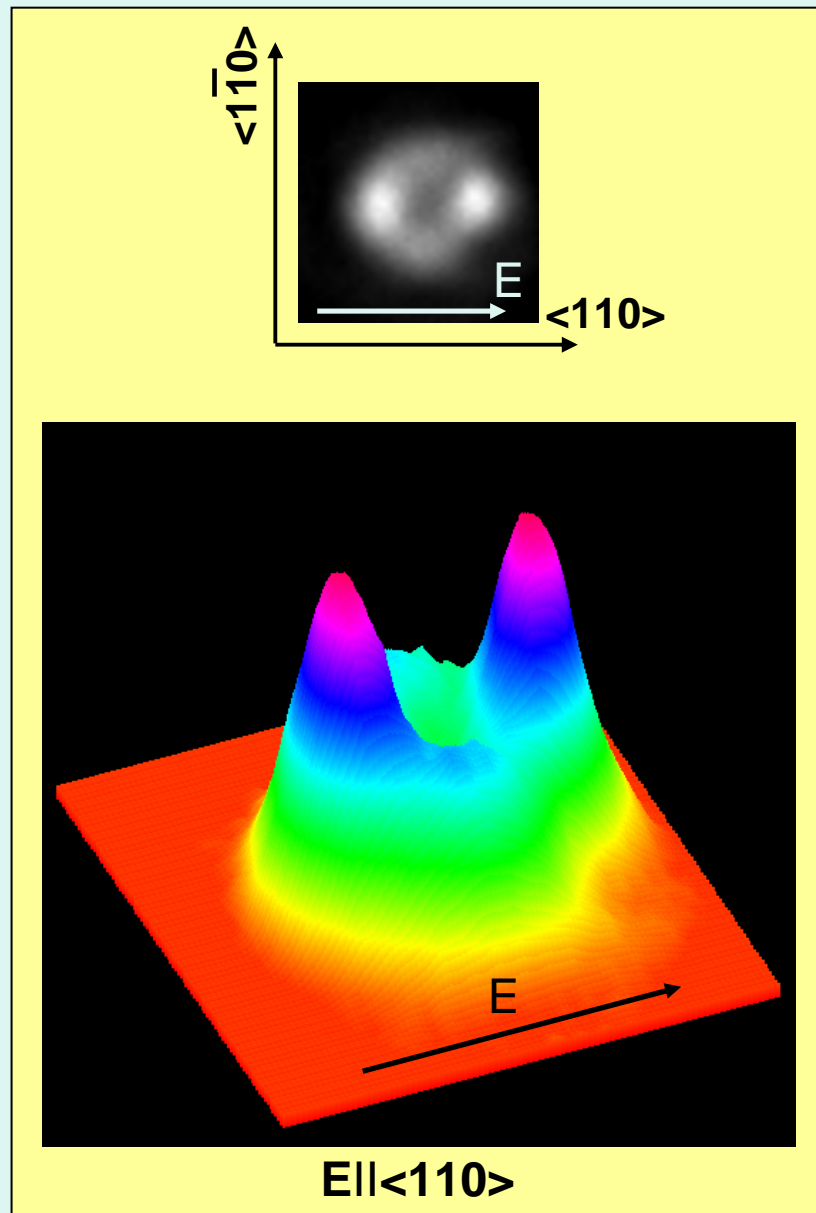


The Phase Diagram of BEC of Dipolar Excitons

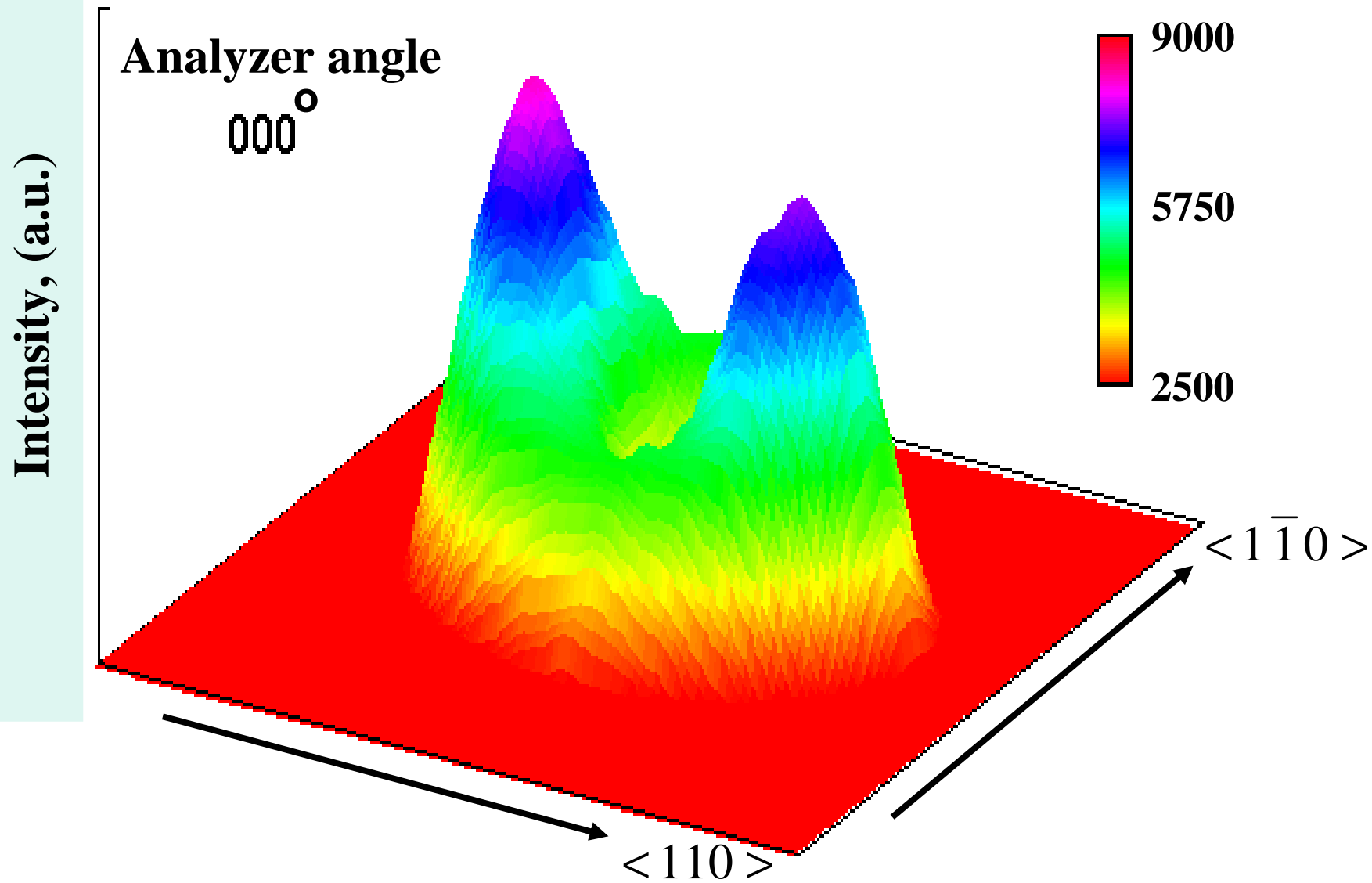


$$I_T \sim (1 - T/T_C)$$

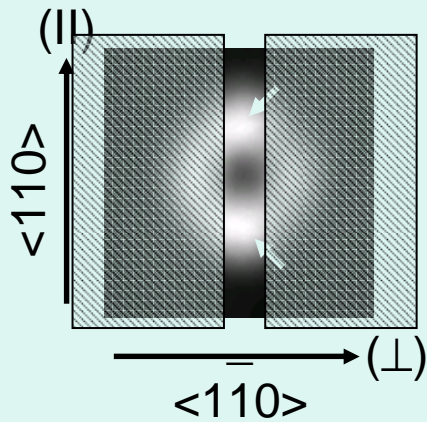
Linear polarization of luminescence at the Bose condensation of dipolar excitons: spatial distribution



Linear polarization of luminescence at the Bose condensation of dipolar excitons: angular dependence

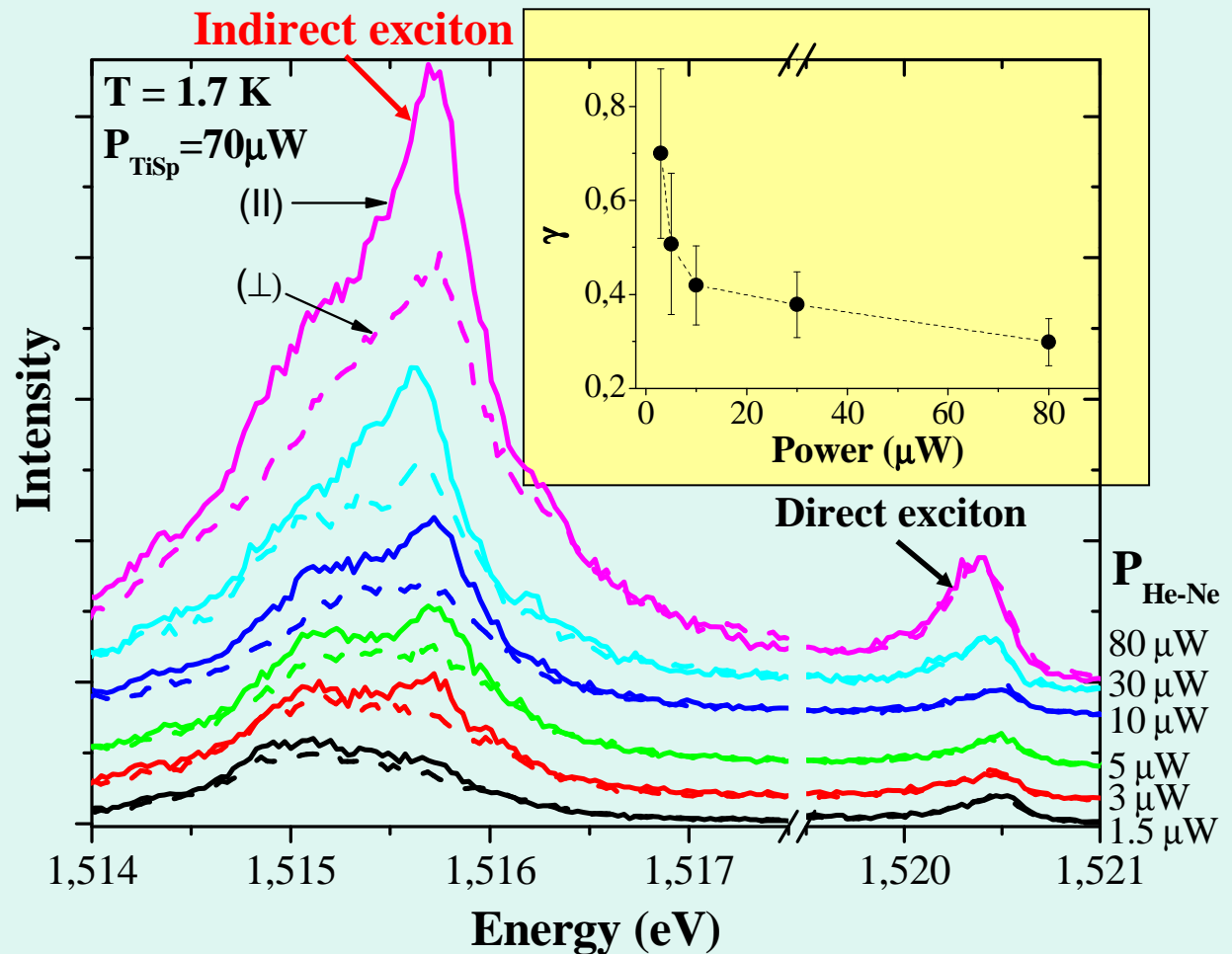


Linear polarization of luminescence at the Bose condensation of dipolar excitons: spectral measurements



Strongly polarized narrow line of indirect exciton ($\Delta E_{FWHM} \approx 300 \mu\text{eV}$) appears with pumping at the blue edge of unpolarized background.

Direct exciton line remains unpolarized.



Polarization degree γ is maximal ($\sim 70\%$) at the condensation threshold. It diminishes gradually with stronger pumping due to the heating-induced condensate depletion.

Anisotropic e-h exchange as a reason of linear polarization

The heavy hole dipolar exciton is fourfold degenerate:

$$\mathbf{m} = \mathbf{S}_{e,Z} + \mathbf{J}_{h,Z} = \pm 1, \pm 2$$

$$\mathcal{H} = a_Z \mathbf{J}_{h,Z} \times \mathbf{S}_{e,Z} + \sum b_i \mathbf{J}_{h,i}^3 \times \mathbf{S}_{e,i}$$

The states with $m = \pm 1$ and $m = \pm 2$ are split by :

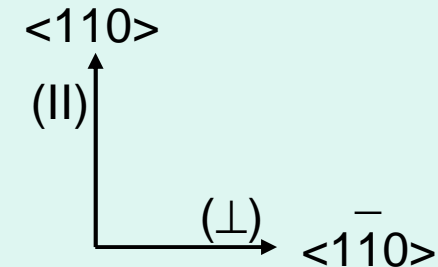
$$E_{\text{ex}} = 1.5 a_Z + 3.375 b_Z$$

An asymmetry of the confinement potential leads to the anisotropic e-h exchange ($b_x \neq b_y$). The spin states are linear combinations of the $m = \pm 1$ excitons:

$$|L_{1/2}\rangle = 1/\sqrt{2} (\alpha|+1\rangle \pm \beta|-1\rangle), \quad \alpha/\beta \approx 1$$

The mixing results finally in a linear polarization of dipolar exciton emission.

The directions of split components are related to the random potential fluctuations, i.e. to crystallography.

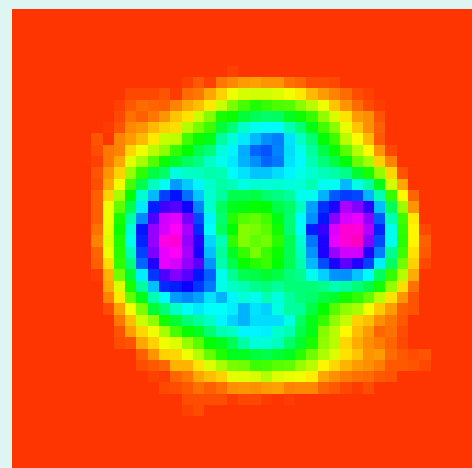


The energy splitting between two orthogonally polarized components is extremely small: $\Delta_{\text{exc}} \leq 50 \mu\text{eV} \ll k_B T$ → polarization should not be observed in normal situation. However, at Bose condensation the lowest split state is preferentially occupied → Linear polarization appears.

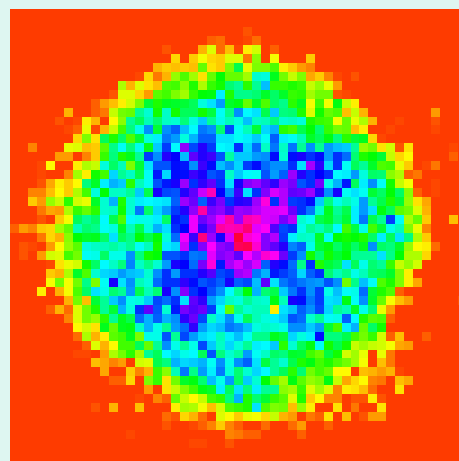
We suppose that the observed phenomenon is an additional evidence of Bose-Einstein condensation of dipolar excitons.

R-space

K-space

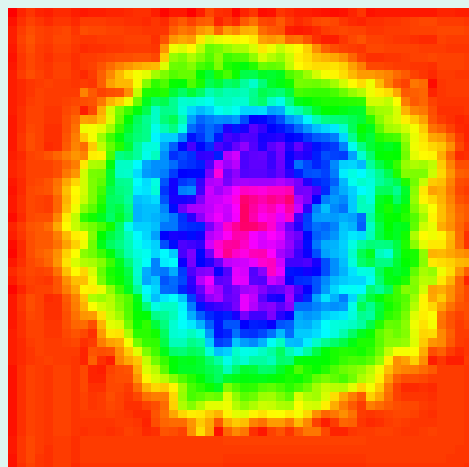


Angle [degree]
-15 0 15



-2 0 2

Wave Vector [10^4 cm^{-1}]



Fourier-transformations with evidence demonstrate the destructive interference. It means that

1. collective state of dipolar excitons is spatially coherent,

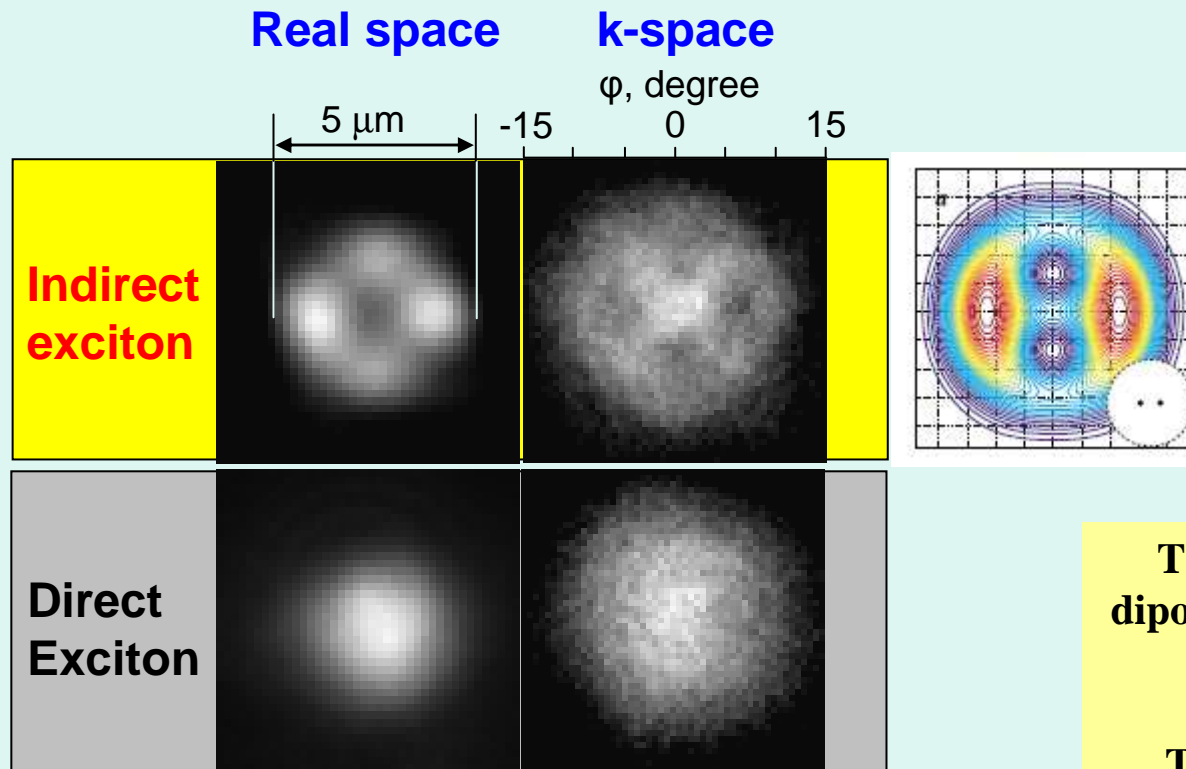
2. luminescence of condensate is directed in a cone with an opening angle around

$$\Delta\varphi \approx \lambda / D \cong 0.23 \text{ rad}$$

3. the whole pattern of equidistant spots is described by a common wave function



Patterning of dipolar exciton luminescence both in real and k-space: optical Fourier-transform



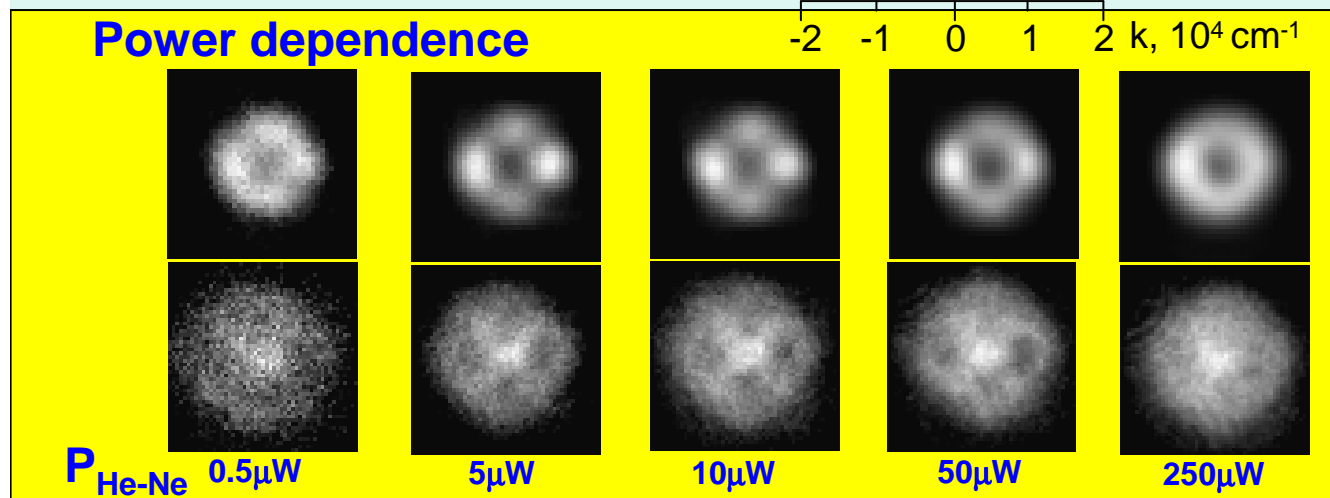
J.Keeling, L.S.Levitov,
P.B.Littlewood
Phys.Rev.Lett. 92,
176402 (2004)

This collective state of dipolar excitons is spatially coherent.

The luminescent ring pattern with equidistant bright spots is described by a common wave function.

BEC emission concentrates close to the normal within angular cone:

$$\Delta\varphi \approx \lambda/D \approx 0.16 \approx 9^\circ.$$



$P_{\text{He-Ne}}$ 0.5 μW

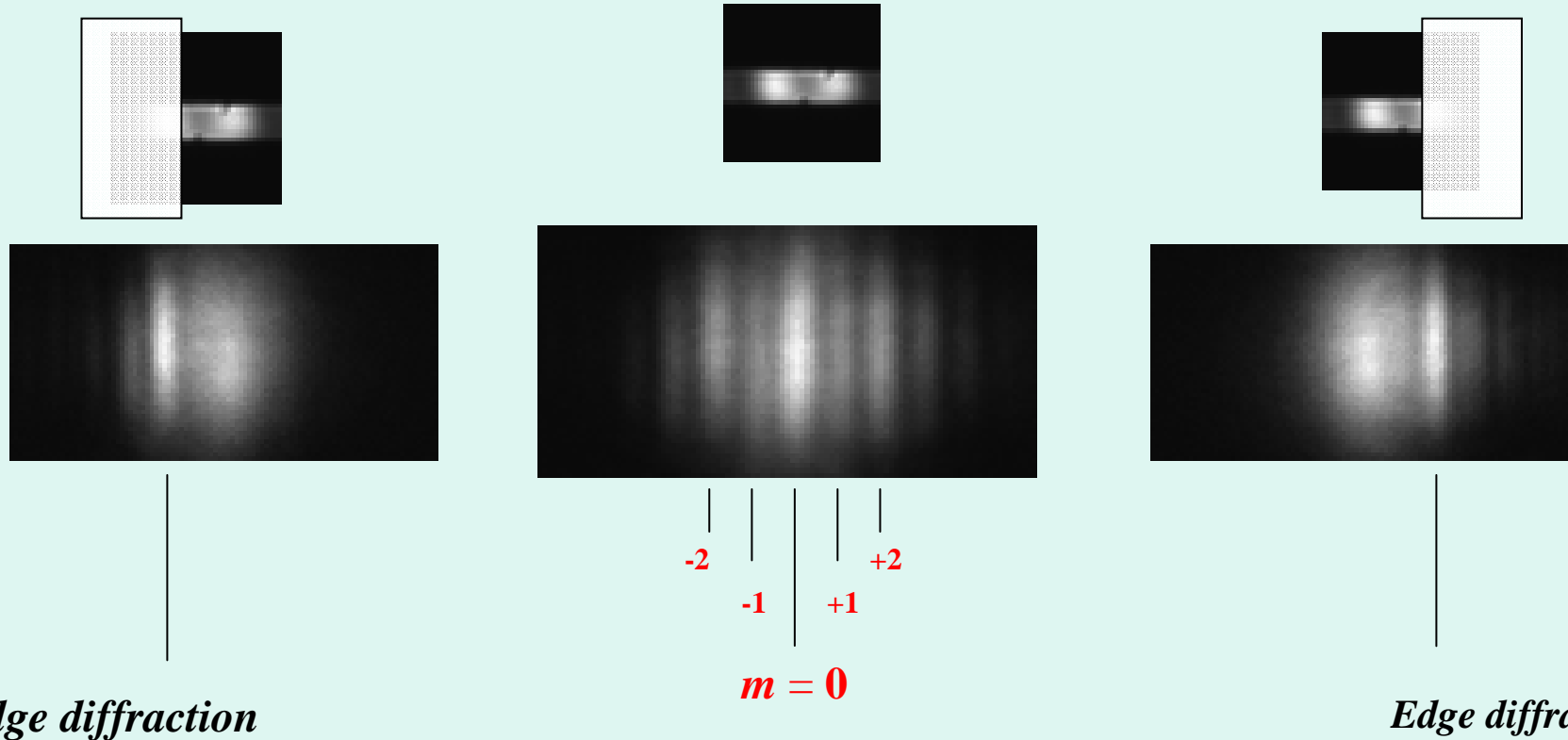
5 μW

10 μW

50 μW

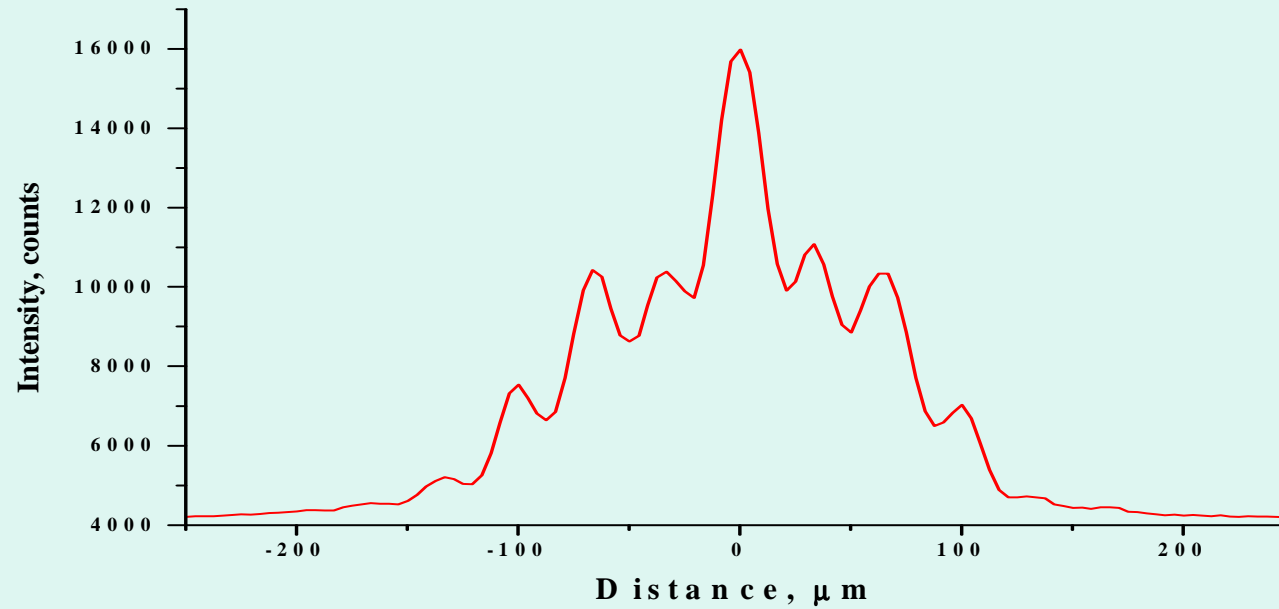
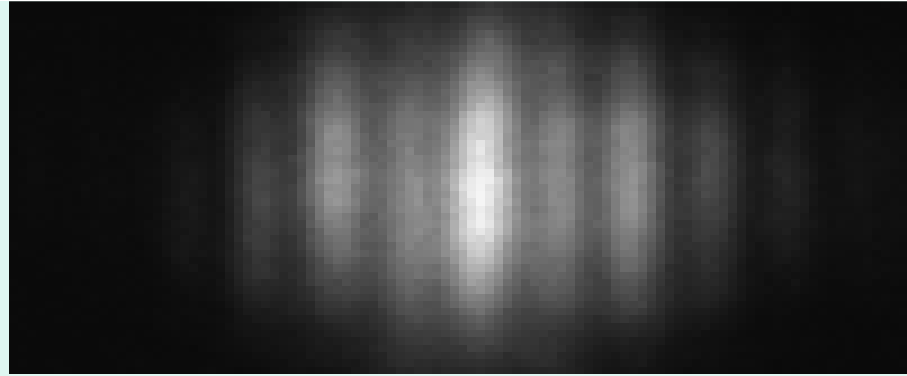
250 μW

Interference from two selected spots in the frame (analogue of Young experiment)



Interference of two coherent sources



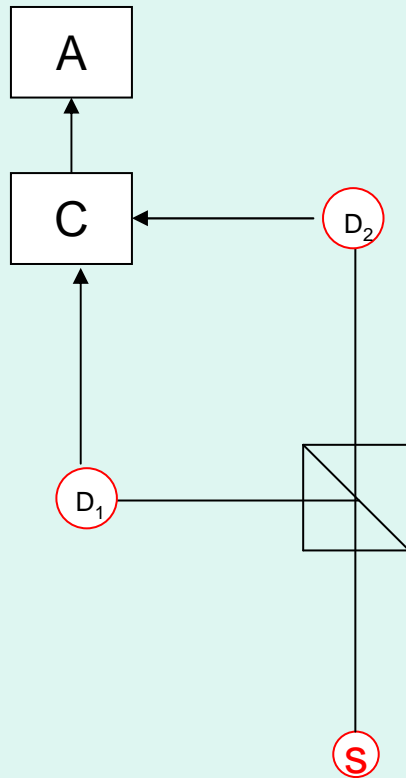


$$g^{(1)}(r, r') = \frac{\langle E^*(r)E(r') \rangle}{\langle E^*(r) \rangle \langle E(r') \rangle}$$



Hanbury Brown-Twiss – интерферометр

(Интерферометр интенсивностей)



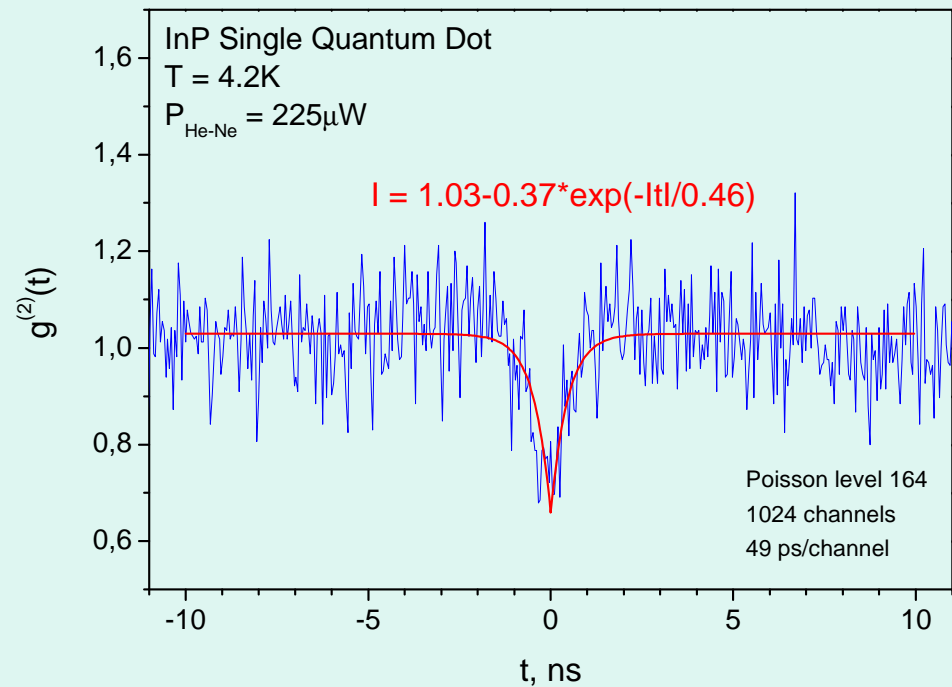
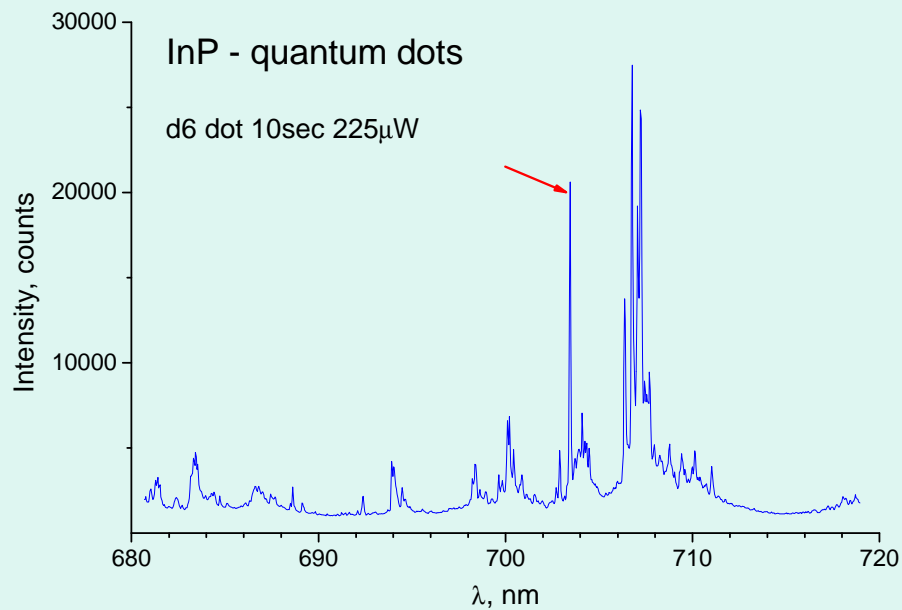
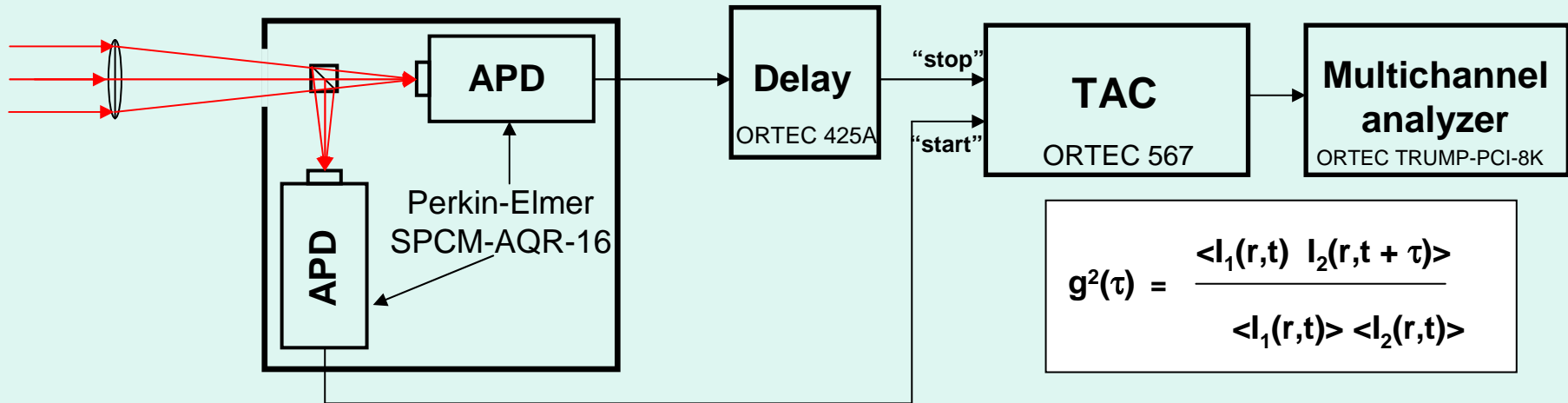
Такой интерферометр позволяет измерять коррелятор второго порядка (корреляции пар фотонов), $g^{(2)}(\tau)$ или $g^{(2)}(r)$

$$G^2(\tau) = \frac{\langle I_1(r,t) I_2(r,t + \tau) \rangle}{\langle I_1(r,t) \rangle \langle I_2(r,t) \rangle}$$

Корреляции между фотонами возникают только при некогерентном смешивании или суперпозиции когерентных состояний. Поэтому корреляционная функция для одномодового лазера в точности равна единице, ибо такой лазер, по сути, проистекает из единого квантового состояния. В таком же смысле коррелятор второго порядка для бозе-конденсата (конденсата бозе-атомов, экситонного бозе-конденсата и т.д.) также должен быть равен единице, (Glauber, 1963)

Корреляции между фотонами проявляются вблизи порога фазового перехода, где наиболее сильны флуктуации поля бозонов (например, вблизи порога лазерной генерации, или вблизи порога бозе-конденсации атомов-бозонов или экситонного бозе-газа и пр.)

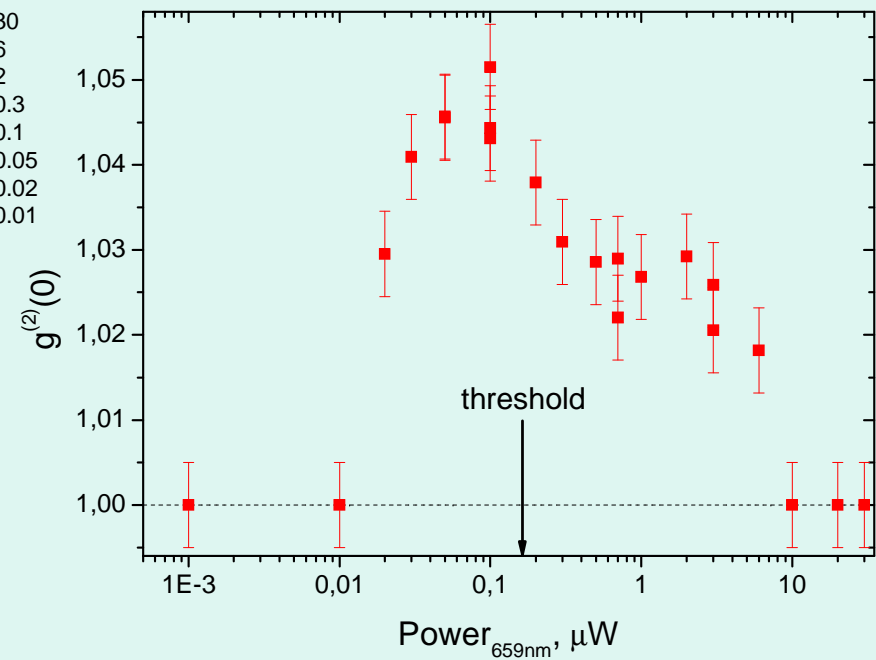
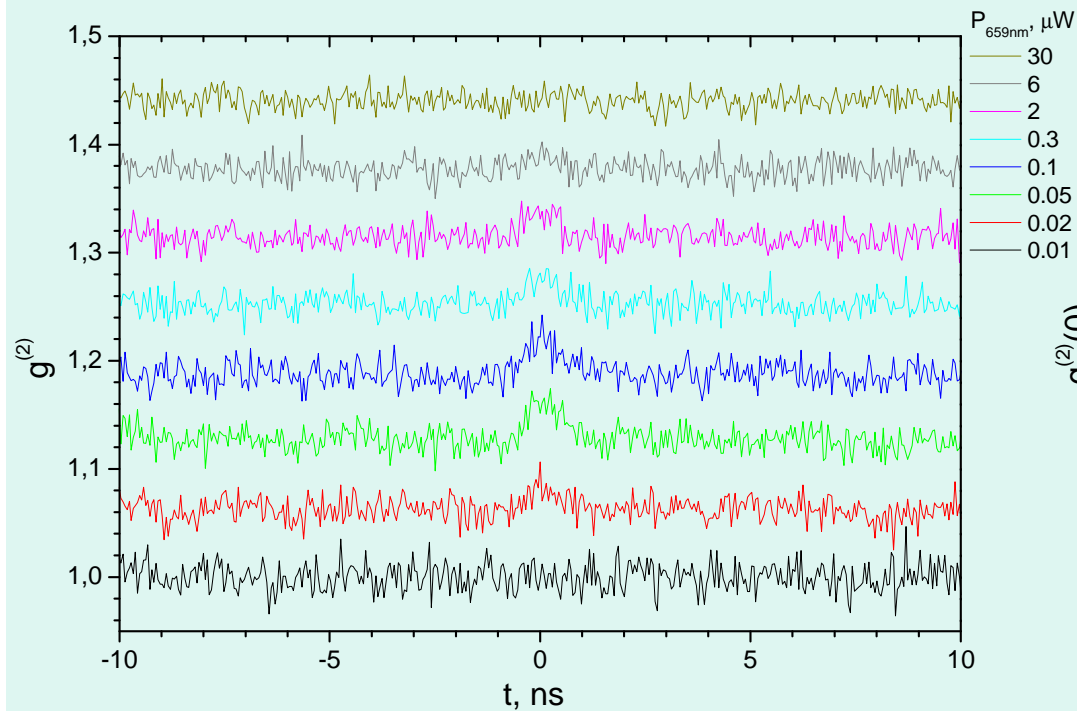
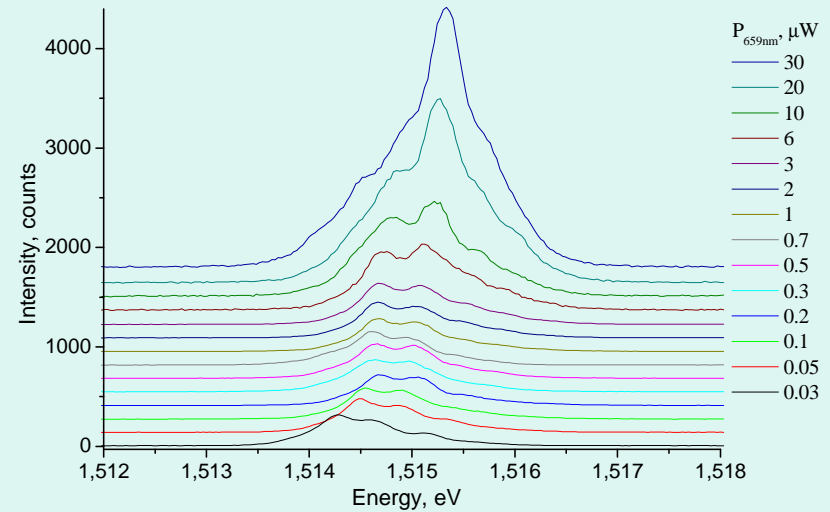
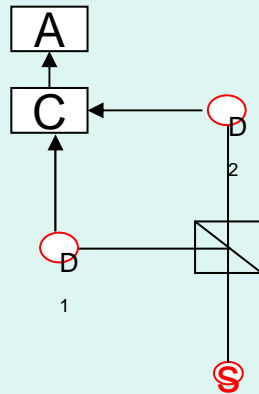
Hanbury Brown-Twiss – interferometer for two-photon correlation, $g^2(\tau)$, measurements



Two-photon correlator of the luminescence, $g^2(\tau)$, in the regime of BEC

$T = 0.45$ K

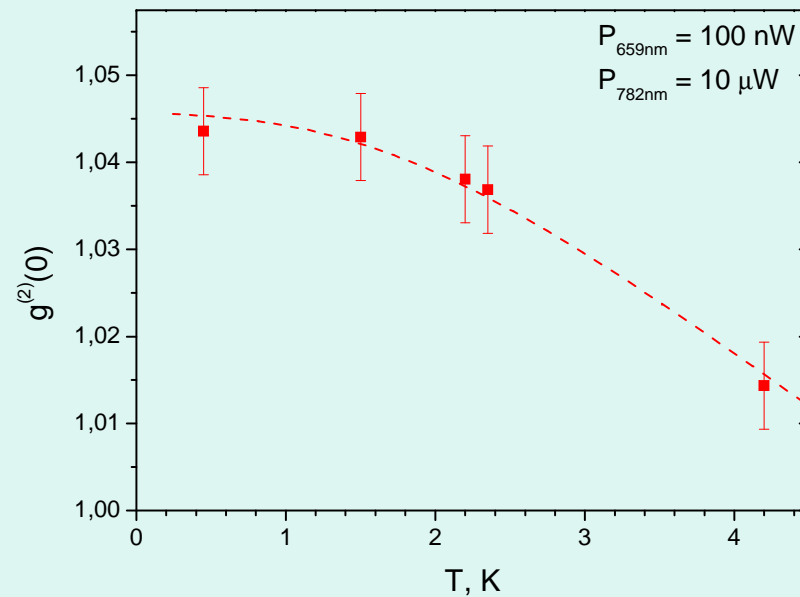
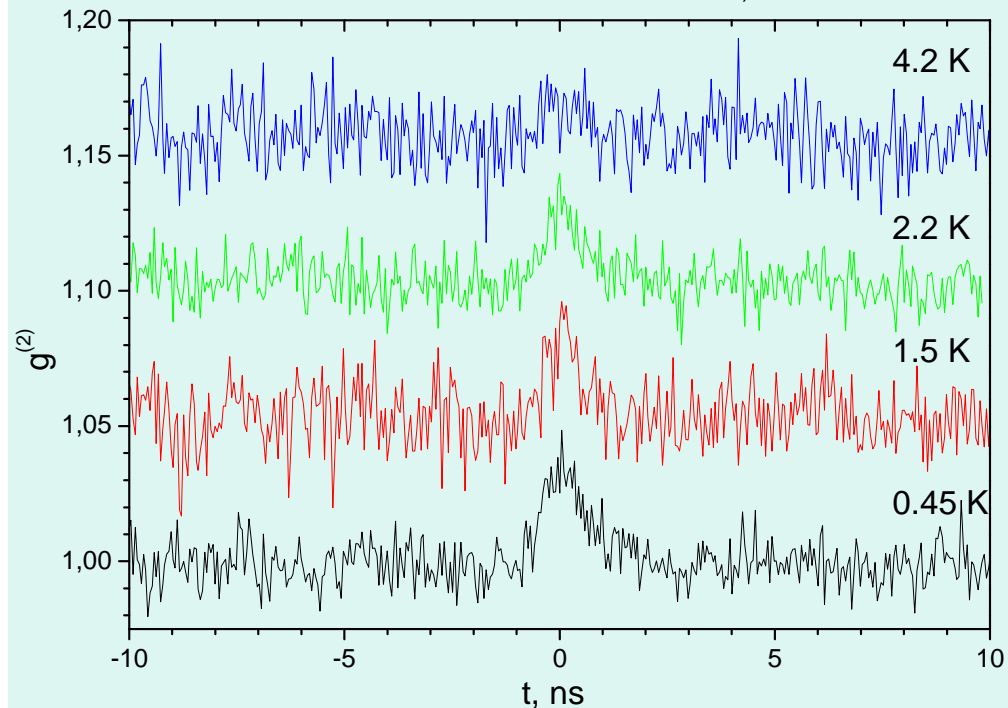
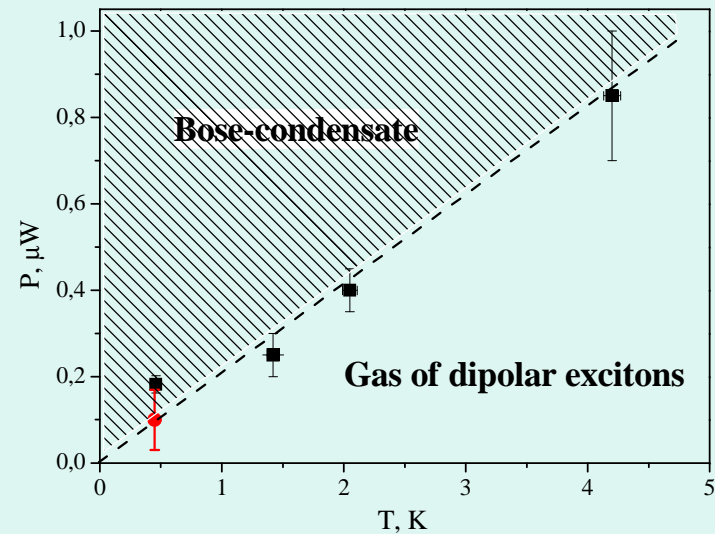
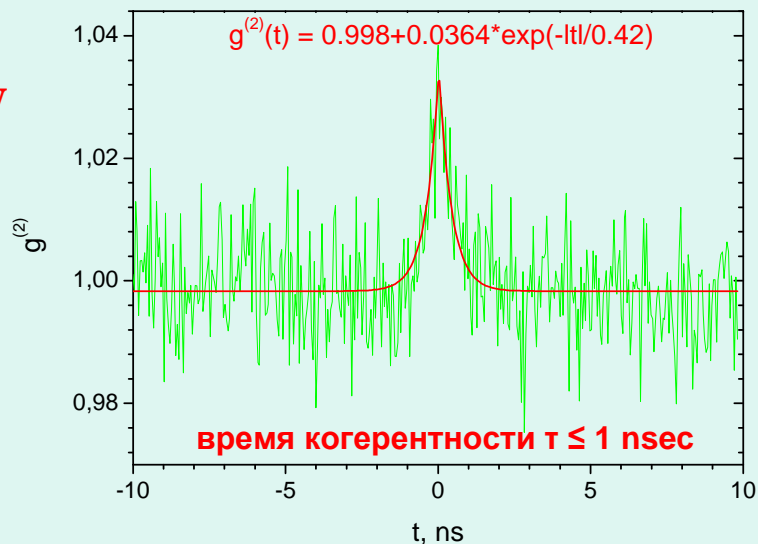
$P_{782\text{nm}} = 10$ mW



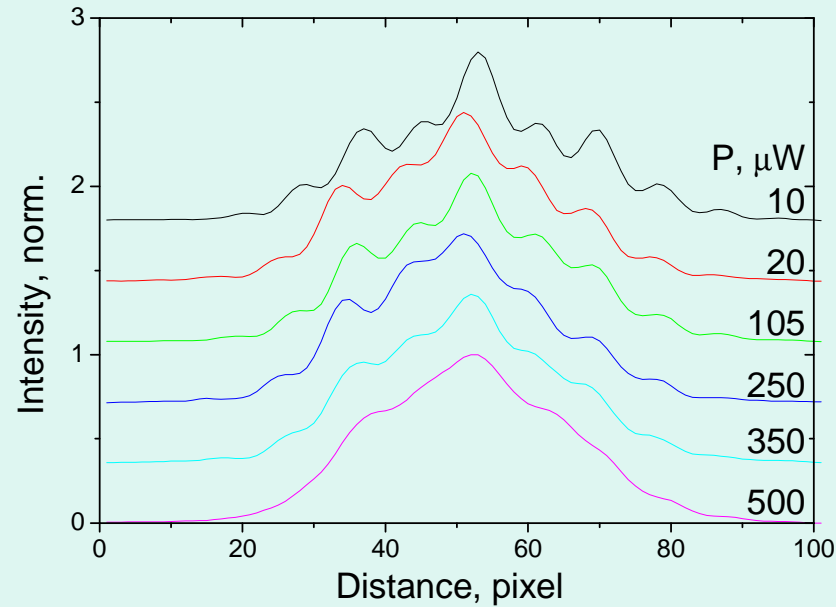
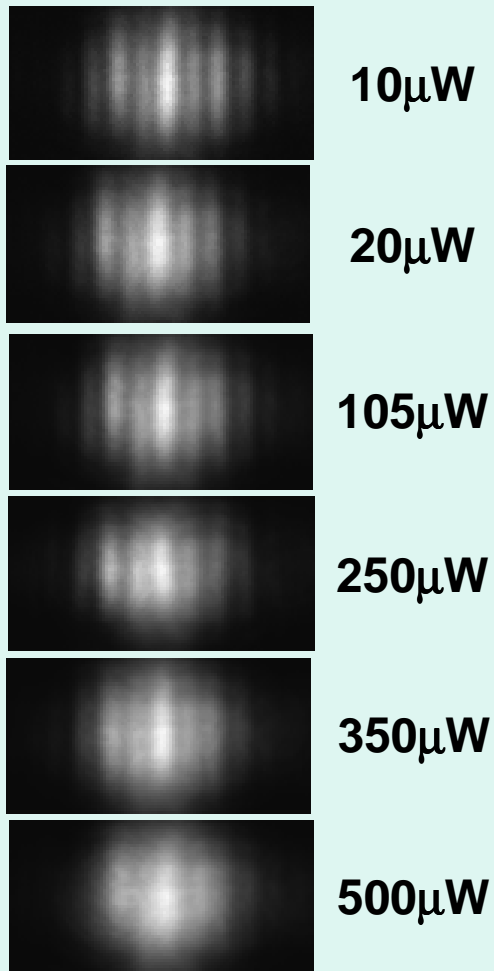
Two-photon correlator, $g^2(t)$, on the temperature variation

$P = 100 \text{ nW}$

$P_{782\text{nm}} = 10 \text{ mW}$
 $P_{659\text{nm}} = 100 \text{ nW}$



Two-beam interference from pair of spots in the frame
Excitation power behavior. $T = 1.7$ K.



Interference is seen in the region where BEC is observed:
 $g^{(1)}(r) = 0,2$.
Only in the region of high excitation, where excitons
are destroyed, $g^{(1)}(r) \rightarrow 0$.

Conclusion

condensation of laterally trapped Bose gas of interacting dipolar excitons is manifested by

1. exciton accumulation at $K \approx 0$: appearance of a sharp line of condensed part of excitons, power low decrease of line intensity on temperature growth ;
2. a sequence of temporal coherence of exciton condensate : increasing of radiative decay rate and decreasing of spin relaxation rate of excitons in condensate ;
3. patterned structure of equidistant luminescence spots of exciton condensate in a ring lateral trap in real and K -space is the signature of quantum bosonic state;
4. found collective state is coherent (the large-scale spatial coherence is equal to the perimeter of a ring trap), we assume that this state is described by a common wave function;
5. macroscopically coherent Bose-condensate of dipolar exciton appears *spontaneously* in the reservoir of interacting excitons;
6. observed linear polarization of PL patterned structure is an exhibition of *spontaneous symmetry breaking*
7. spatial long-range coherence appears with a time delay with respect to excitation pulse; time delay is determined by the effect of thermalization of photoexcited e-h system

Acknowledgements

we are grateful to acknowledge very fruitful collaboration in the course of this work with

A.V.Gorbunov, A.V.Larionov, A.A.Dremin, S.V.Dubonos, J.M.Hvam, C.Soerensen, W.Ditsche

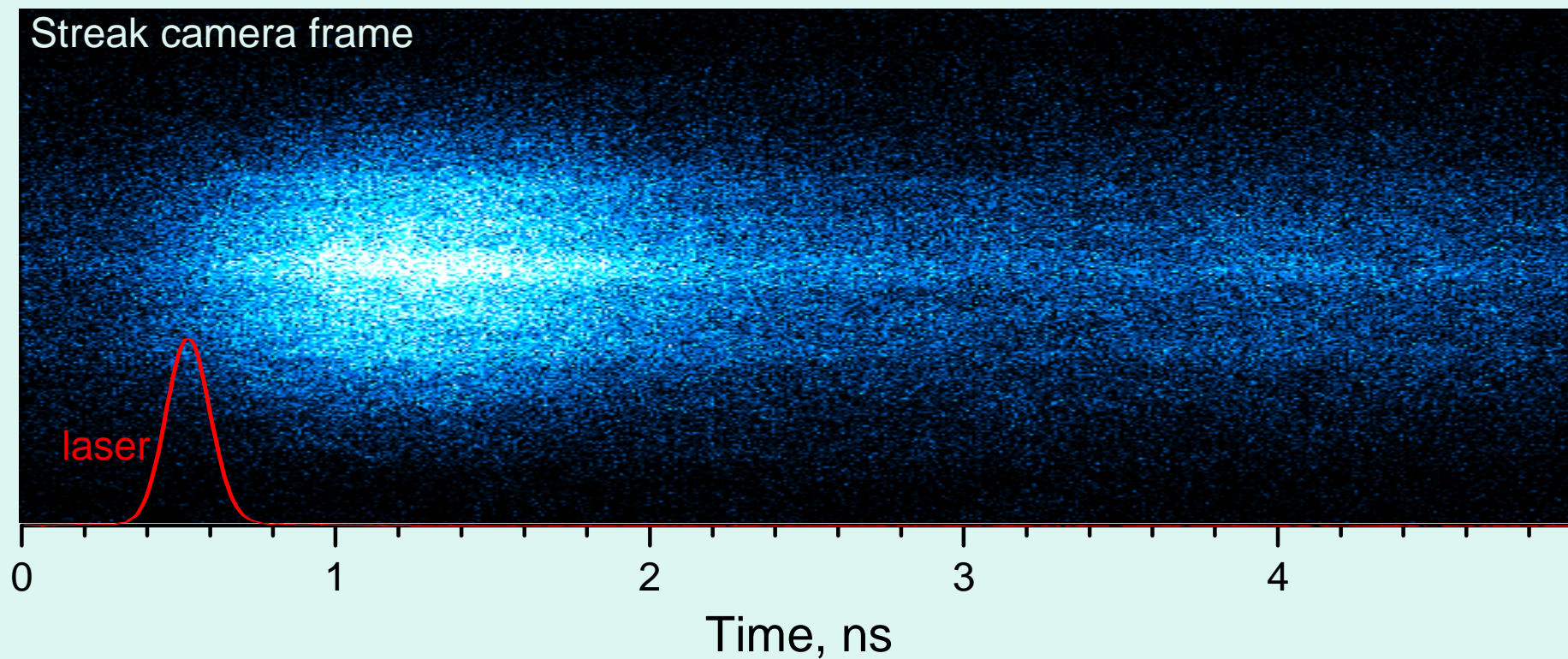
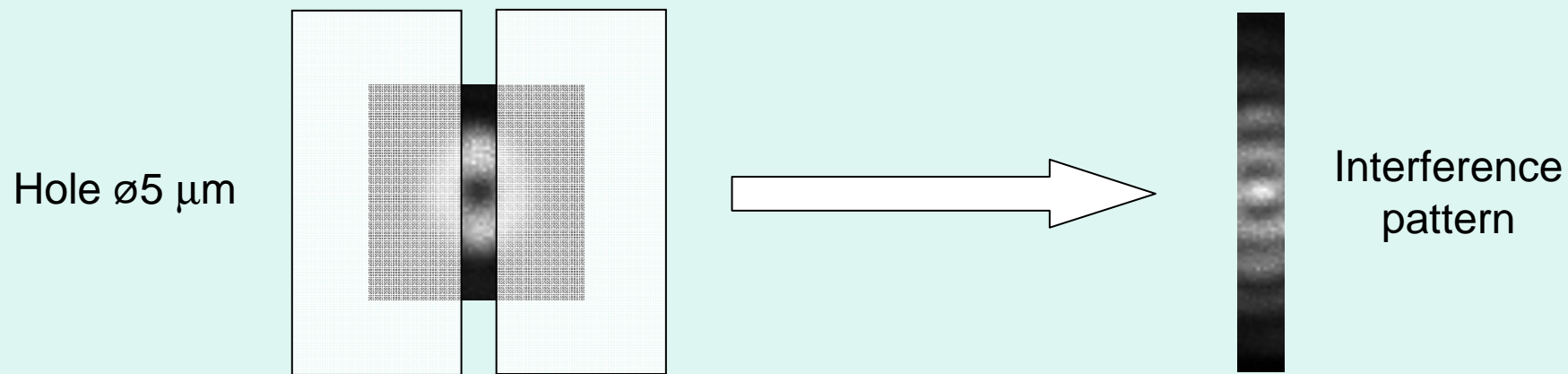
we are indebted for valuable and stimulating discussions to

L.V.Keldysh, V.D.Kulakovskii, I.V.Kukushkin, Yu.M.Kagan, Yu.E.Lozerovik, S.V.Iordanskii, V.G.Lyssenko, L.P.Pitaevskii, V.I.Sugakov, G.M.Eliashberg

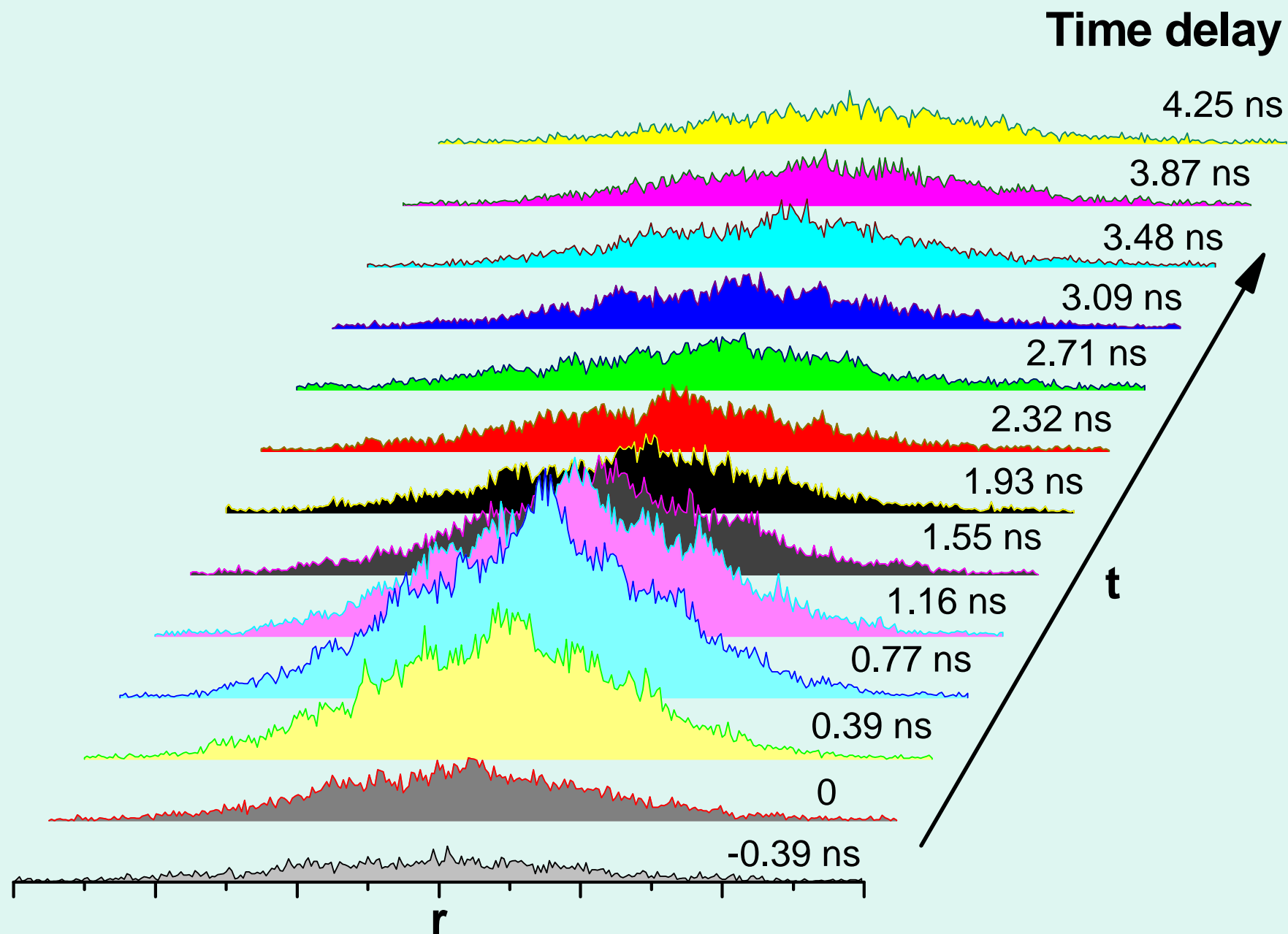


Time-resolved interference

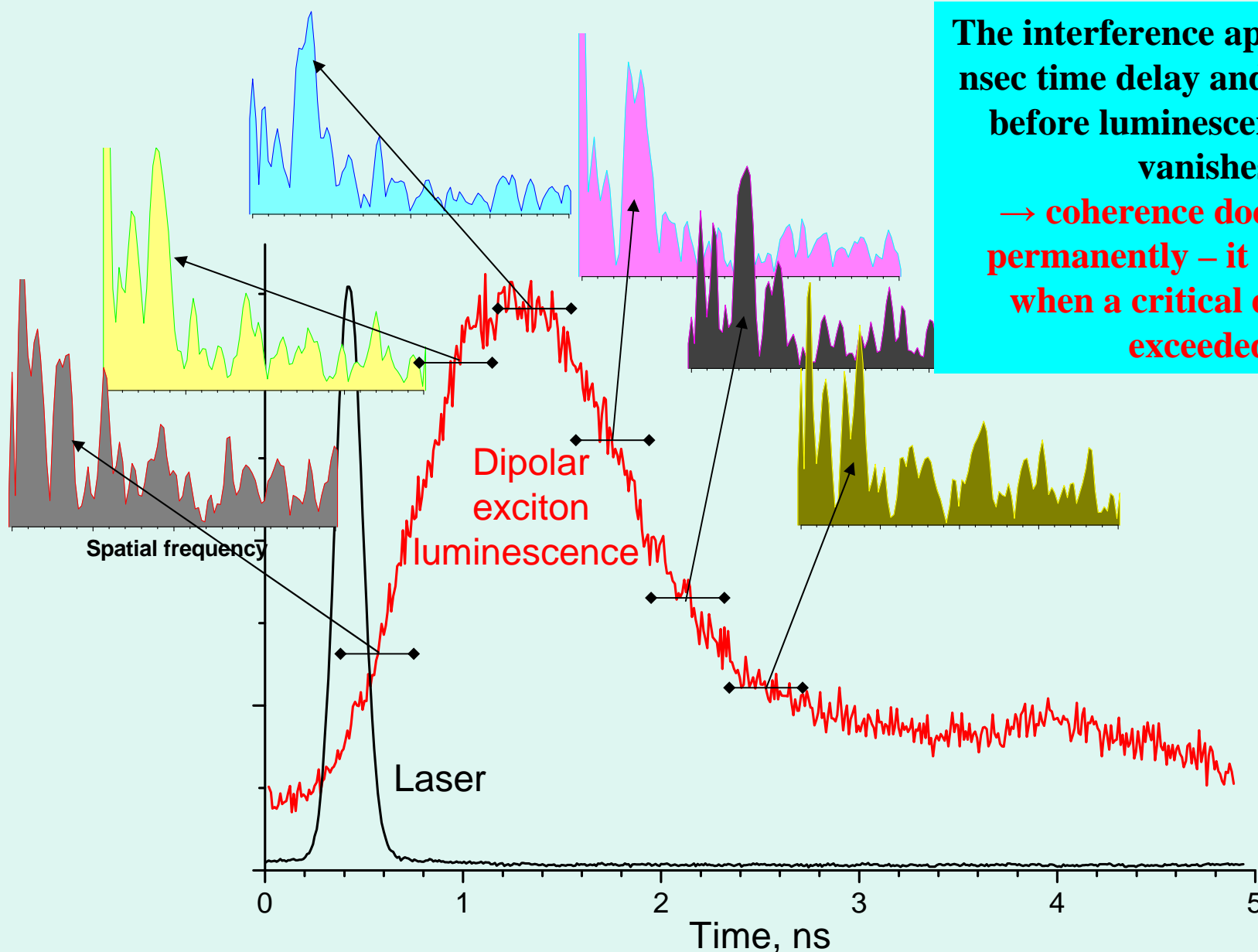
(combined excitation: pulsed above-barrier (100ps/10MHz) + CW in-barrier)



Time-resolved interference (2)



Time-resolved interference (3): Fourier-spectra



The interference appears with a nsec time delay and disappears before luminescence totally vanishes
→ coherence does not live permanently – it exists only when a critical density is exceeded.

Hanbury Brown Twiss Effect for Ultracold Quantum Gases

M. Schellekens,¹ R. Hoppeler,¹ A. Perrin,¹ J. Viana Gomes,^{1,2}
D. Boiron,¹ A. Aspect,¹ C. I. Westbrook^{1*}

M. Schellekens, *et al.*
Science **310**, 648 (2005);

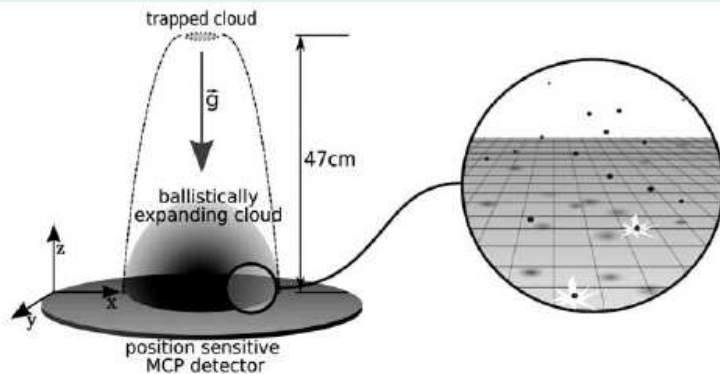
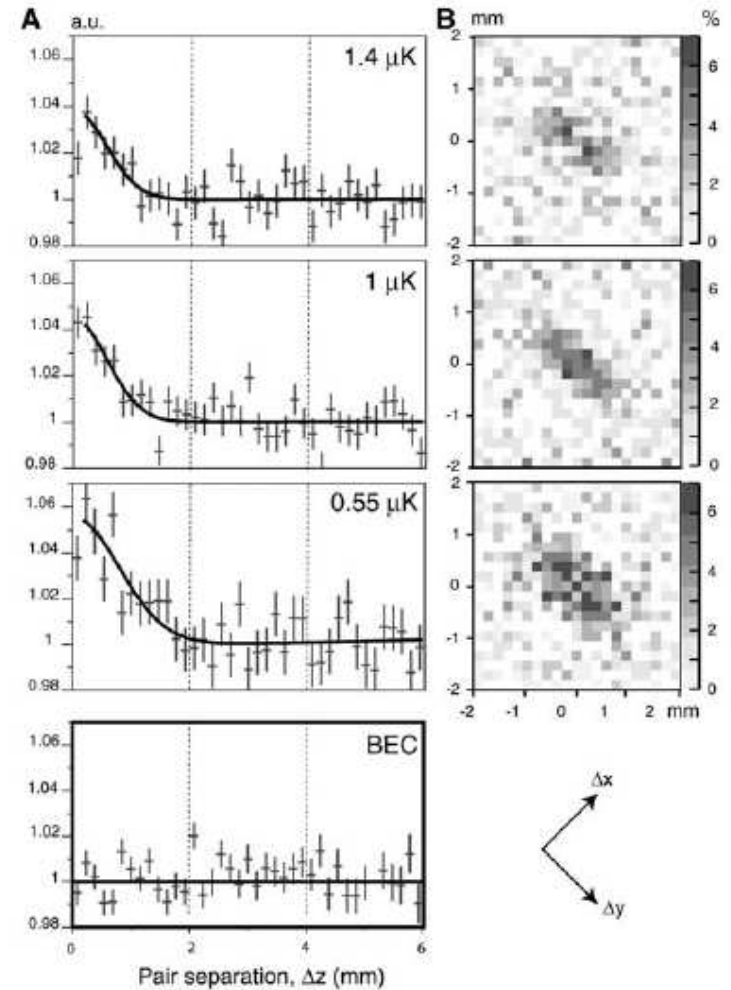


Fig. 1. Schematic of the apparatus. The trapped cloud has a cylindrical symmetry with oscillation frequencies of $\omega_x/2\pi = 47$ Hz and $\omega_y/2\pi = \omega_z/2\pi = 1150$ Hz. During its free fall toward the detector, a thermal cloud acquires a spherical shape. A 1- μ K temperature yields a cloud with an rms radius of about 3 cm at the detector. Single particle detection of the neutral atoms is possible because of each atom's 20-eV internal energy that is released at contact with the MCP. Position sensitivity is obtained through a delay-line anode at the rear side of the MCP.

Fig. 2. (A) Normalized correlation functions along the vertical (z) axis for thermal gases at three different temperatures and for a BEC. For the thermal clouds, each plot corresponds to the average of a large number of clouds at the same temperature. Error bars correspond to the square root of the number of pairs. a.u., arbitrary units. (B) Normalized correlation functions in the $\Delta x - \Delta y$ plane for the three thermal gas runs. The arrows at the bottom show the 45° rotation of our coordinate system with respect to the axes of the detector. The inverted ellipticity of the correlation function relative to the trapped cloud is visible.



Comparison of the Hanbury Brown–Twiss effect for bosons and fermions

T. Jeltes¹, J. M. McNamara¹, W. Hogervorst¹, W. Vassen¹, V. Krachmalnicoff², M. Schellekens², A. Perrin², H. Chang², D. Boiron², A. Aspect² & C. I. Westbrook²

Vol 445 | 25 January 2007 | doi:10.1038/nature05513

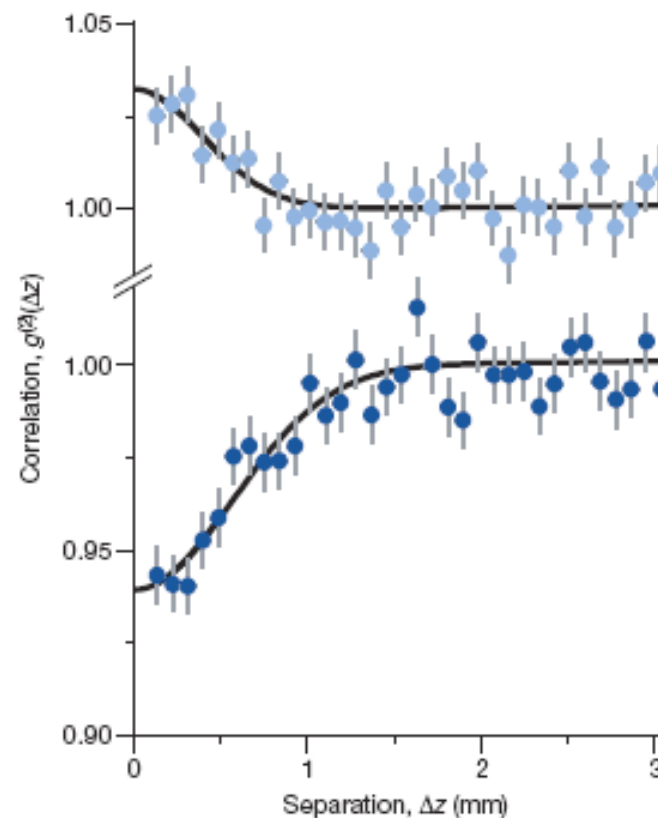
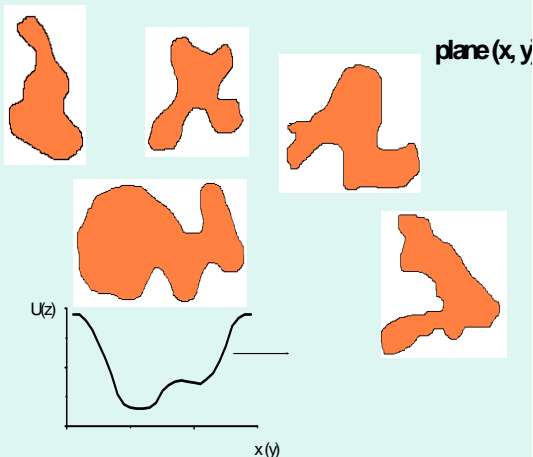


Figure 2 | Normalized correlation functions for ${}^4\text{He}^*$ (bosons) in the upper plot, and ${}^3\text{He}^*$ (fermions) in the lower plot. Both functions are measured at the same cloud temperature ($0.5\ \mu\text{K}$), and with identical trap parameters. Error bars correspond to the square root of the number of pairs in each bin. The line is a fit to a gaussian function. The bosons show a bunching effect, and the fermions show antibunching. The correlation length for ${}^3\text{He}^*$ is expected to be 33% larger than that for ${}^4\text{He}^*$ owing to the smaller mass. We find $1/e$ values for the correlation lengths of $0.75 \pm 0.07\ \text{mm}$ and $0.56 \pm 0.08\ \text{mm}$ for fermions and bosons, respectively.

Ловушки, связанные с крупномасштабными флуктуациями случайного потенциала

The lateral random potential fluctuations



$$\mu(n(r)) + U(r) = \mu$$

$$|\mu(r)| < |\mu|$$

$$\mu(n) = -|E_{ex}| + |\delta U|$$

$$T_C = \frac{2\pi\hbar^2 N_{ex} / g}{m_{ex} k_B \ln(SN_{ex} / g)}$$

Непрозрачная маска с отверстиями микронных размеров (вплоть до 0.5 μm) на поверхности образца для отбора отдельных доменов в случайном

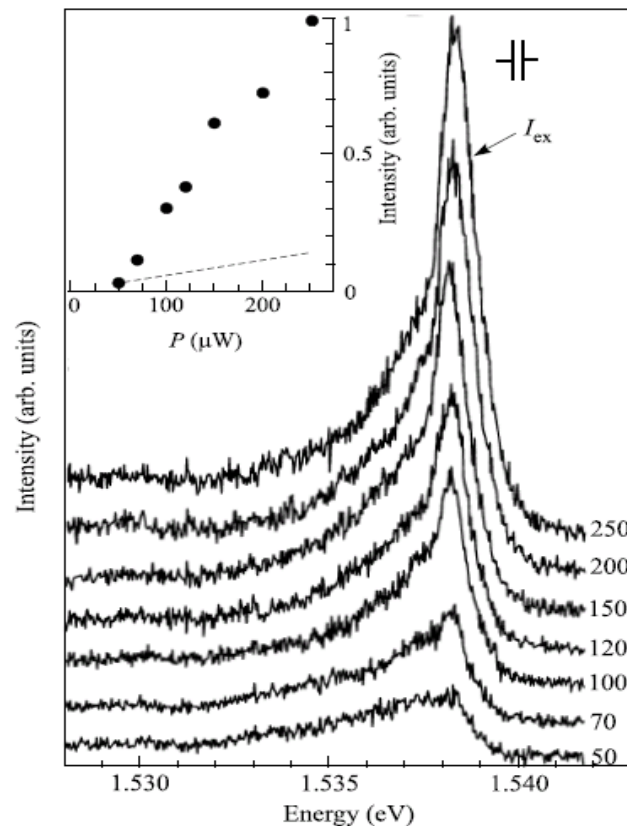


Рис.2. Спектры ФЛ межъямного экситона (линия I_{ex}) при различных мощностях резонансного возбуждения прямого 1sHH экситона, приложенном смещении $U = 0.3$ В и $T = 1.51$ К. Цифры справа от спектров соответствуют мощности возбуждения в мкВт. Вверху справа указано спектральное разрешение прибора. На вставке представлена зависимость интенсивности линии МЭ (точки) в функции мощности оптического возбуждения. Штриховая линия – экстраполяция линейной зависимости интенсивности фона под линией

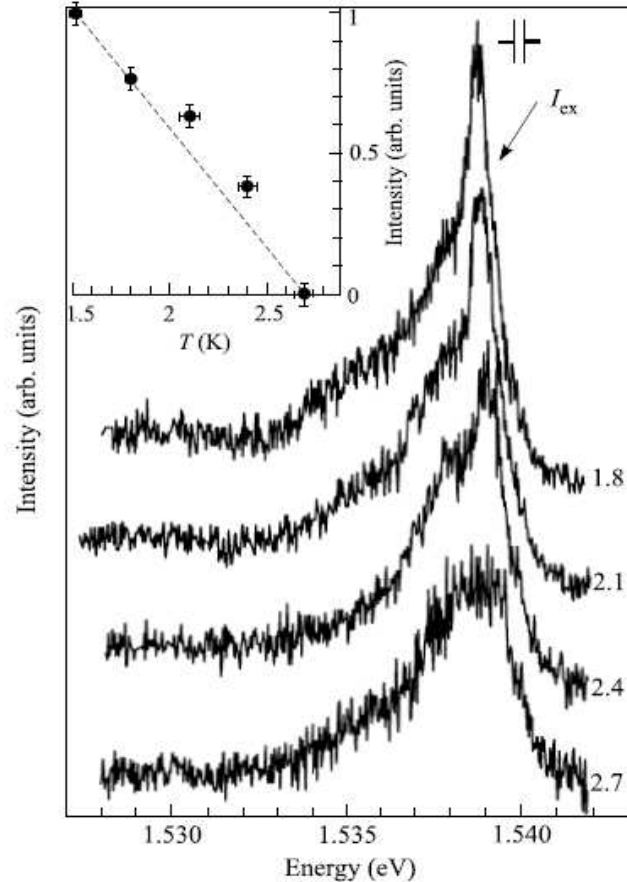


Рис.3. Температурная зависимость интенсивности линии фотолуминесценции МЭ при возбуждении $P = 150$ мкВт и приложенном электрическом смещении $U = 0.3$ В. Цифры справа соответствуют температуре в кельвинах. Точки на вставке показывают поведение интенсивности линии МЭ от температуры, штриховая кривая – экстраполяция зависимости $I_T \propto (1 - T/T_c)$

Photon Statistics of Semiconductor Microcavity Lasers

S. M. Ulrich,^{1,*} C. Gies,² S. Ates,¹ J. Wiersig,² S. Reitzenstein,³ C. Hofmann,³ A. Löffler,³
A. Forchel,³ F. Jahnke,² and P. Michler¹¹*Institut für Strahlenphysik, Universität Stuttgart, Germany*²*Institut für Theoretische Physik, Universität Bremen, Germany*³*Lehrstuhl für Technische Physik, Universität Würzburg, Germany*

(Received 2 March 2006; published 25 January 2007)

We present measurements of first- and second-order coherence of quantum-dot micropillar lasers together with a semiconductor laser theory. Our results show a broad threshold region for the observed high- β microcavities. The intensity jump is accompanied by both pronounced photon intensity fluctuations and strong coherence length changes. The investigations clearly visualize a smooth transition from spontaneous to predominantly stimulated emission which becomes harder to determine for high β . In our theory, a microscopic approach is used to incorporate the semiconductor nature of quantum dots. The results are in agreement with the experimental intensity traces and the photon statistics measurements.

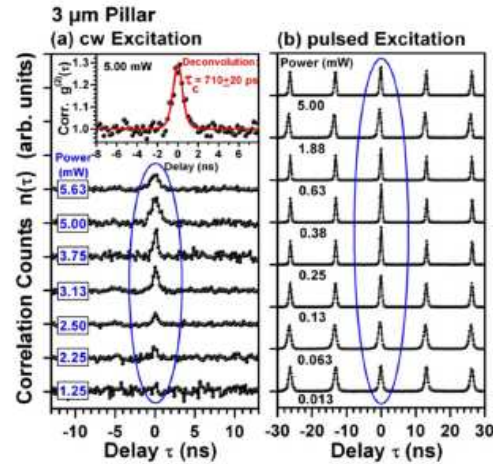


FIG. 2 (color online). (a) $\bar{g}^{(2)}(\tau)$ correlation series for the 3 μm fundamental pillar mode under varying cw excitation, clearly revealing photon bunching $\bar{g}^{(2)}(0) > 1$. Inset: Coherence time fit to the 5.0 mW trace under convolution with the temporal IRF ($\Delta t_{\text{IRF}} \approx 600$ ps). (b) Power-dependent autocorrelation series of the same micropillar under pulsed excitation, again reflecting a strong bunching effect at $\tau = 0$.

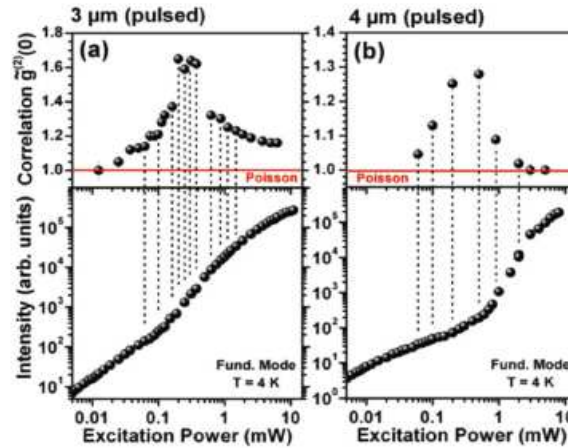


FIG. 3 (color online). (a),(b) Integrated intensities (bottom) for the 3 (4 μm) pillars under nonresonant pulsed excitation. Strong photon bunching $\bar{g}^{(2)}(0) > 1$ is found from corresponding correlation measurements (top) over a broadened regime around the threshold.

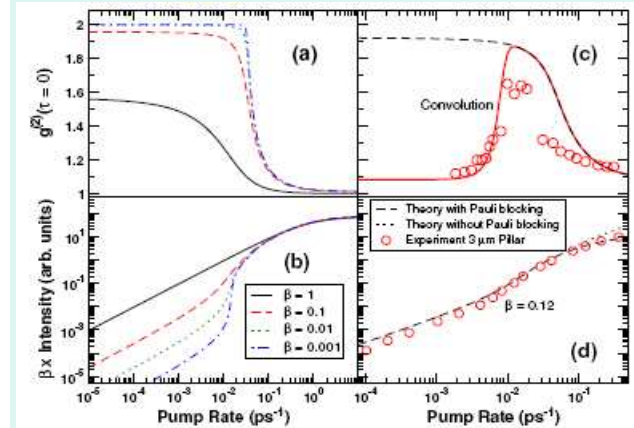
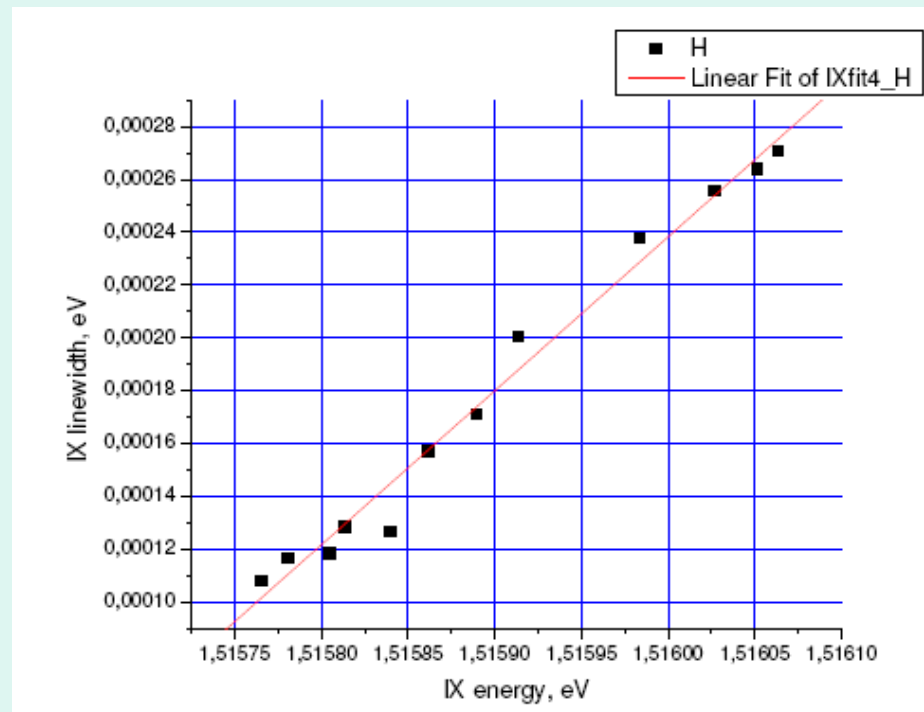


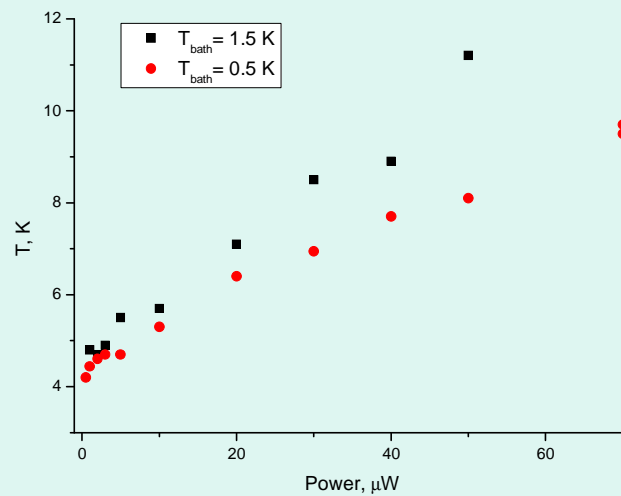
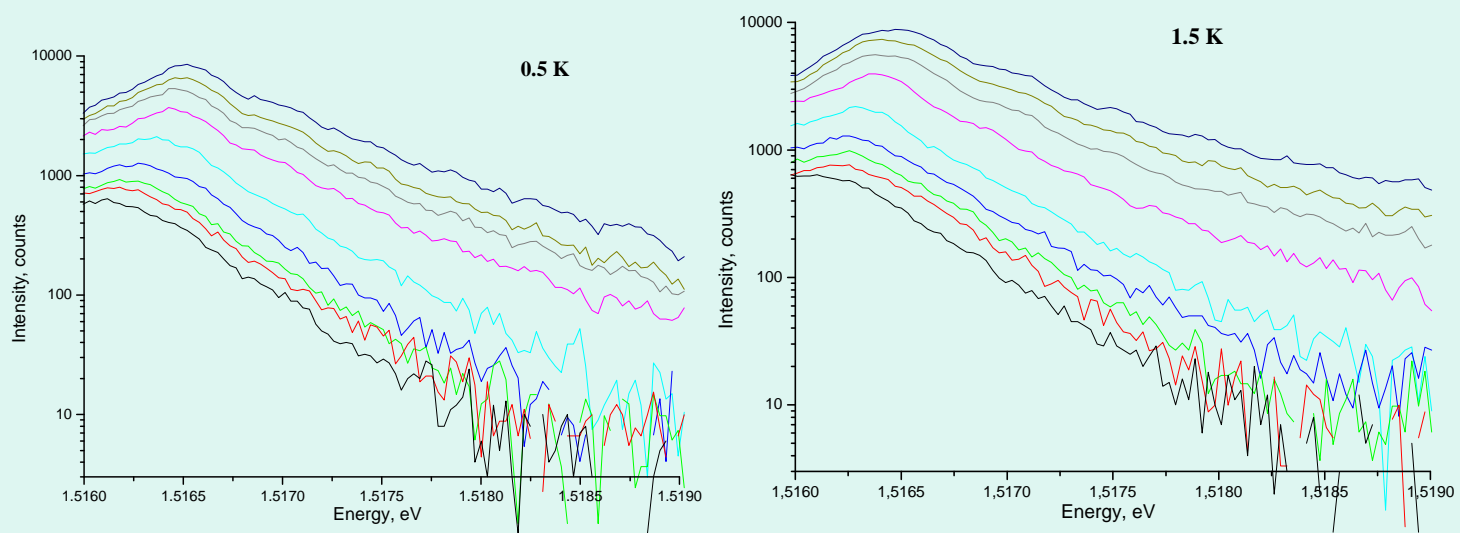
FIG. 5 (color online). (a),(b) Calculated output curves (bottom) and $g^{(2)}(0)$ (top) for various β . (c),(d) Calculated results vs experimental data (pulsed) from Fig. 3(a) for the 3 μm pillar. In (c), a convolution (solid line) with the experimental temporal resolution τ_c is shown. (d) Corresponding I/O curves, explicitly indicating the effects of pump saturation.

FWHM (M_1) and centre of weight (M_2) of the narrow line of condensate under variation of pumping

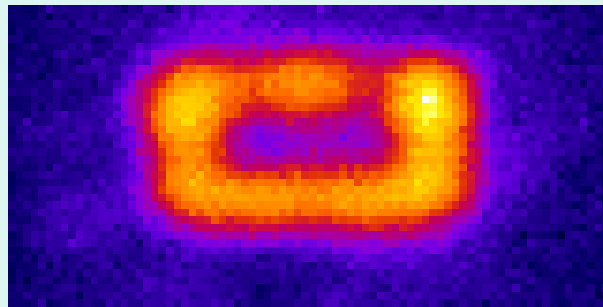


$$M_1/M_2 \cong 1.25$$

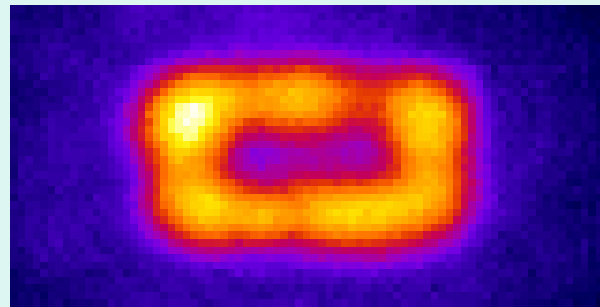
The above condensate excitations and the temperature of dipolar exciton gas



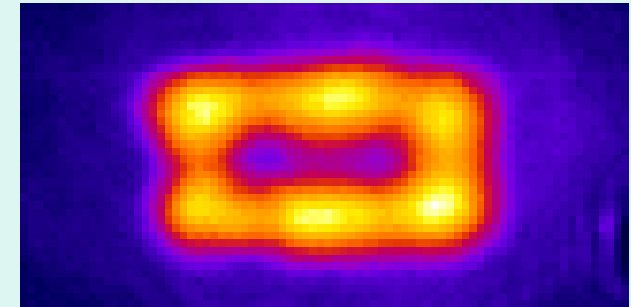
Rectangular hole D2 (5 x 10 μm)



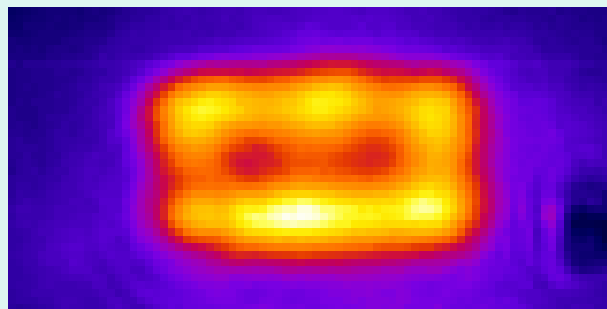
0.5 μW



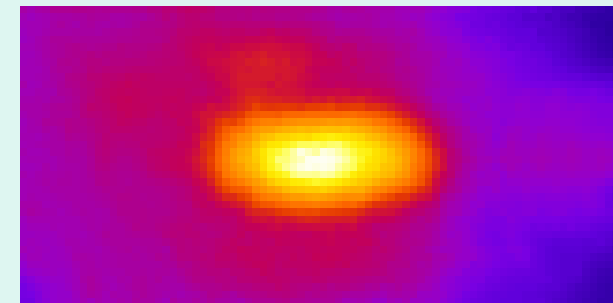
2 μW



25 μW



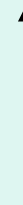
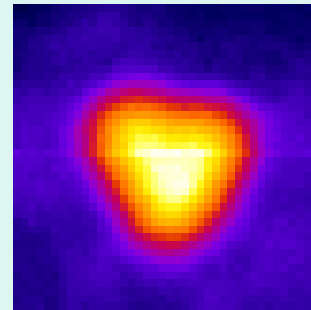
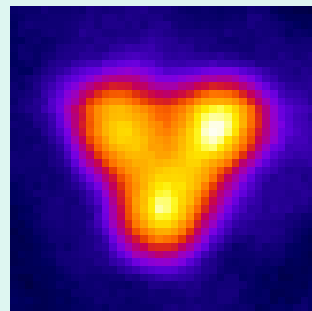
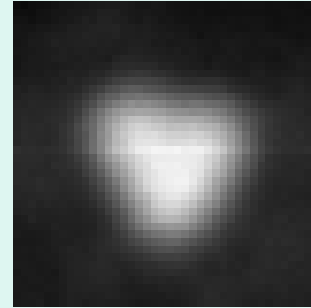
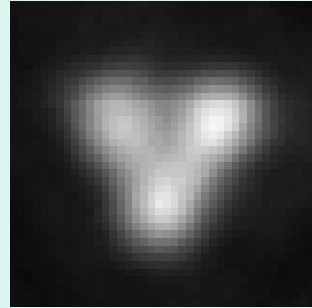
100 μW



25 μW

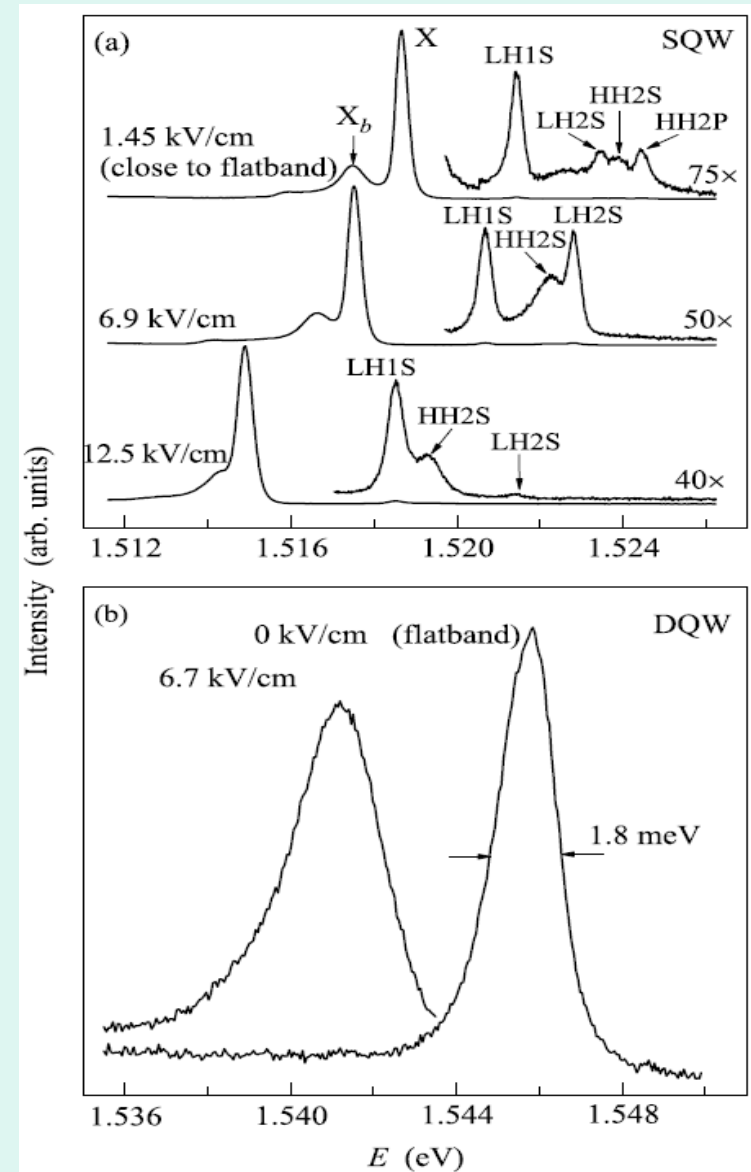
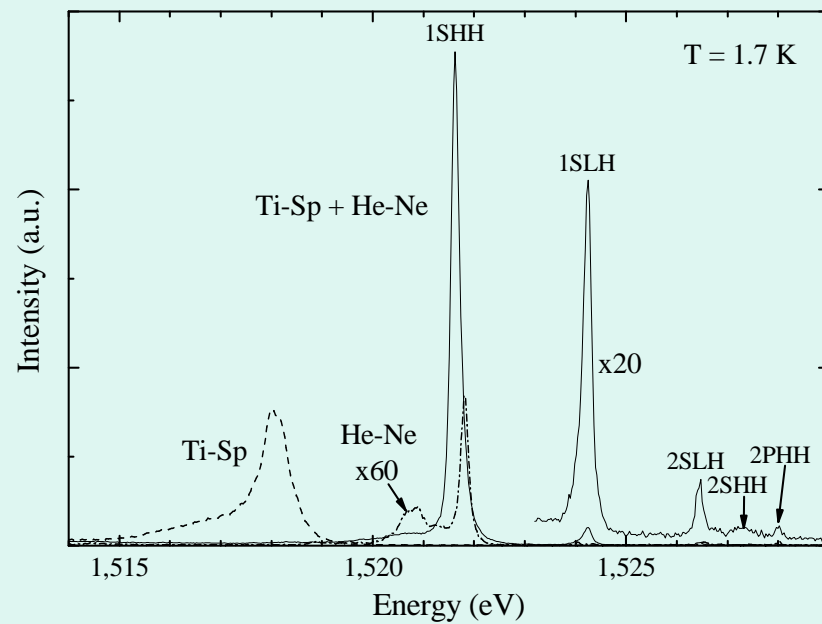
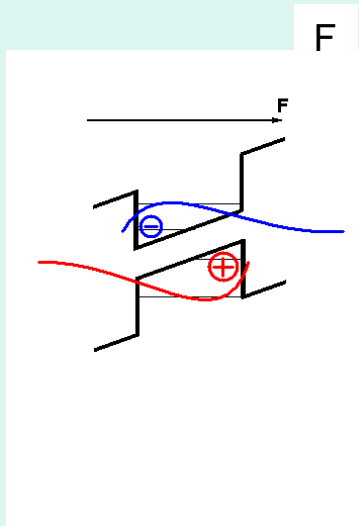
Direct exciton PL in the central part of a window exhibits homogeneous (!) distribution

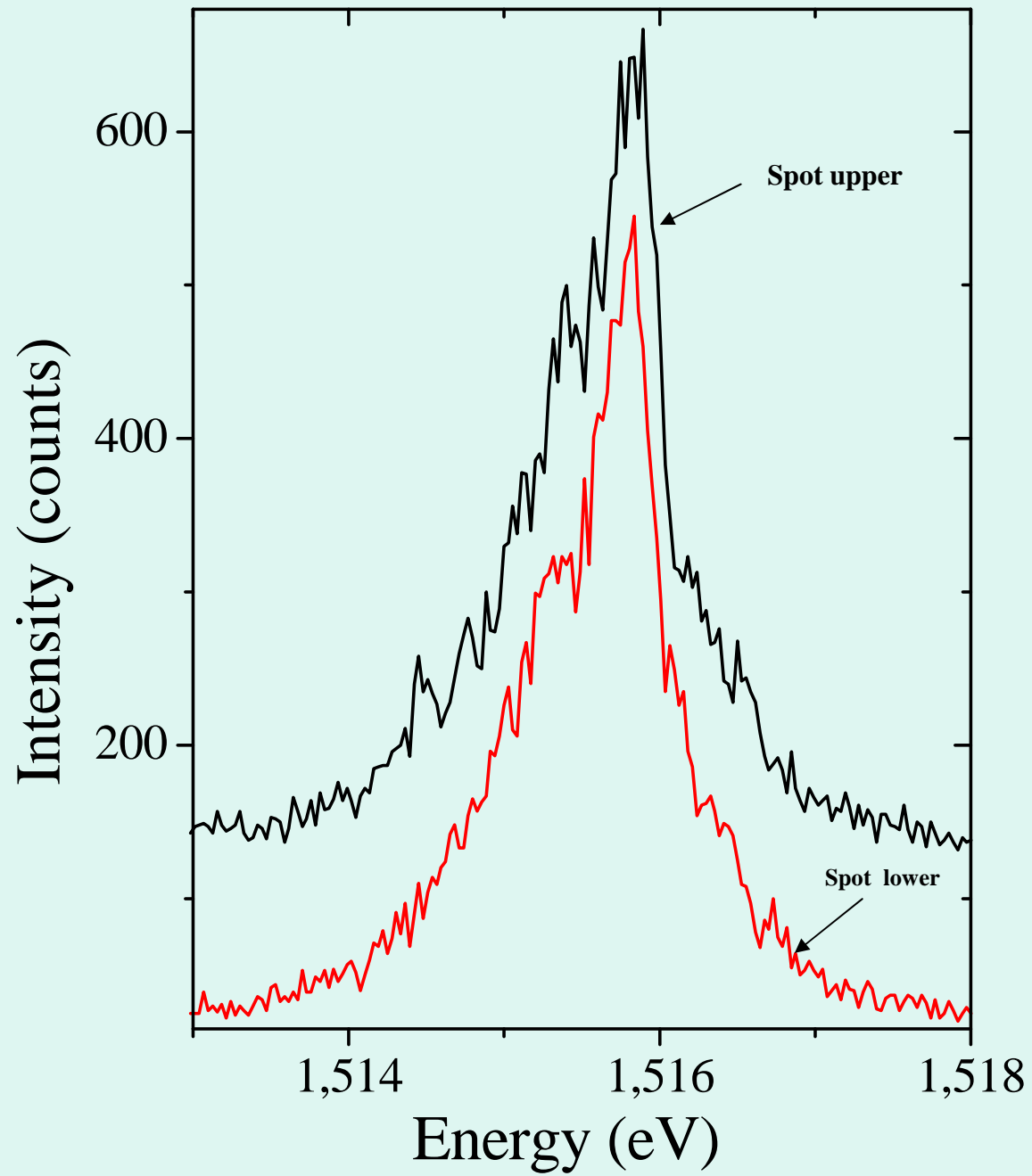
Triangular hole (C3), side length $6\mu\text{m}$



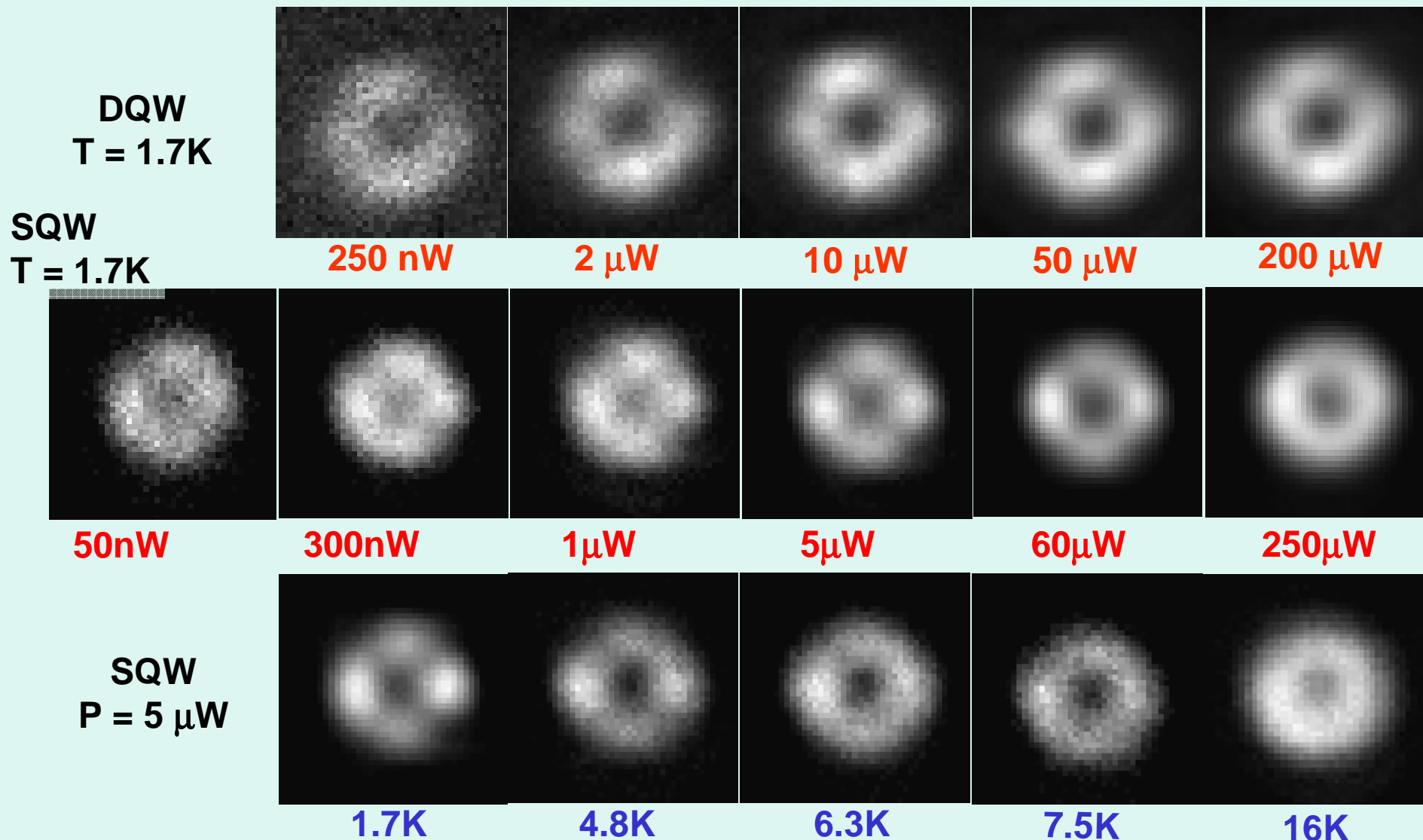
Exciton PL in the central part of a window is homogeneous

Compensation of extra charges in SQW with the use of in- and above barrier photoexcitations





Пространственное распределение люминесценции непрямого (диполярного) экситона внутри отверстия $\varnothing 5\mu\text{m}$ в непрозрачном электроде на поверхности двойной (DQW) GaAs/AlGaAs 120/12/120Å и одиночной (SQW) GaAs/AlGaAs 250Å квантовой ямы

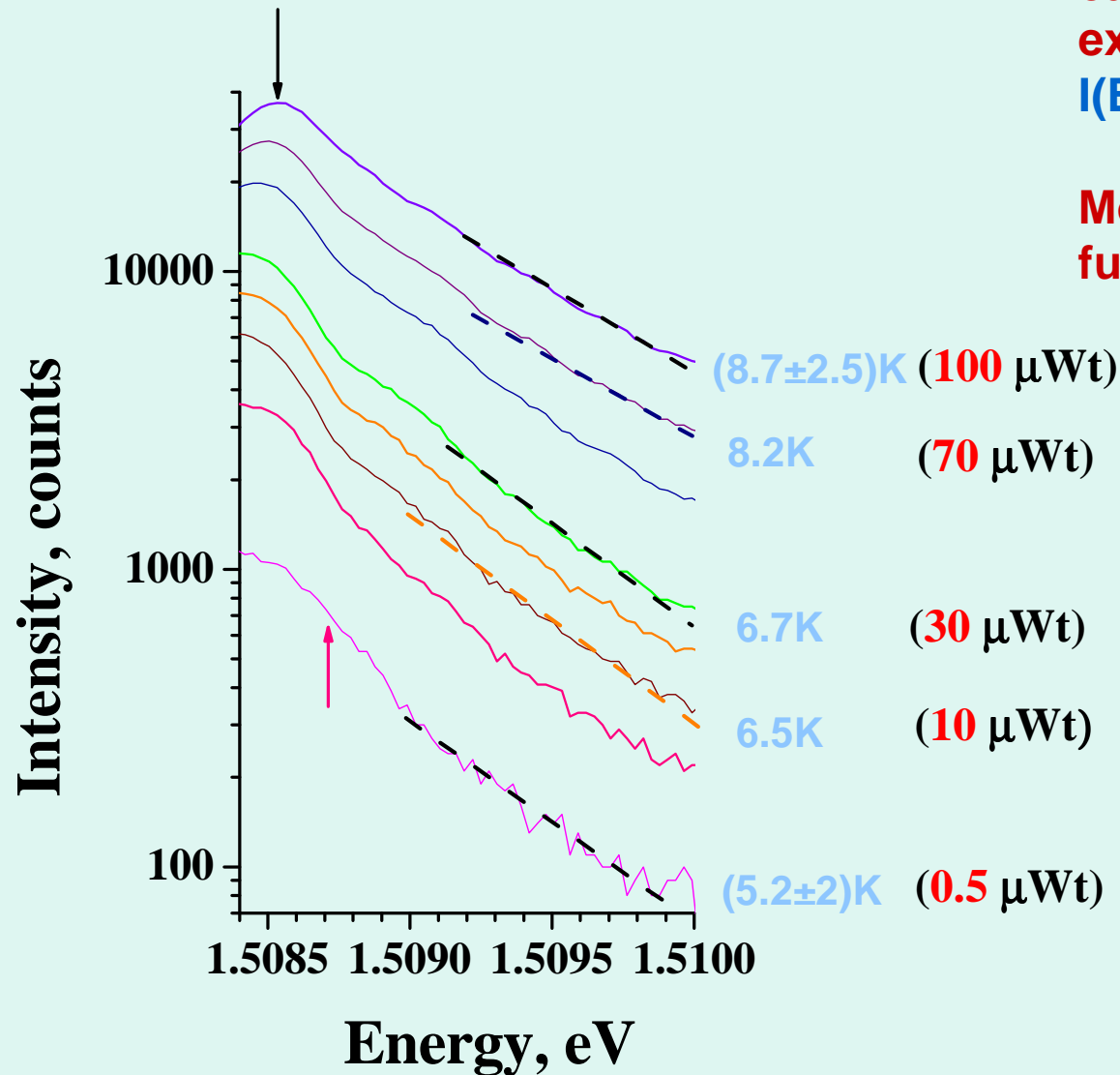


Excitations in BEC are under thermal quasi equilibrium

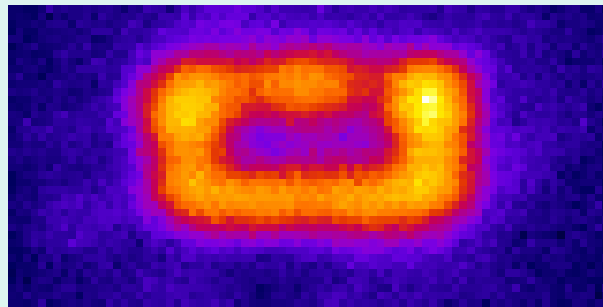
The temperature of excitations can be found from high energy exponential tail of exciton line $I(E) \sim N_q \sim \exp(-E/kT)$, at $E > kT$

Momentum conservation is fulfilled due to collisions and recoil processes

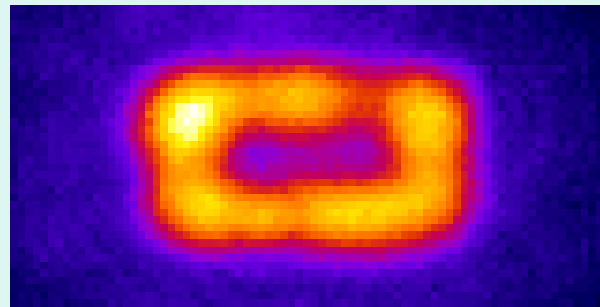
Condensation occurs under thermal quasi equilibrium



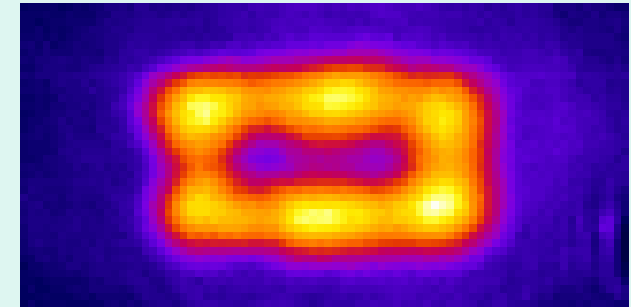
Rectangular hole D2 (5 x 10 μm)



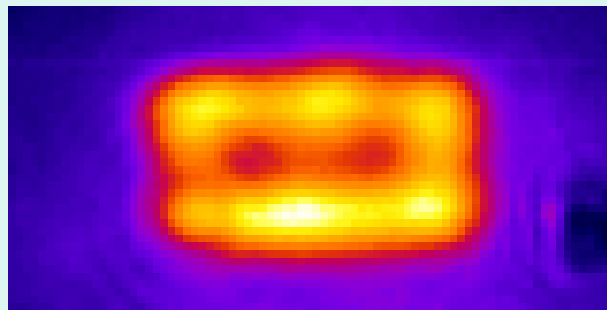
0.5 μW



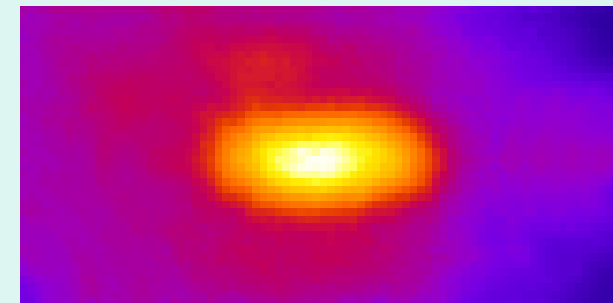
2 μW



25 μW



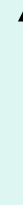
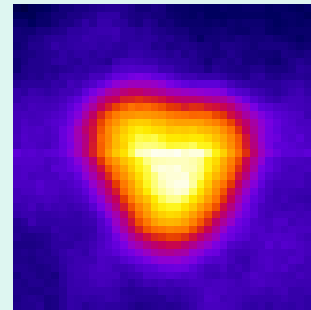
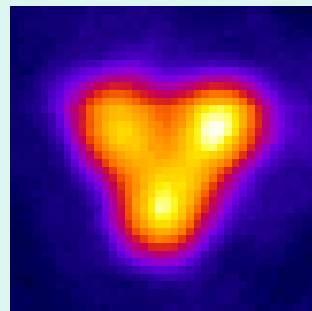
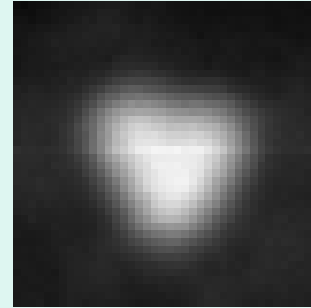
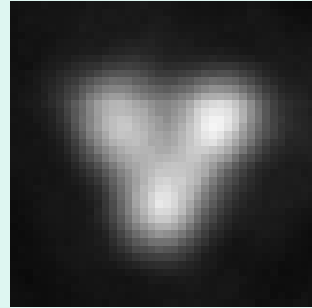
100 μW



25 μW

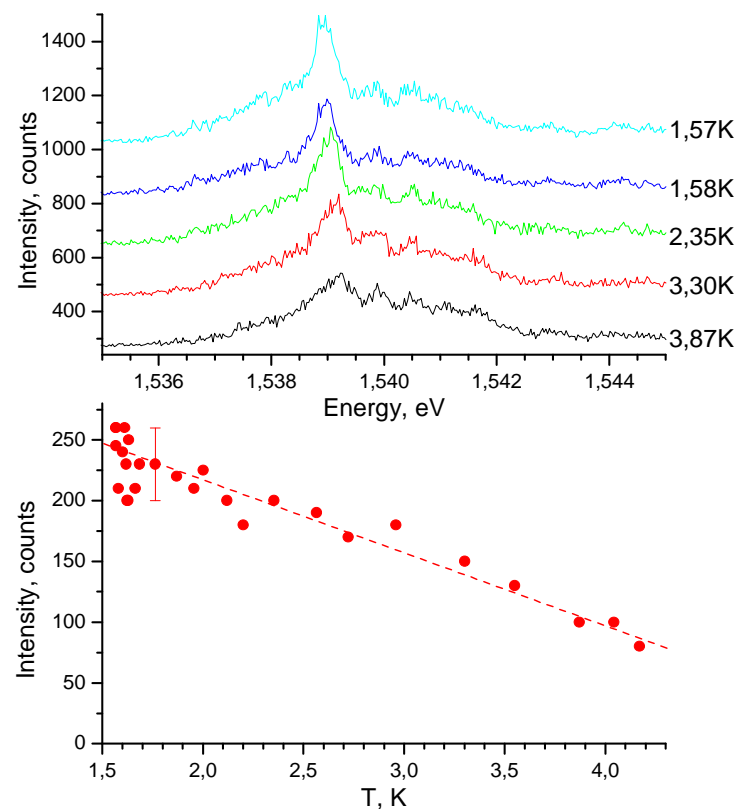
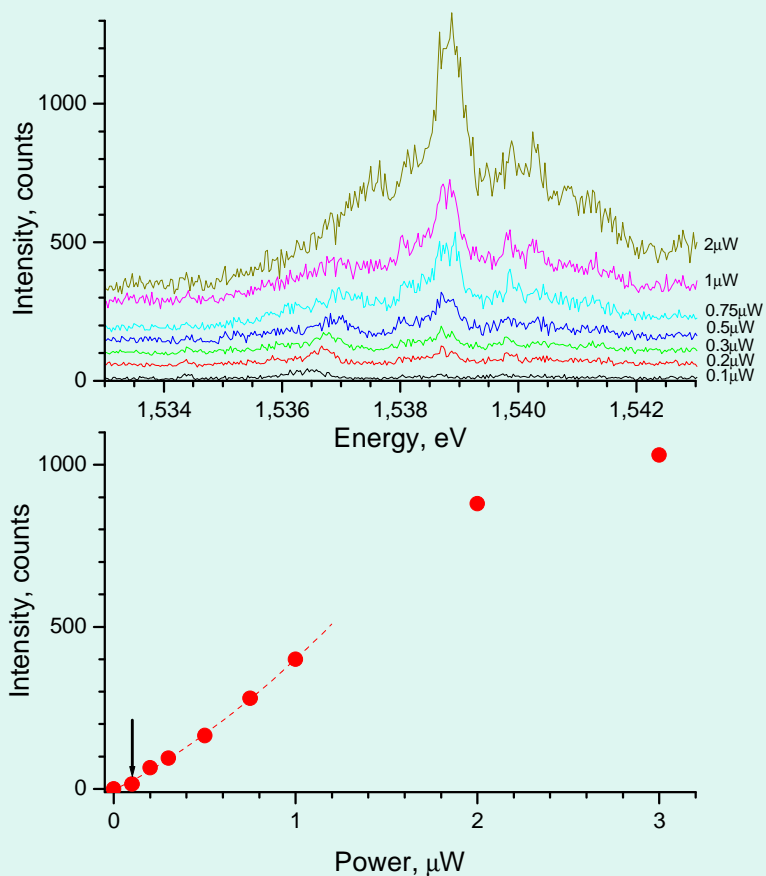
Direct exciton PL in the central part of a window exhibits homogeneous (!) distribution

Triangular hole (C3), side length $6\mu\text{m}$

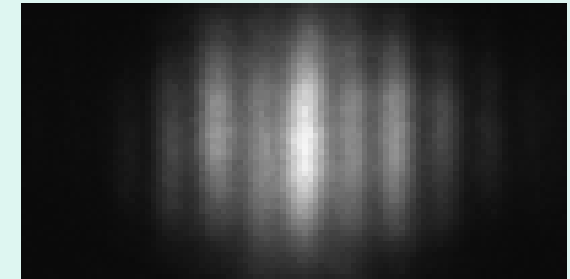
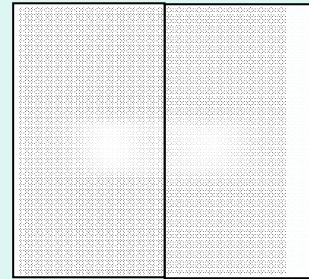
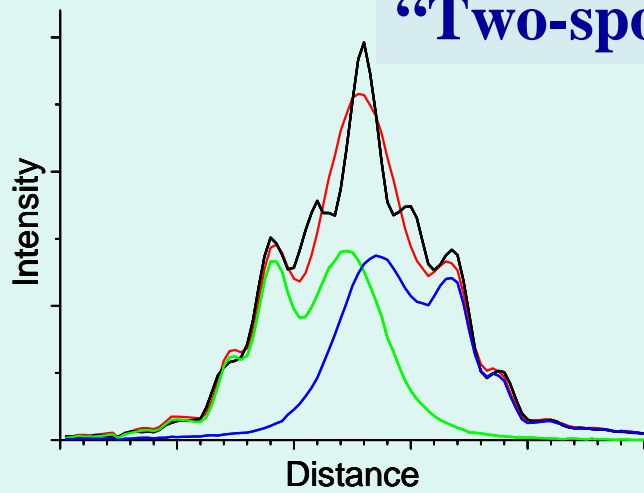


Exciton PL in the central part of a window is homogeneous

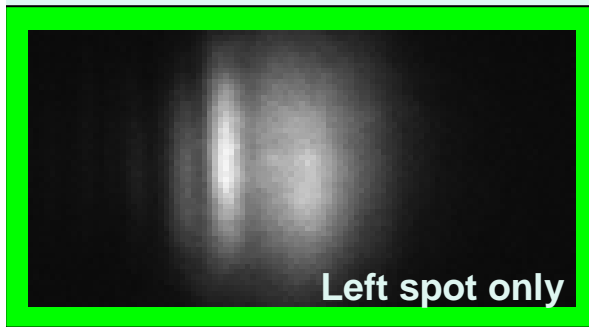
Luminescence spectra of interwell excitons in DQW from 5 μm window under excitation power and temperature variations



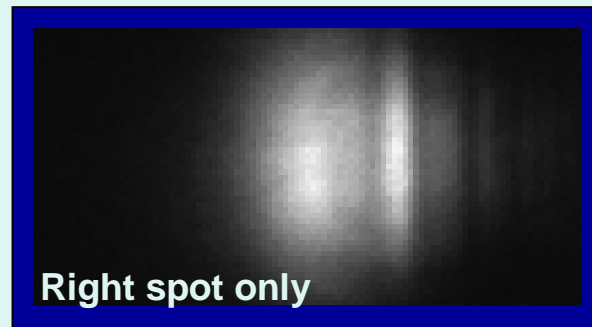
“Two-spot” interference: overcoming edge diffraction



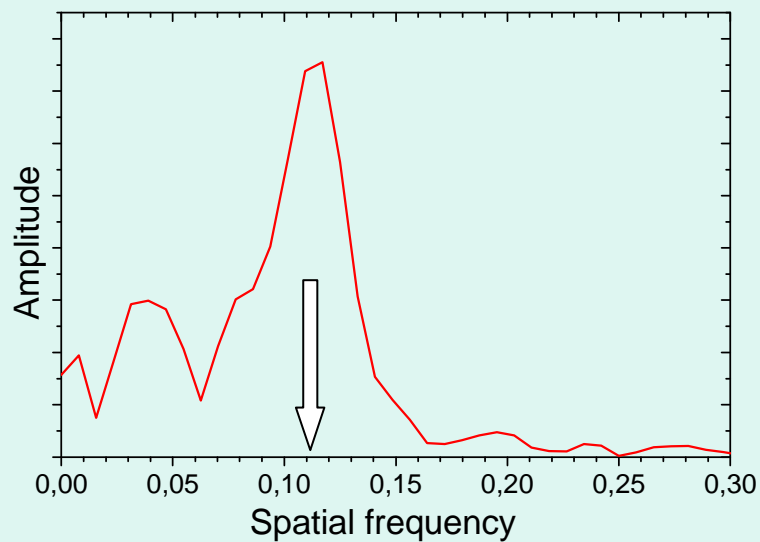
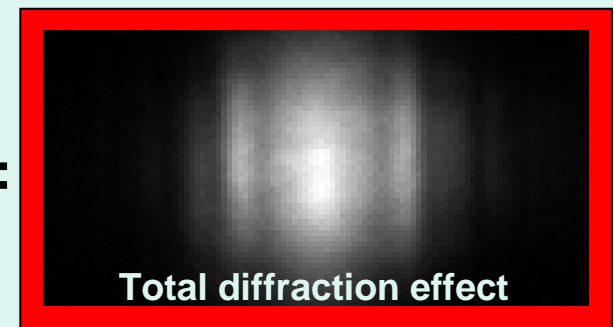
—



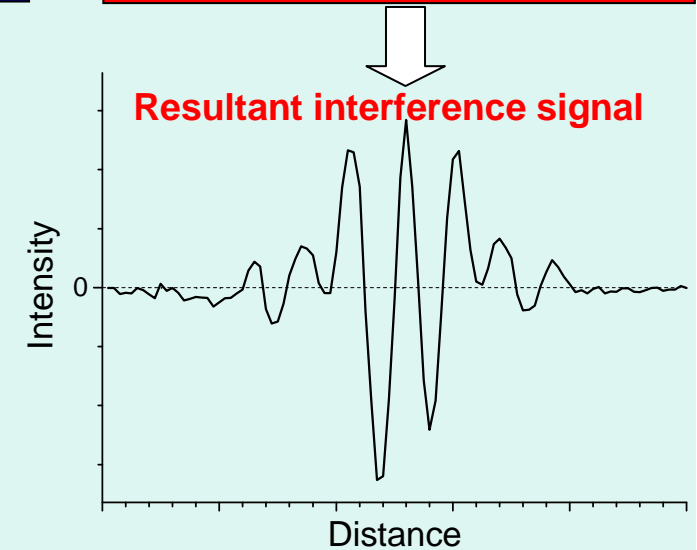
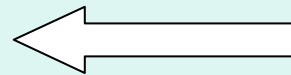
+



=

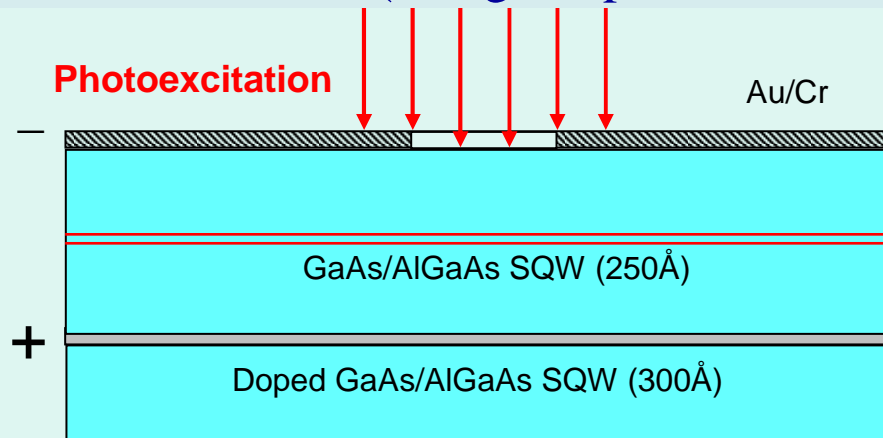


Fourier-transform



Ring-shaped lateral trap for indirect excitons in Schottky-diod

(along the perimeter of a window in top Schottky gate)

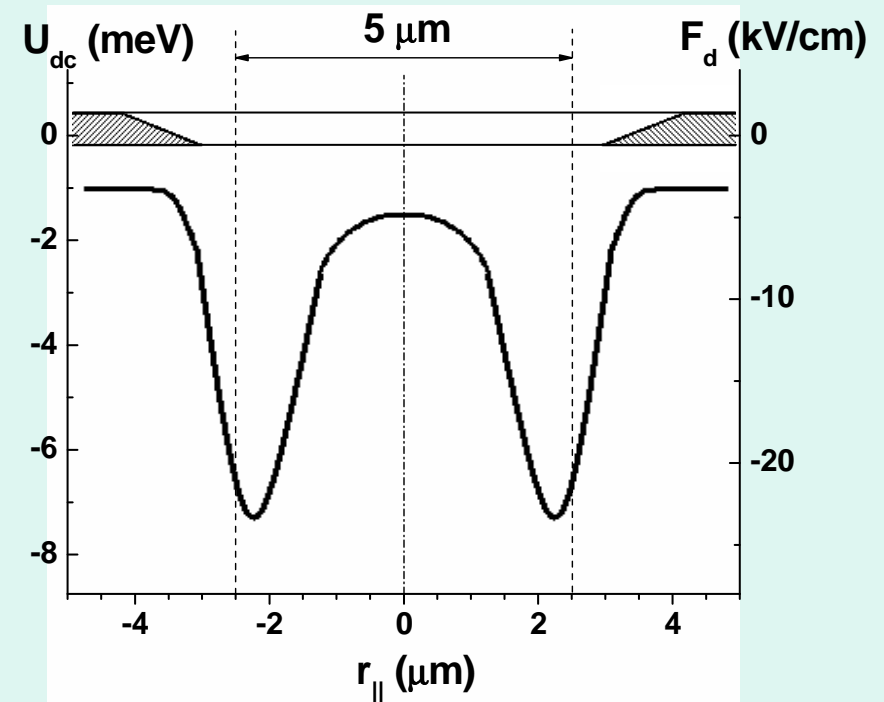
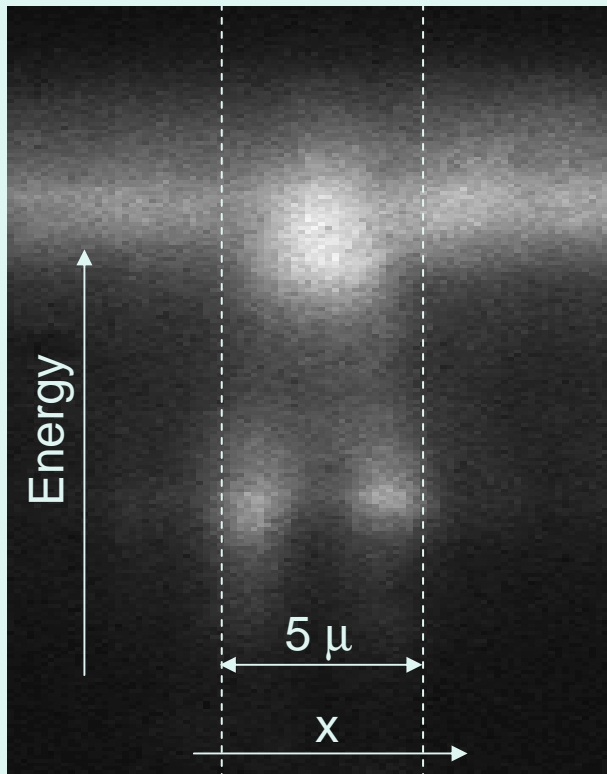


The potential profile of the trap can be described near bottom as:

$$V(r) = \alpha r_{\parallel}^2,$$

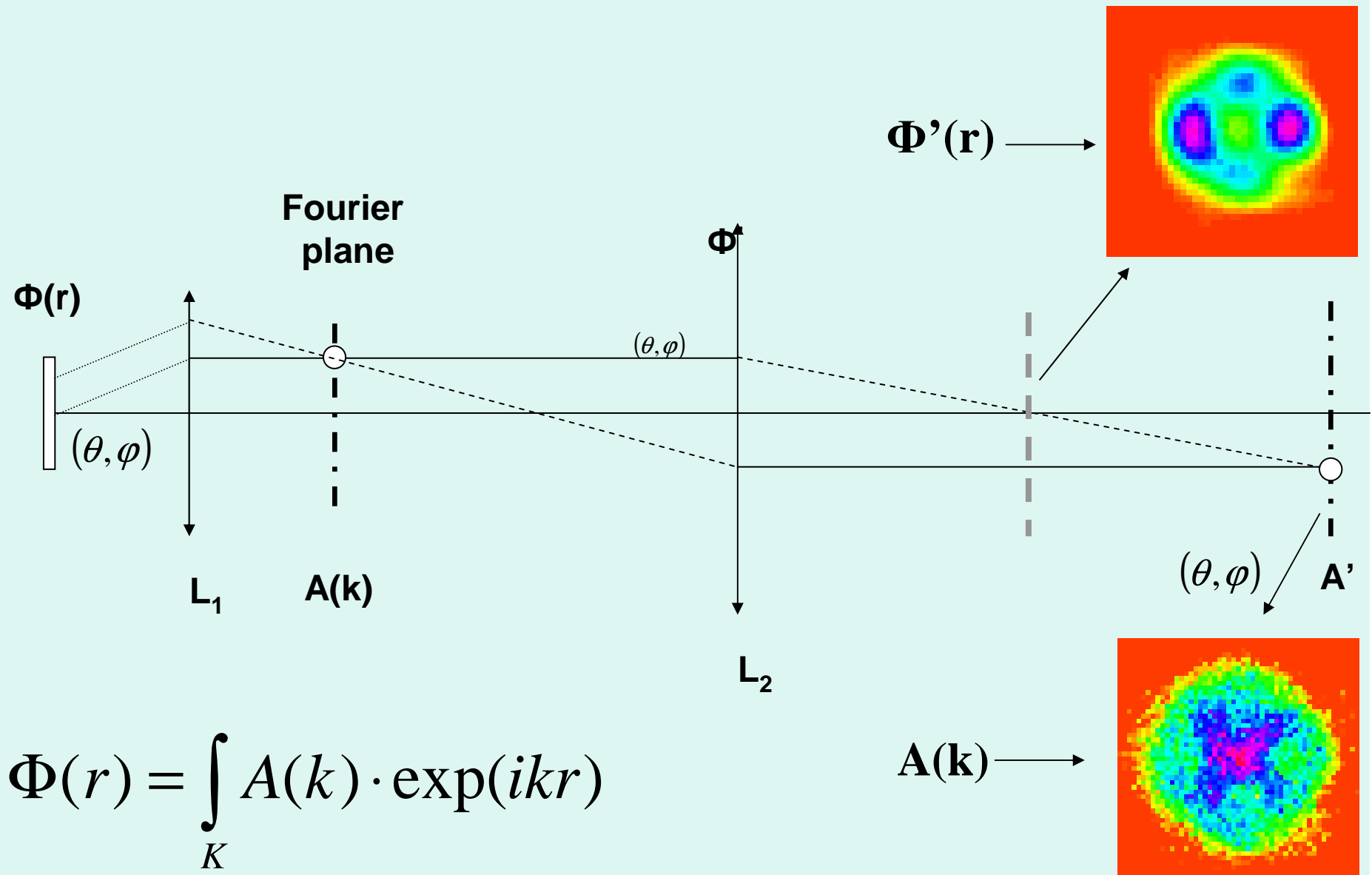
with force constant $\alpha \approx 2.2 \text{ meV}/\mu\text{m}^2$.

Barrier height $\Delta V \approx 5 \text{ meV} \gg kT$.

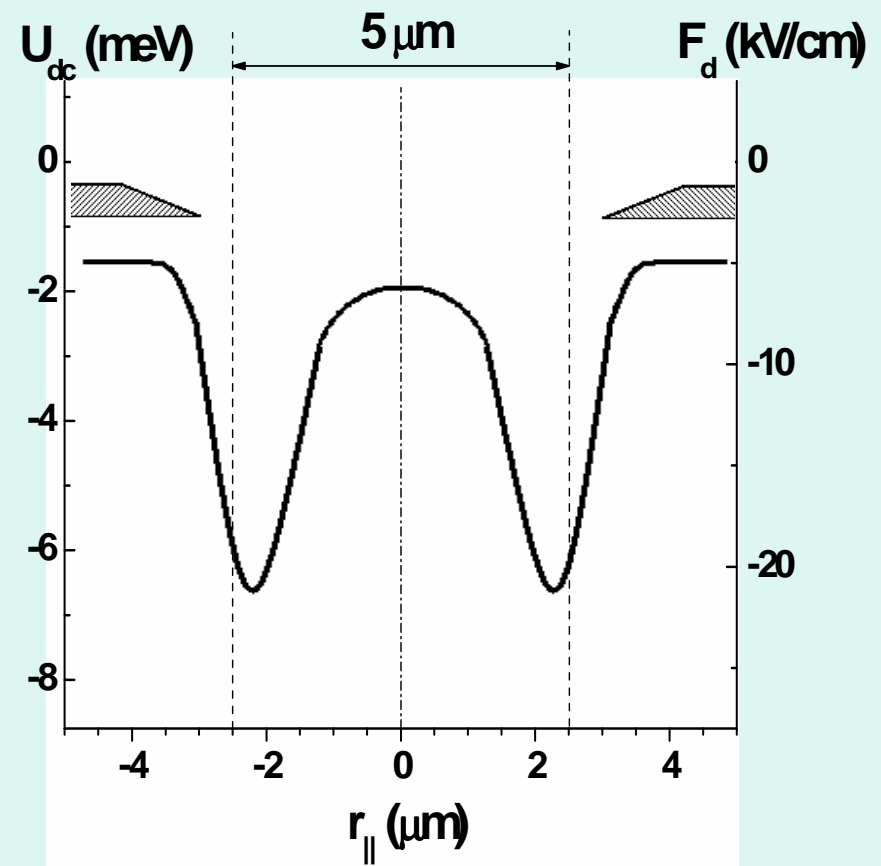
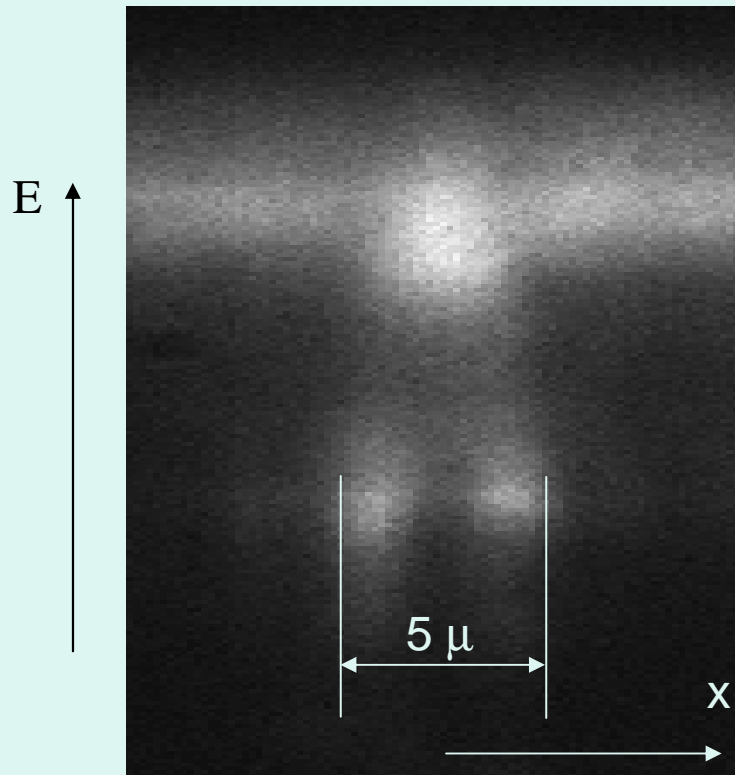


$\langle d_{ex} \rangle = 115 \text{ \AA}$ (F=20 kV/cm)

K-space imaging – Fourier transformation



Confining energy $U_{dc}(r_{\parallel})$ of circular electrostatic trap for dipolar excitons



$$\langle d_{\text{ex}} \rangle = 115 \text{ \AA} \quad (F=20 \text{ kV/cm})$$

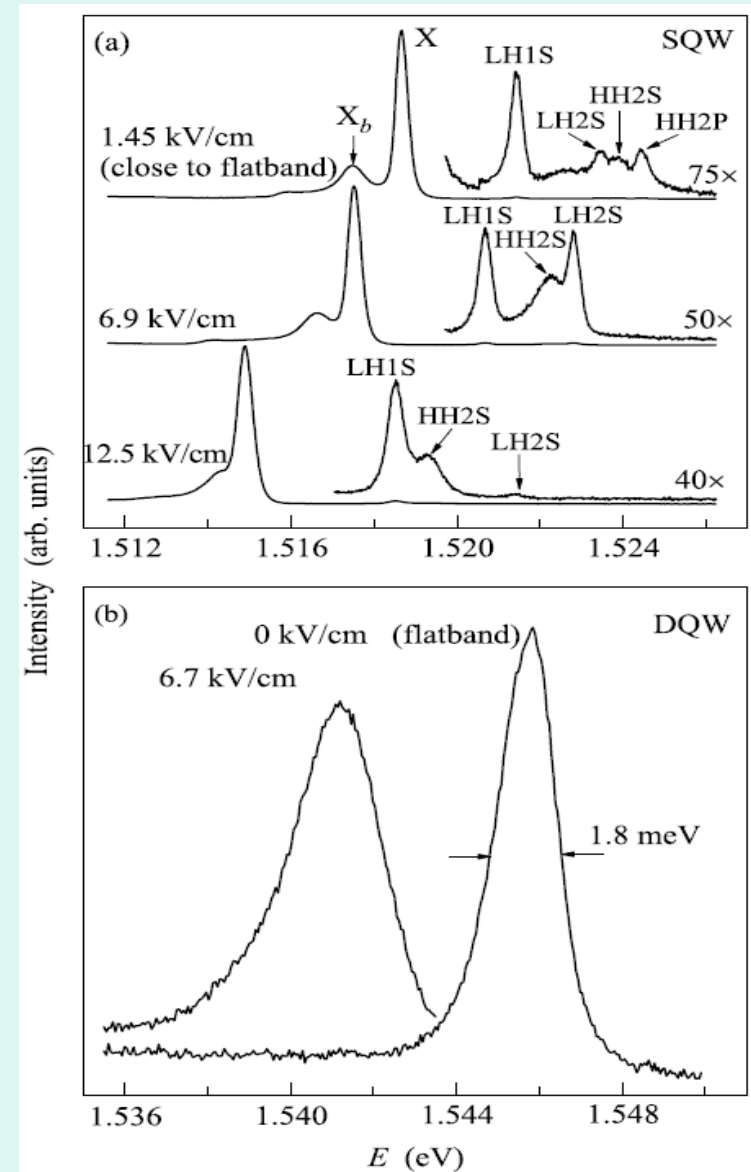
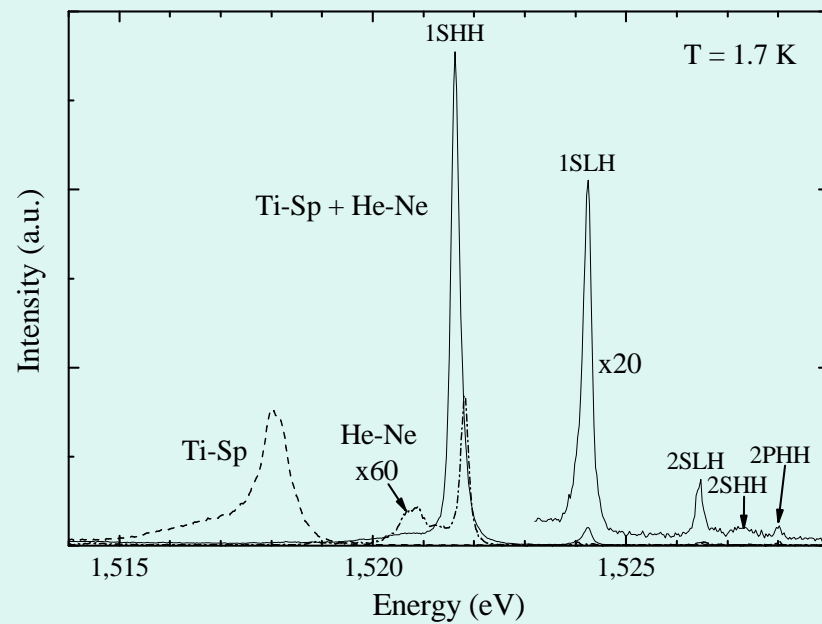
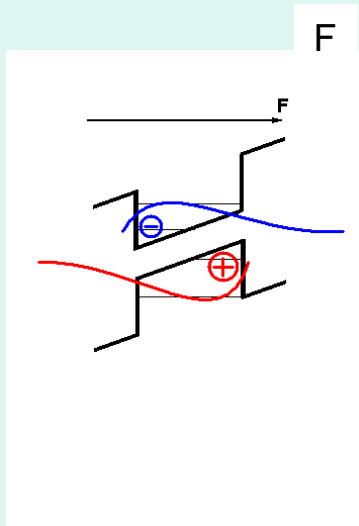
The potential profile of the trap can be described near bottom as:

$$V(r) = \alpha r_{\parallel}^2,$$

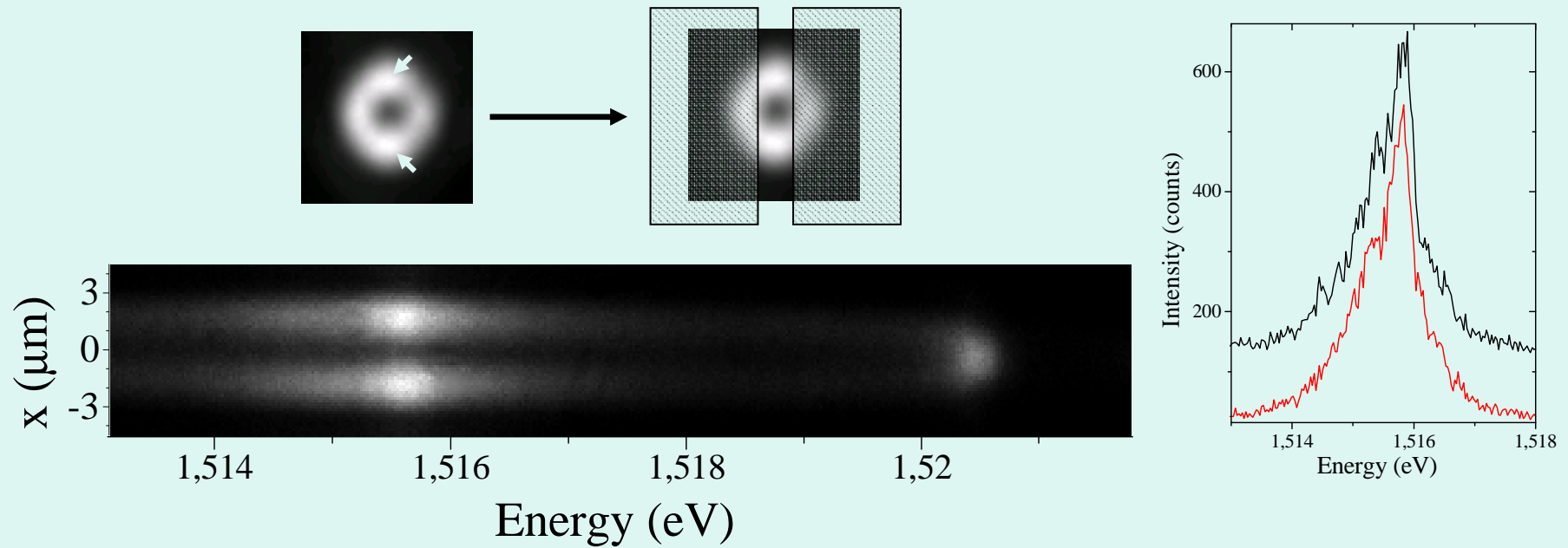
with force constant $\alpha \approx 2.2 \text{ meV}/\mu\text{m}^2$.

Barrier height $\Delta V \approx 5 \text{ meV} \gg kT$.

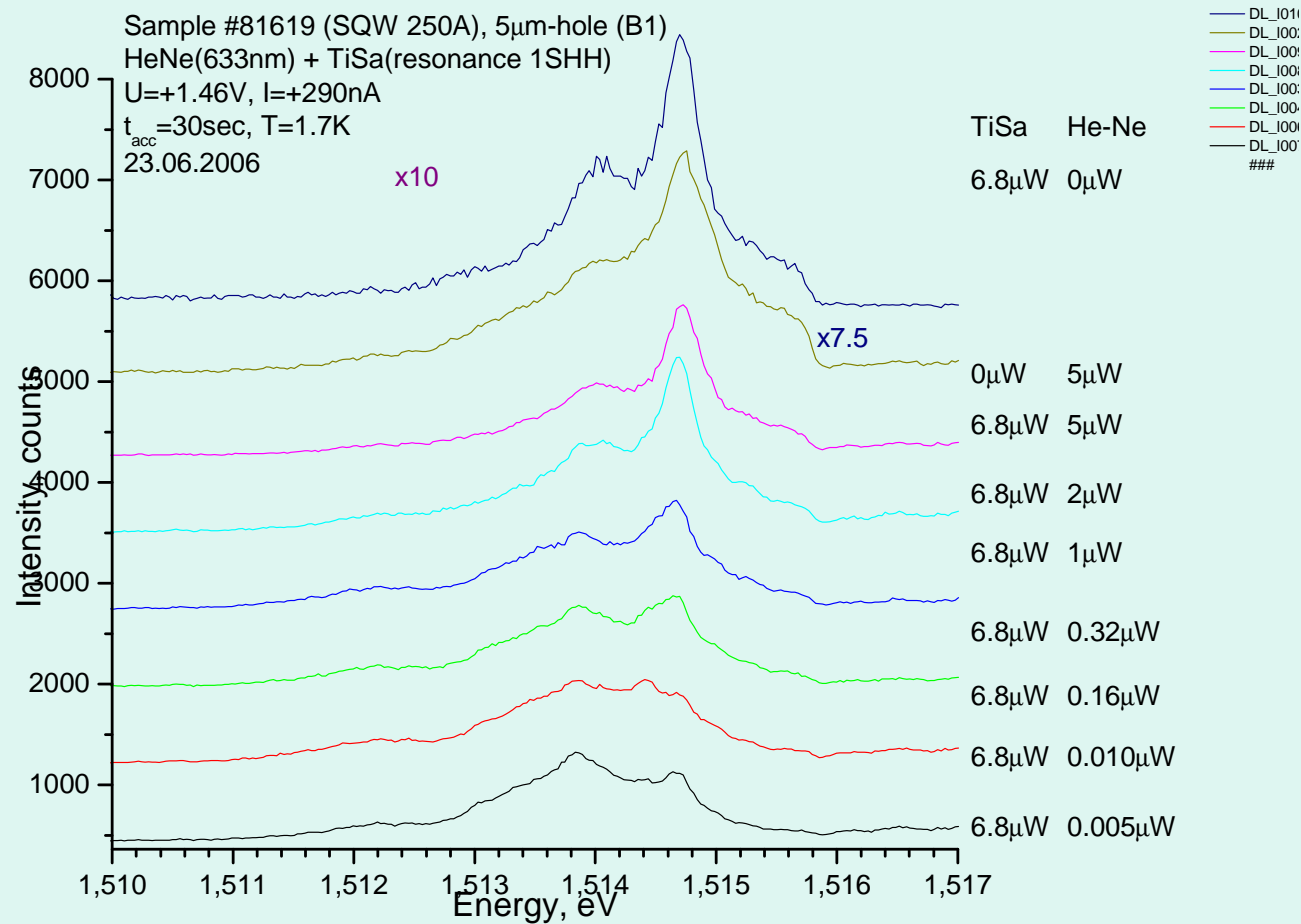
Compensation of extra charges in SQW with the use of in- and above barrier photoexcitations



Luminescence spectra measured under projection of circular window ($\varnothing 5 \mu\text{m}$) on the entrance spectrometer slit for DQW and SQW

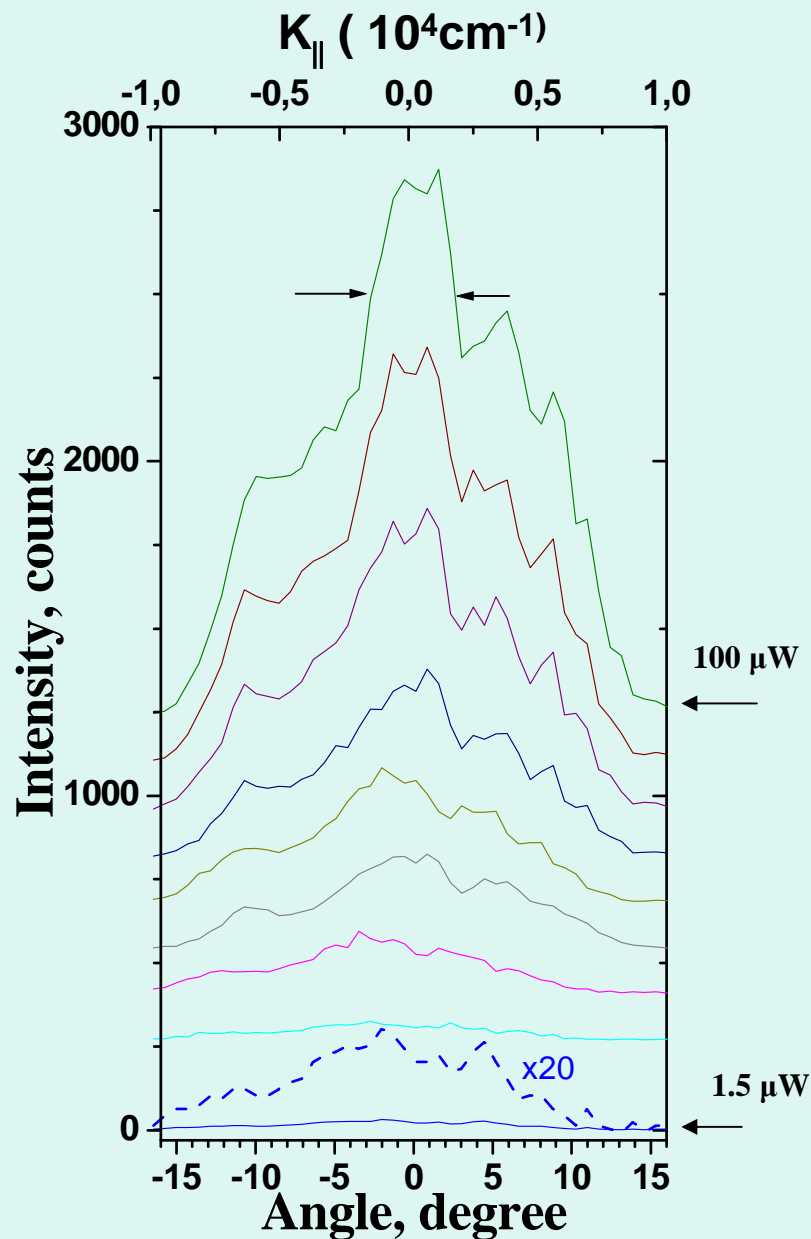


Luminescence spectra of interwell excitons in SQW from 5 μm window under excitation power variation



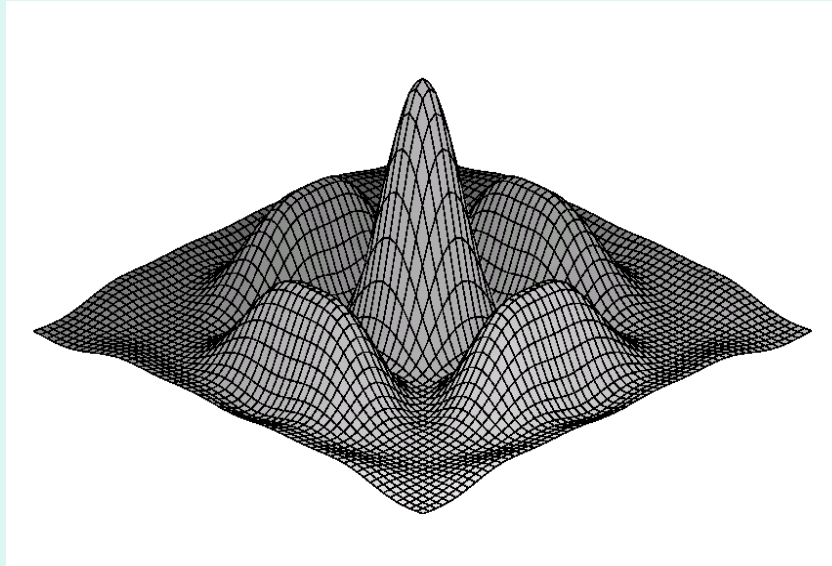
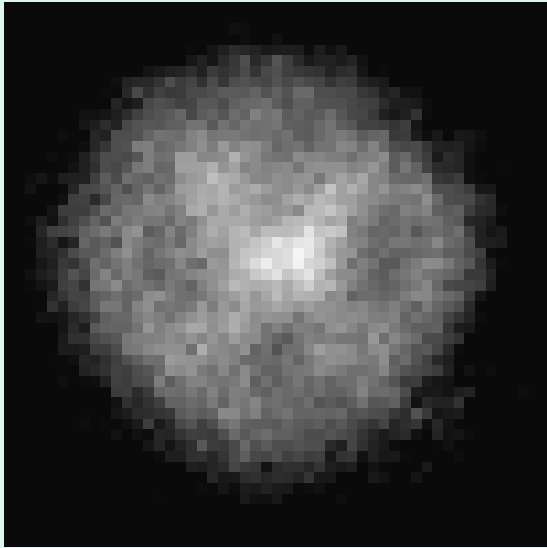
Found FWHM of the line $\delta E=180\mu\text{eV}$ is less than kT

Narrowing of exciton distribution in a far zone (K-space)



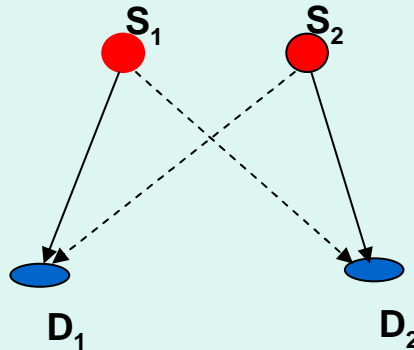
- Excitons are condensed at $K \approx 0$

- Uncertainty $\Delta K_{||} \approx 10^4 \text{ cm}^{-1}$ corresponds to the radial width of the circular trap, $\Delta r \approx 1 \mu\text{m}$ ($\Delta K_{||} \Delta r \sim 1$)



**Condensed dipolar exciton system
confined in a ring trap with 4 vortices.
Theoretical calculations of angular profile
of luminescence – $I(\mathbf{K})$, which is proportional
to the moment distribution of excitons (i.e. to
Fourier-transformed density matrix within
Thomas-Fermi approximation).**

By Yu.E.Lozovik and A.G.Semenov (2006)



Hanbury Brown and Twiss (HBT), 1956

Nature, 177, 27 (1956).

Для бозонов амплитуды $\langle D_1 | S_1 \rangle \langle D_2 | S_2 \rangle$ и $\langle D_1 S_2 \rangle \langle D_2 | S_1 \rangle$ складываются и дают результирующий фактор 2 в комбинированной вероятности детектирования фотонов при условии, что эти две амплитуды имеют одну и ту же фазу (!). Здесь термин амплитуда подразумевает амплитуду квантового состояния $|a_k\rangle$. Суммирование амплитуд по всем парам точек ($S_1 S_2$) в источнике стирает интерференцию, если разность расстояний между детекторами и источником начнет превосходить длину когерентности. HBT использовали этот факт для измерения углового размера звезд (в частности Сириуса, 1956 г.)

Результирующая плотность вероятности регистрации фотонов детектором D_1 в момент времени t_1 и детектором D_2 в момент t_2 равна

$$W(t_1, t_2) = w_1 w_2 \cdot C(r_1 t_1 r_2 t_2) \quad \text{Roy J. Glauber (1963)}$$

C – корреляционная функция, ее отличие от единицы выражает тенденцию двух событий быть коррелированными (т.е. отличаться от пуассоновского распределения при регистрации двух событий в случае испускания стохастическим источником; например, при регистрации α -частиц при радиоактивном распаде)

Если состояние поля определяется оператором плотности поля в форме $\prod_k |a_k\rangle \langle a_k|$ (здесь a_k – квантовая амплитуда поля), то корреляционная функция тождественно равна единице, $C = 1$.

Корреляции между фотонами возникают только при некогерентном смешивании или суперпозиции когерентных состояний. Поэтому корреляционная функция для одномодового лазера в точности равна единице, ибо такой лазер, по сути, происходит из единого квантового состояния. В таком же смысле коррелятор второго порядка для бозе-конденсата (конденсат бозе-атомов, бозе-экситонов и т.д.) также должен быть равен единице. Корреляции между фотонами проявляются вблизи порога фазового перехода, где наиболее сильны флуктуации поля бозонов (например, вблизи порога лазерной генерации, или вблизи порога бозе-конденсации атомов-бозонов или **экситонного бозе-газа** и пр.)